CSTEP®
CENTER FOR STUDY OF SCIENCE, TECHNOLOGY & POLICY

# CSTEP'S SOLAR TECHNO-ECONOMIC MODEL FOR PHOTOVOLTAICS (CSTEM PV): SOLAR AND FINANCIAL MODELS

# CSTEP's Solar Techno-Economic Model for Photovoltaics (CSTEM PV): Solar and Financial Models

*Author*
Harshid Sridhar

**Center for Study of Science, Technology and Policy (CSTEP)**

**September 2019**

The Center for Study of Science, Technology and Policy (CSTEP) is a private, not-for-profit (Section 25) Research Corporation registered in 2005.

Designed and edited by CSTEP

Disclaimer

While every effort has been made for the correctness of data/information used in this report, neither the authors nor CSTEP accepts any legal liability for the accuracy or inferences for the material contained in this report and for any consequences arising from the use of this material.

© 2019 Center for Study of Science, Technology and Policy (CSTEP)

Any reproduction, in full or part, of this publication must mention the title and/or citation, which is provided below. Due credit must be provided regarding the copyright owners of this product.

Contributor: *Harshid Sridhar*

This report should be cited as: CSTEP. (2019). CSTEP's *Solar Techno-Economic Model for Photovoltaics (CSTEM PV): Solar and Financial models*. (CSTEP-RR-2019-05).

September 2019

**Center for Study of Science, Technology and Policy**

**Bengaluru Office**
No. 18, 10th Cross, Mayura Street,
Papanna Layout, Nagashettyhalli, RMV II Stage,
Bengaluru-560094, Karnataka (India)
Tel.: +91 (80) 6690-2500
Fax: +91 (80) 2351-4269

**Noida Office**
Studio No. 206, International Home Deco Park (IHDP),
Plot No. 7, Sector 127, Taj Expressway,
Noida-201301, Uttar Pradesh (India)
Tel.: +91 (121) 484-4003

**Email:** cpe@cstep.in
**Website:** www.cstep.in

## Acknowledgements

The author is grateful to Thirumalai N.C, Principal Research Scientist, CSTEP, Prof M. A. Ramaswamy, Advisor, CSTEP and Prof. V. S. Chandrasekaran, Advisor, CSTEP for their mentorship and guidance. Their support led to a better understanding of the fundamentals of solar energy and engineering analysis.

The support and encouragement provided by CSTEP'S Executive Director, Dr Anshu Bharadwaj, Research Co-ordinator, Dr Jai Asundi, and Principal Research Scientist, Dr Mridula Dixit Bharadwaj is deeply appreciated.

The author is also thankful to N. S. Suresh, Senior Research Engineer, CSTEP for his critical review. CSTEP's Chief Financial Officer, Dr K. C. Bellarmine provided insights that helped the development of the financial model. The author appreciates the input provided by Dr Vinay Kandagal and Dr Ammu Susanna Jacob.

The author sincerely thanks the current and former members of the IT team at CSTEP, including Ranganathan P, Surbhi Sinha, Rohith S. S., Mohana Kumari, Sunil Kumar Chaurasia, Ananth Hegde and Dr Gaurav Kapoor.

The author is thankful to the National Renewable Energy Laboratory (NREL), USA, for providing the Typical Meteorological Year Solar Datasets for India.

Finally, the author wishes to thank the editorial team Sreerekha Pillai, Merlin Francis, Devaditya Bhattacharya, Abhinav Mishra, India Aishani Ashok, and Bhawna Welturkar for their support.

## Executive Summary

CSTEP's Solar Techno Economic Model for Photovoltaics (CSTEM-PV) is a web-based open access tool, which can be used to derive insights regarding a plant's net utilisable solar resource, technical performance, and financial viability. This report aims to serve as a reference document for interested stakeholders who wish to obtain an in-depth understanding of the CSTEM PV tool. It details the basis, considerations, and applications of the solar and financial models supporting the tool. These models can perform pre-feasibility analysis of a potential solar photovoltaic plant (utility and mini grid) in India.

The report comprises of a brief introduction and context, with respect to the core idea of the tool. We explain the overall modelling framework and present the structure, basis, and details of the solar model. This includes aspects ranging from determining the position of the sun, as seen by the location, to estimation of a plant's area, and the power output over its lifetime. The financial model has been built to assess the plant's viability. Itis based on considerations provided by the Central Electricity Regulatory Commission and other relevant stakeholders. Finally, we illustrate the workings of the model via a simulated case and draw relevant insights and conclusions.

# Table of Contents

## List of Figures

## List of Tables

## Nomenclature

| Symbol | Remark | Unit |
|---|---|---|
| $\Phi$ | Latitude of the location | ° |
| $L_{Standard}$ | Longitude of reference location for Indian Standard Time | ° |
| $L_{Local}$ | Longitude of the location | ° |
| $T_{Solar}$ | Estimated Solar Time | min |
| $T_{Std}$ | Indian Standard Time | min |
| EoLD | Effect of longitudinal difference | min |
| EoT | Equation of Time | min |
| N | Day number as per Julian calendar | - |
| $Day_{min}$ | Minute counter for a day post applying solar time correction | min |
| $Day_{hour}$ | Hour counter for a day post applying solar time correction | hour |
| $Hour_{0to23}$ | Hour counter for a day in solar time | hour |
| $\omega_{hour}$ or $\omega$ | Hour angle | ° |
| $\omega_{min}$ or $\omega$ | Minute angle | ° |
| $\delta$ | Declination angle | ° |
| $\omega_{rise/set}$ | Daily hour angle for sun-rise and sun-set | ° |
| $T_{rise/set}$ | Hour of sun-rise and sun-set | hour |
| $\beta$ | Tilt of panel | ° |
| $\gamma$ | Surface Azimuth angle | ° |
| $\alpha_s$ | Solar altitude angle | ° |
| $\theta_z$ | Zenith angle | ° |
| $\theta$ | Incidence angle | ° |
| $\gamma_s$ | Solar azimuth angle | ° |
| DNI | Direct Normal Irradiance also known as beam radiation component | $W/m^2$ |
| DHI | Diffused Horizontal Irradiance | $W/m^2$ |
| GHI | Global Horizontal Irradiance | $W/m^2$ |
| $R_b$ | Tilt factor for DNI component | - |
| $R_d$ | Tilt factor for DHI component | - |
| $R_g$ | Tilt factor for GHI component | - |
| $G_T$ | Net effective radiation incident on the tilted panel | $W/m^2$ |
| $G_{ref}$ | Reference net effective radiation incident on the tilted panel = 1000 $W/m^2$ | $W/m^2$ |
| $\rho$ | Diffuse reflectance of the surroundings for total radiation (GHI) | - |
| $T_{cell}$ | Module cell temperature | °C |
| $T_{cell\text{-}ref}$ | Reference module cell temperature = 25 ºC | °C |
| $T_{amb}$ | Ambient temperature at location | °C |
| WS | Wind speed at location at standard 10-m height | m/s |
| $a_{CT}$ | Empirically-determined coefficient establishing the upper limit for module temperature at low wind speeds and high solar irradiance | °C / $(W/m^2)$ |
| $b_{CT}$ | Empirically-determined coefficient establishing the rate at which module temperature drops as wind speed increases | °C / (W/ms) |

| Symbol | Remark | Unit |
|---|---|---|
| $\Delta T$ | Temperature difference between the cell and the module back surface at an irradiance level of 1000 $W/m^2$. | °C |
| STC | Standard Testing Conditions | - |
| NOCT | Nominal Operating Cell Temperature | - |
| $I_{sc}$ | Short circuit current | A |
| $I_{sc\text{-}ref}$ | Short circuit current at STC | A |
| $V_{oc}$ | Open circuit Voltage | V |
| $V_{oc\text{-}ref}$ | Open circuit voltage at STC | V |
| MPP | Maximum Power Point | (V,A) |
| $V_{mpp}$ or $V_{mp}$ | Voltage at Maximum Power Point | V |
| $I_{mpp}$ or $I_{mp}$ | Current at Maximum Power Point | A |
| $P_{mpp}$ or $P_{mp}$ | Power at Maximum Power Point | W |
| $P_{module\_output}$ | Power output from the PV module | W |
| $P_{max}$ or $P_{mod}$ | Maximum power rating of the module (typically power rating at STC) | W |
| $P_{mod\text{-}max}$ | Maximum power output from the module | W |
| $K_{T\text{-}Voc}$ | Temperature Coefficient of Open Circuit Voltage | %/°C |
| $K_{T\text{-}Isc}$ | Temperature Coefficient of Short Circuit Current | %/°C |
| $K_{T\text{-}Pmp}$ | Temperature Coefficient of Maximum power | %/°C |
| $L_{mod}$ | Length of the module | M |
| $B_{mod}$ | Breadth of the module | M |
| $W_{mod}$ | Width of the module | M |
| $N_{cell}$ | Number of cells in a module | - |
| $\eta_{mod}$ | Efficiency of the module | % |
| $P_{PCU\ AC}$ | Maximum Continuous AC Output Power | kVA or MVA |
| $\eta_{PCU}$ | Efficiency of the PCU | % |
| $P_{nomDC}$ | Nominal DC Power Rating of the PCU | kW or MW |
| $P_{PCU\text{-}DC\text{-}Max}$ | Maximum DC Power seen by the PCU | kW or MW |
| $V_{start}$ | PCU Start Voltage | V |
| $V_{DC\_max}$ | Maximum permissible voltage on the DC side of PCU | V |
| $V_{mppmin}$ | Lower end of voltage range for MPP operation of PCU | V |
| $V_{mppmax}$ | Upper end of voltage range for MPP operation of PCU | V |
| $V_{mid}$ | Mean voltage of $V_{mppmin}$ and $V_{mppmax}$ of PCU | V |
| $V_{PCU\text{-}ref}$ | Reference PCU voltage | V |
| $I_{mppmin}$ | Current at $V_{mppmin}$ for rated $P_{DC}$ | A |
| $I_{start}$ | Current at $V_{start}$ for rated $P_{DC}$ | A |
| $I_{mid}$ | Current at $V_{mid}$ for rated $P_{DC}$ | A |
| $I_{mppmax}$ | Current at $V_{mppmax}$ for rated $P_{DC}$ | A |
| $I_{nomDC}$ | Nominal Operating DC current of PCU | A |
| $I_{DC\ max}$ | Maximum permissible current from PV array to PCU in DC side | A |
| $I_{PCU\text{-}Ref}$ | Reference PCU current | A |
| $RP_{mod}$ | Resource to Module Power Factor | - |
| $RP_{mod\text{-}max}$ | Maximum Resource to Module Power Factor | - |
| $P_{plamt\text{-}target}$ | Target plant capacity | MWp |
| $N_{PCU}$ | Number of PCUs for the plant | - |
| m | Number of modules in series per string | - |
| m_change | Number of module strings added or removed to optimize plant size | - |
| n | Number of strings in parallel per array | - |
| y | Number of arrays per PCU | - |

| Symbol | Remark | Unit |
|---|---|---|
| h | Height of array structure not considering ground clearance | m |
| $N_{mod\text{-}PCU}$ | Number of modules per PCU | - |
| $N_{plant}$ | Number of modules for the plant | - |
| $P_{plant}$ | Rated Plant DC Capacity | MWp |
| $P_{plant\text{-}PCU}$ | Rated Plant AC Capacity | MVA |
| $y_{area}$ | Number of arrays per PCU for area estimation | - |
| $D_{row}$ | Inter-row spacing for a specific time/generation window | m |
| $D_{col}$ | Inter-column spacing for a specific time/generation window | m |
| $D_r$ | Inter-row spacing for all generation windows | m |
| $D_c$ | Inter-column spacing for all generation windows | m |
| PD | Packing Density | - |
| DF | Deviation Factor | - |
| $RP_{plant}$ | Resource to Plant AC Power Factor | - |
| $P_{plant\text{-}AC}$ | Hourly plant AC power generation | MW |
| $Q_{year}$ or $Q_{PV,\ year}$ | Annual PV Generation for a specific year | MWh |
| Net $P_{mod}$ | Net module rating for a year considering module degradation | Wp |
| $CUF_{year}$ | Capacity Utilisation Factor for a specific year | % |
| $PR_{year}$ | Performance Ratio for a specific year | % |
| $SEE_{year}$ | Solar to Electric Efficiency for a specific year | % |
| $Q_{Aux,\ year}$ | Auxiliary Plant Energy Consumption for a specific year | MWh |
| $Q_{Net\ Energy,\ year}$ | Net Saleable Energy | MU |
| $Q_{met\ load,\ year}$ | Quantum of energy demand met for a specific year | MU |
| $Q_{from\ grid,\ year}$ | Quantum of energy imported from grid for a specific year | MU |
| $Q_{load,\ year}$ | Quantum of load from grid for a specific year | MU |
| $Q_{unmet\ load,\ year}$ | Quantum of unmet demand for a specific year | MU |
| $Q_{to\ grid,\ year}$ | Quantum of energy exported to grid for a specific year | MU |
| $Q_{not\ utilized,\ year}$ | Quantum of energy not utilized for a specific year | MU |
| EBIDTA | Earnings Before Interest Depreciation Tax and Amortisation | ₹ Lakhs |
| MAT | Minimum Alternate Tax | ₹ Lakhs |
| IT | Income Tax | ₹ Lakhs |
| LCOE | Levelised Cost of Energy | ₹ / kWh |
| r | Discount rate | % |
| IRR | Internal Rate of Return | % |
| $Tax_{year}$ | Estimated Tax for a specific year | ₹ Lakhs |
| PAT | Profit After Tax | ₹ Lakhs |
| DSCR | Debt Service Coverage Ratio | - |

# 1. Introduction

## 1.1 Solar Power in the Indian Context

India is blessed with solar energy. It receives about 5000 trillion kWh (5 quadrillion or 5 x $10^{15}$ Units or 50,00,000 BU) of energy per year over its landmass (MNRE, 2019b). The global electricity generation in 2018 is reported as 26,672 BU (IEA, 2019). In comparison, India's anticipated electricity generation for 2018 was reported to be 1,399 BU (CEA, 2018c). Even if we consider a conservative assumption,[1] the incident solar energy could still power about 21% and 393% of the global and Indian electricity needs respectively.

Recognising this immense potential, the government of India, in 2015, set up an ambitious target of about 100 GW of installed solar power capacity by 2022 (PIB, 2015). Furthermore, NITI Aayog— the Government of India's premier policy think tank — put forth a broader report about the overall renewable energy (RE) target of 175 GW (includes 100 GW from solar) by 2022 (NITI Aayog, 2016). This ambitious target bolstered the country's solar market and triggered the jump in solar plant installations[2] indicated in Figure 1 and Figure 2, (CEA, 2018b, 2018a; MNRE, 2019a). Although the pace of capacity addition has been brisk, India is still a long way from meeting the targets.

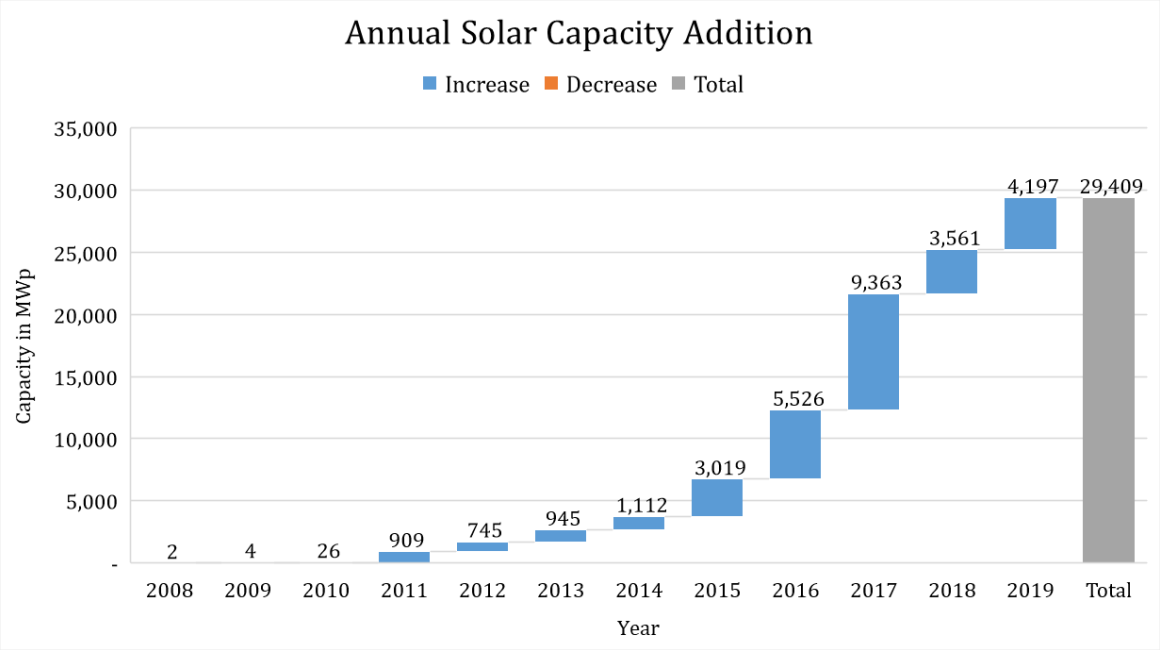


*Figure 1: Year-on-year solar plant capacity addition*

[1] Solar to electric efficiency of 11% and translating only 1% of the Indian landmass for solar energy generation
[2] as on May 2019

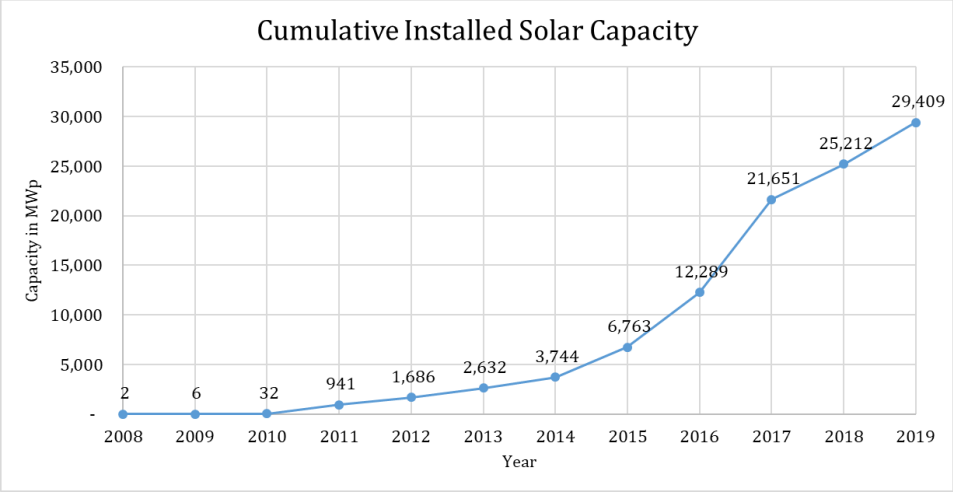


*Figure 2: Cumulative installed solar capacity*

The targets also fostered competition and resulted in lowering solar plants' bids, as illustrated in Figure 3 (Bridge To India, 2019). Here, the average represents the weighted average of the winning bids for that year. The narrowing range of bids indicate that we are approaching a point of bid tariff stabilisations.

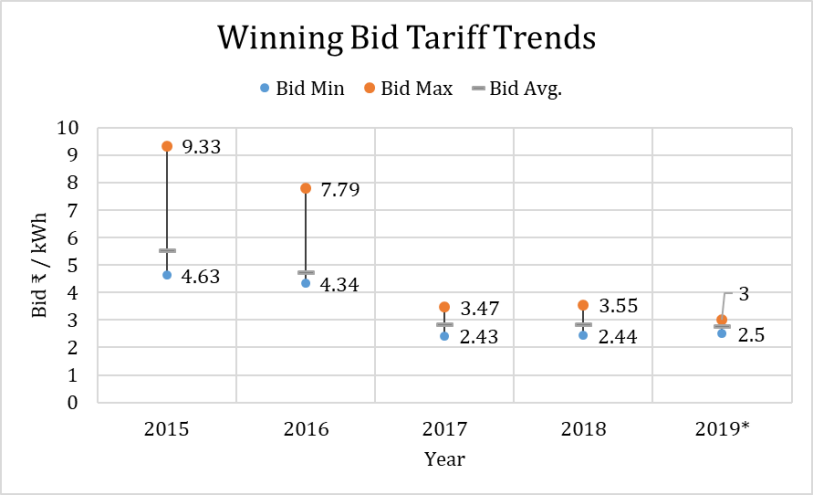


*Figure 3: Solar bid tariff trends*

**Note: Numbers were projected by Bridge To India, 2019*

The report focuses on utility scale and mini grid applications. In this context, the currently installed solar capacity is close to achieving only 50% (~30 GW) of the 2022 target for the utility scale plants (60 of 100 GW). Furthermore, in pursuit of the climate goals, India aspires to work towards 411 GW of RE by 2035 (CEA, 2016) Solar energy is expected to play a dominant role in the nation's ambitious targets. Achieving this would require integrated planning considering resource, energy, infrastructure, and economic aspects. It is in our interest to identify suitable regions for solar installations. Ramachandra, Jain, & Krishnadas, 2011 elegantly coin these regions as 'Solar hotspots' and refer to them as "regions characterised by an exceptional solar power potential suitable for decentralized commercial exploitation of energy

with the favourable techno-economic prospects and organisational infrastructure support to augment solar based power generation in the country". This statement has been visually illustrated in Figure 4.

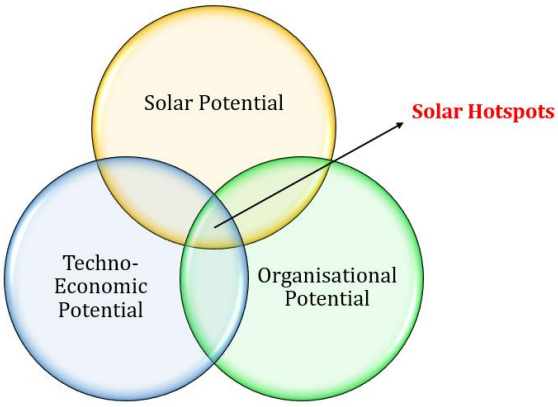


*Figure 4: Conceptual representation of 'Solar Hotspots'*

## 1.2 Brief Story of CSTEM

The Center for Study of Science, Technology and Policy (CSTEP) recognised that a multi-dimensional analysis approach was the need of the hour. This includes integrating perspectives of resource availability, engineering design, and plant economics. Considering the premise that the organisational potential is driven by the industry and government policies, CSTEP built the CSTEP's Techno-Economic Model (CSTEM). This was built with support from the Ministry of New and Renewable Energy (MNRE) for solar thermal technologies in 2011. The outcome of this work is covered in a detailed report by Ramaswamy et al., 2012.

The core deliverable of this work was a desktop-based software, which could compute the techno-economics of a Concentrating Solar Power (CSP) plant. This effort was expanded under the Solar Energy Research Institute for India and United States (SERIIUS) project (SERIIUS, 2012), the US-India Partnership to Advance Clean Energy Research (PACE-R) in 2012. The core deliverable here was a web-based computational tool named CSTEM for Photovoltaics (CSTEM PV), which operated on *publicly available/open data* (CSTEP, 2017).

The objective of this platform was to serve as a useful tool for prefeasibility analysis of utility scale solar PV plants from a techno-economic standpoint. It was aimed to cater to policy makers, researchers, and industry trackers for informed decision making. While the platform was built for PV-based utility scale plants, computational models were also built for mini grid[3] and roof top systems[4]. Realising that there is merit in developing an integrated solar photovoltaics model for utility scale and mini grid applications with storage technologies, CSTEP pursed the development of version 2 (V2) of the CSTEM PV tool, with support from the Good Energies Foundation.

This report is an effort to record the details of the solar and financial models of CSTEM PV V2. It covers, in detail, the methodology, structure, technical basis, assumptions, and considerations of

[3] Supported by Wipro Ltd. Under SERIIUS
[4] Based on a custom request by MNRE

the model. Additional reports will be released detailing the models on-storage technologies, load management, and solar module tracking soon.

A brief contrast of the features covered in V1 and V2 of the CSTEM PV tool has been provided in Table 1.

*Table 1: Comparing V1 and V2 of CSTEM PV*

| Feature | V1 | V2 |
|---|---|---|
| **Time Reference** | Solar Time | Zone Time |
| **Application** | Utility scale PV plants | • Utility scale PV plants<br>• Mini Grids<br>  ○ Grid connected<br>  ○ Off Grid |
| **Technology** | PV only | PV with storage (for mini grid systems, lead acid-based systems) |
| **Financial Assessment** | Levelised Cost of Energy (LCOE) and Internal Rate of Return (IRR) | • LCOE and IRR (for all applications)<br>• Bid analysis (for utility scale plants)<br>• Feed in Tariff (for mini grid cases only) |
| **Scope** | 22 locations | Pan India at approximately 10 km x 10 km resolution (Solar Data Source: NREL) |
| **Other Enhancements** | • Plant area estimation (block-based estimation to spiral pattern-based plant design)<br>• Plant design configurations reduced to one optimal design<br>• Effect of module degradation (algorithm revised for faster computation)<br>• 5-year roll over for Minimum Alternate Tax added<br>• Detailed resource estimation modules built<br>• Revamped the entire look and feel of the tool to make it more intuitive and useful | |

## 1.3 Model Outline

Figure 5 presents the overview of the inputs, outputs, and outcomes of the integrated model.

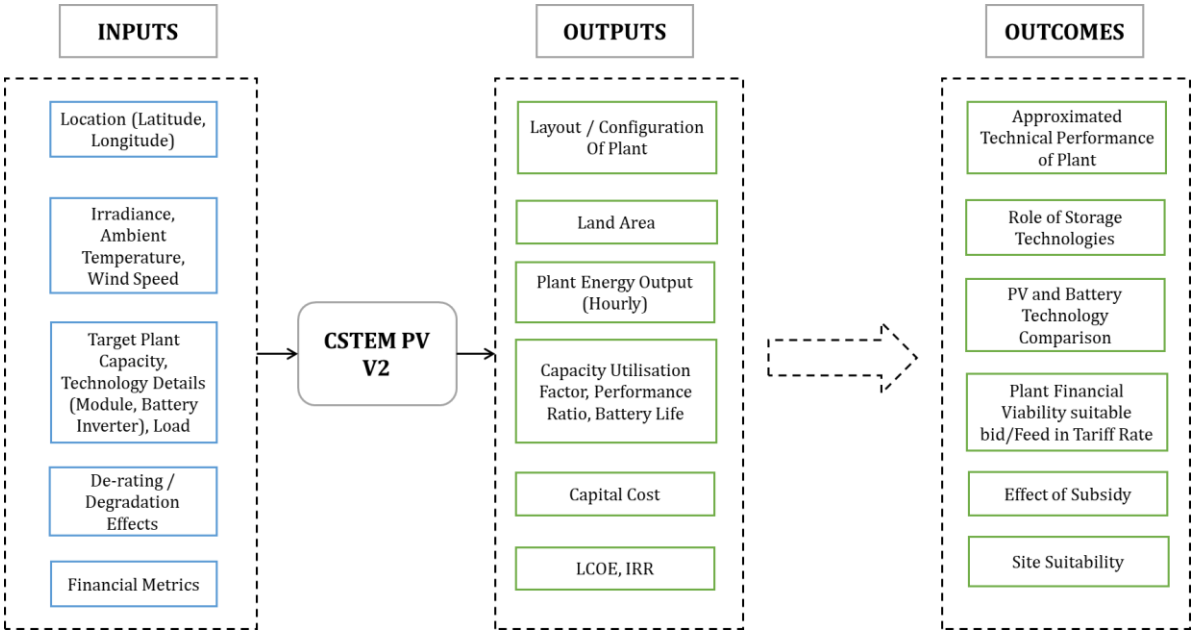


*Figure 5: Overview of inputs, outputs, and outcomes of the CSTEM PV V2*

### 1.3.1 Inputs

The model's inputs are provided by the user in the following steps:

- Basis for design choice
- Location and plant details
- Technology details
- Costs and financial metrics

The basis for design choice is first presented to the user. This section collects details about the plant design and financial assessment of interest. The details are as follows:

- Design of PV plant - This can be PV plant capacity-based (currently available and elaborated in this report) or available area-based (will be released as an add-on to the model).
- Application - Here, the choice is large-scale grid connected utility plant (0.5 to 5000 MWp) or mini grid application (10 to 500 kWp). The mini grid plant can also be a grid-connected or off-grid set up.
- Financial Assessment - The user is provided with three kinds of assessments:-
    - Estimation of LCOE, available of both utility-scale and mini grid cases.
    - Bid analysis is suitable for checking the viability of the bids during reverse auction and is available for utility-scale plants alone
    - Feed in tariff evaluates the viability of a prescribed tariff of mini grid systems.
- Technology - The choice is limited to either a PV-only plant (applicable for utility-scale plants only) or PV with storage plant (currently available for mini grid cases only, but it will be expanded to utility plants)
- Tracking - The module tracking option can be chosen by the user. At present, only fixed tilt is available and elaborated in this report. Single and dual axis tracking options will be included as add-ons and the details of the model will be published in a separate report soon.

Based on the above choices, the next the set of inputs include:

- Location of interest (determining the latitude (φ) and longitude (L) of interest)
- Type of ground to choose the albedo value (ρ)
- The target capacity of the PV plant (Pplant-target) in kWp or MWp
- Array-related details, including orientation and tilt of the PV array [surface azimuth angle (γ), tilt angle (β)], array height (h) in m, ground clearance (GC) in m, and boundary spacing along length and breadth in m (a, b)
- Other plant-related parameters include plant life in years and reference plant area in acres/MWp.

Next, the user can choose technology-related inputs, which includes:

- Module - Choice of module technology (multi crystalline, mono crystalline or thin film), manufacturer and module model details, module mount details, and module degradation-related details
- PCU or Inverter - Manufacturer and PCU model details
- Battery and demand - Choice of manufacturer, window of back up hours, and details of load curve.
- Others - Details of auxiliary consumption, soiling and electrical loss details.

Finally, the user can choose cost and financial metrics, which includes the following:

- Capital cost - Benchmark cost for module in ₹/Wp, battery in ₹/kWh and land in ₹/acre. Further costs related to mounting structure, civil and general works, inverter, power evacuation infrastructure, preliminary and preoperative expenses, and miscellaneous expenses are in ₹ lakhs/MWp or ₹ lakhs/kWp. Finally, the quantum of bulk capital subsidy availed, if applicable, is considered as a percentage of the total capital cost.
- Operation cost - Comprises of baseline operation and maintenance (O&M) expenses at the end of year 1, and the year-on-year escalation rate for O&M expenses
- Financial metrics - Comprises term loan and working capital, return on equity, depreciation, and taxes.

### 1.3.2 Methodology

Figure 6 illustrates a simplified methodology of the process[5]. Based on the inputs provided by the user, the following points summarise the methodology of the CSTEM PV model:

- The first step is to mathematically model how the location of interest sees the sun. This is done by simulating the sun's path, with respect to the tilted module. The reference for the calculation is set in zone time (it was set in solar time in V1). Hence, appropriate time corrections[6] and solar geometry-related metrics were estimated and applied based on the coordinates of the location. The solar geometry-related metrics includes solar angles such as declination angle (δ), hour angle (ω), solar zenith angle ($\theta_z$), solar altitude angle ($\alpha_s$), solar azimuth angle ($\gamma_s$) and solar incidence angles (θ). Furthermore, the sunrise and sunset times, along with the duration of each day has been estimated. The works of Duffie & Beckman, 2013; Iqbal, 1983; and Stine & Geyer, 2001, served as

[5] *Figure 5* and *Figure 6* are slightly modified versions from that presented in Sridhar & N. C., 2018, to accommodate the current enhancement.
[6] This is because of differences in the latitudinal and longitudinal displacement of the location from the location of time reference.

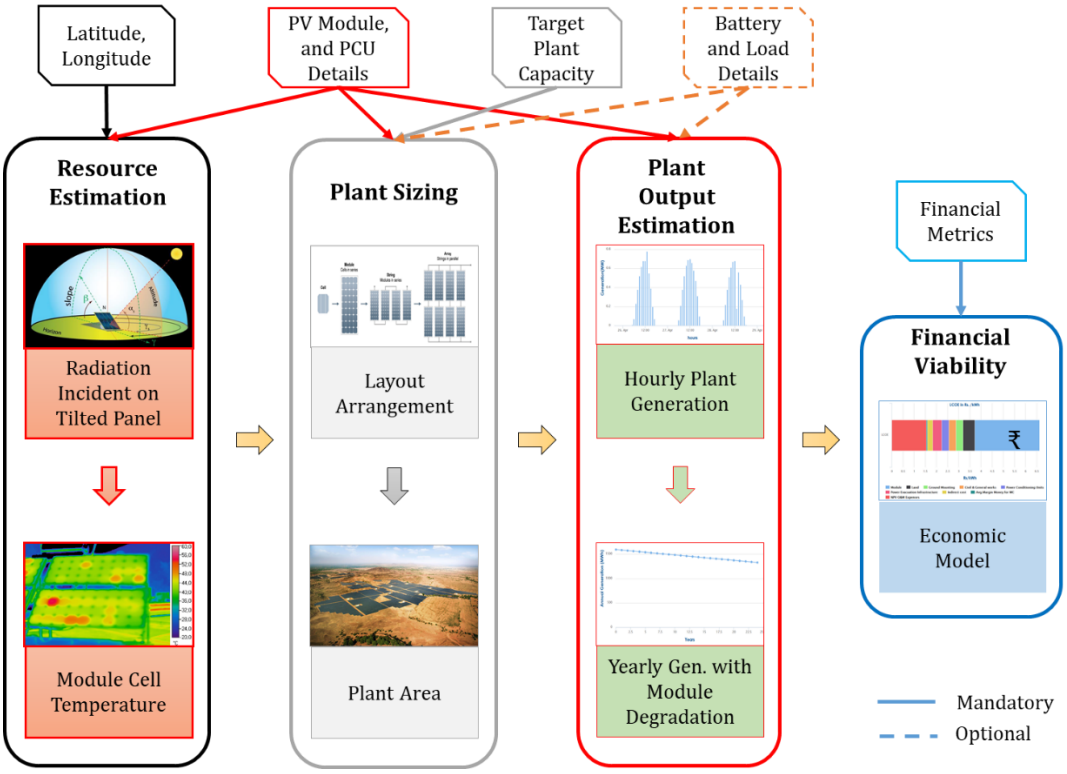


*Figure 6: Generic Computational flow of CSTEM PV V2*

*Note: PCU – Power Conditioning Unit is also known as Inverter, Image sources: Azure Power, 2015;* CSTEP, 2017*; Paiva, Pimentel, Marra, & de Alvarenga, 2015; Tsanakas & Botsaris, 2009; Your Home (Govt. Of Australia), n.d.*

references. Using these solar angles, the net radiation incident on the tilted panel was estimated, using 2D isotropic radiation model (Liu & Jordan, 1960). Finally, King, Boyson, & Kratochvil, 2004 served as a reference for estimating the cell temperature of the PV module, considering effects of ambient temperature and wind speeds.

- Next, we determine the electrical arrangement of solar PV modules and batteries (if applicable) as per the design considerations chosen by the user (utility/mini grid, grid connected/off-grid, PV only or PV with storage systems). By electrical arrangements, we refer to the number of PV modules and/or batteries in series and parallel, as per considerations of PCU and/or load. The works of Hegedus & Luque, 2011; Honsberg & Bowden, n.d.; Kalogirou, 2009; Markvart & Castaner, 2013; Mertens, 2014; Roger & Jerry, 2005; Solanki, 2015; Teodorescu, Liserre, & Rodriguez, 2011 served as references for the PV model. The battery sizing models for the mini grid cases were built based on the maximum energy demand for the hours of backup, battery efficiency, and battery depth of discharge (DoD). The plant area estimation model (especially the utility scale application) was built based on our original research, inspired by the mathematical construct of the prime spiral/ulam spiral (Stein, Ulam, & Wells, 1964).
- The next section focuses on estimating the PV module and PV plant output. The works of Bai et al., 2015; De Soto, 2004; Townsend, 1989; and Whitaker et al., 1991 were considered for this section. The basic PV power estimation section has been compared with that of select, existing plants, and has been found suitable for policy analysis-related studies (Klima et al., 2018). The module degradation has been accounted for, as per the specifications in the module datasheet. The battery and load management models have been built taking into consideration the works of Hittinger, Wiley, Kluza, & Whitacre, 2015; Langella, Testa, & Ventre, 2014; Shi, Xu, Tan, Kirschen, & Zhang, 2018.

As mentioned earlier, the battery and load management models, along with the solar module tracking models, will be covered in a separate report that will be made available via the CSTEP website soon.

- Finally, the last section computes LCOE and/or IRR for various cases of financial study such as viability of bid, FIT and impact of subsidy. The works of Brigham & Houston, 2007; Cambell, 2008 and CERC, 2016 were considered. Additional upgrades and revisions were made as per suggestions of stakeholders.

### 1.3.3 Outputs and Outcomes

The outputs from the model aims to address the following aspects:

- Resource availability (solar energy availability, solar hours) and land requirement
- System design and sizing (PV module, PCU and/or battery system)
- Plant output, in terms of generation fed to grid and/or consumed by the load
- Capital and operational cost of the system
- Metrics assessing technical performances like Capacity Utilisation Factor (CUF), Performance Ratio (PR), Packing Density (PD), Solar to Electric Efficiency (SEE), LCOE, and IRR

The broader outcomes of the platform involve its ability to be used to derive insights regarding a plant's net utilisable solar resource, technical performance, and financial viability. Although its applicability can directly assess a site, it can certainly be scaled further to derive regional and national level perspectives. With the appropriate inputs, this tool can be used to perform comparisons of technologies, determine the effect of subsidies, and assess tariff viability. This tool could also be used to conduct sensitivity analysis of various levers available to policy makers for impact assessment, informed decision making, and better planning.

## 1.4 Report Structure

It must be reiterated that the scope of this report is restricted to the overall conceptual architecture of CSTEM PV V2, solar energy, and financial models. The battery and load management systems, and tracking models will be covered in a separate report.

The structure of this report is as follows:
Chapter 1: Introduction to the Indian solar energy context and the story of CSTEM
Chapter 2: Details of the solar energy model
Chapter 3: Description of the financial model
Chapter 4: Presentation of a simulated case
Chapter 5: Conclusions about the model and the way forward

# 2. Solar Energy Model

This chapter details the solar energy model. It details the assumptions and considerations of the solar model (section 2.1). We present the details of the calculations pertaining to the development of the sun's path, as seen by the location of interest. Here, we present conventions and calculations to estimate the various solar angles, considering the fixed module tilt configuration (section 2.2). The basis for estimating the effective radiation on the tilted panel (section 2.3) and the effective cell temperature developed in the module (section 2.4) has also been put forth in this section. Next, a detailed account of the electrical operation of the solar cell and the basis for the choice of model for module power estimation has been presented (section 2.5 and 2.6). Using the insights drawn so far, we developed a method for the sizing of the photovoltaic arrays, and by extension, the system (section 2.7and 2.8). Based on the array structure and solar angles, we determined the area of the solar PV plant (section 2.9). Finally, we determined the output from the solar PV plant, factoring in module degradation, and derive the plant performance metrics (section 2.10).

## 2.1 Assumptions and Considerations

The core idea is to design a plant such that it generates approximately the target plant capacity at the best local environmental conditions. *The overall model framework has been developed such that it relies on information that is readily available in datasheets*. The CSTEM PV V2 solely caters to prefeasibility/potential assessment purposes, designed for policy analysis. An elementary version of the solar power plant model has been tested at a minute-wise resolution and has been found to have an error margin of 6 ± 6 % (Klima et al., 2018). In this model, due to absence of temporally and spatially coincident data, we have incorporated the conclusions of Klima et al., 2018, and have adopted the NREL's TMY data from NSRDB (NREL, 2015) as the primary source of solar resource information. The solar resource dataset used in this model has a spatial resolution of 10 km x 10 km, and an hourly temporal resolution. Despite the measures taken, a margin of ± 20% should be considered when comparing the output with those of operational plants. This is primarily because the TMY data is a representative (most probable) solar data for a location. It does not capture the extreme fluctuations in the solar resource.

The solar model presented here is generic and can be used to design PV systems for both utility and mini grid applications, for a target plant capacity. The model, however, does not cover whether the PV plant capacity is *optimised* for battery technology operation. The battery is expected to adopt the output from the PV plant and adapt, as per the dispatch strategy of the load curve (beyond the scope of this report). The model presented here is for a fixed panel tilt-based system. This option was prioritised, as majority plants in the world are of this configuration, and this is relatively cheaper than tracking-based systems. The plant is designed such that there is no module shading during the hours of recommended operation (time window). Aspects related to module degradation have been considered as per module specifications in the module datasheet.

## 2.2 Solar Geometry

The solar geometry aspect tries to mathematically represent the motion of the sun, as seen by the location of interest throughout the year. We represented this by calculating the appropriate solar angles. The definition and convention of the angles has been provided in Appendix – A.

In V2, the reference of time has been changed to zone time (also known as standard time) from solar time. This is because in reality the power systems and various power sources operate and hence, must be co-ordinated according to zone time. Since solar angles are computed with respect to solar time, this requires the estimation of equivalent solar time from zone time for a chosen location of interest. One possible method to do this has been illustrated by Iqbal, 1983.

The Indian Standard Time is calculated based on 82.5° E longitude, in Shankargarh Fort, Mirzapur (25.15°N, 82.58°E) (in the Allahabad district of Uttar Pradesh), which is nearly on the corresponding longitude reference line. For a location with a given longitude, the time conversion parameters could be calculated by the following relations:

$Solar\ Time\ (T_{Solar}) - Standard\ Time\ (T_{Std}) = Effect\ of\ longitudinal\ difference\ (EoLD) + Equation\ of\ time\ (EoT)$.

$$T_{Solar} - T_{Std} = EoLD + EoT$$

$$T_{solar} = T_{std} + EoLD + EoT$$

Where,

$$EoT = 229.2 \times (0.000075 + 0.001868 \times cos(B) - 0.032077 \times sin(B) - 0.014615 \times cos(2B) - 0.040849 \times sin(2B)$$

$$EoLD = 4 \times (L_{standard} - L_{Local})$$

$$B = (N - 1) \times 360/365$$

Here, $L_{standard}$ represents the standard meridian for the local time zone, while $L_{Local}$ is longitude of the location of interest. EoLD and EoT are in minutes, N represents a day number, as per the Julian calendar (from 1 to 365). Hence, the correction, $T_{Std}$ and $T_{Solar}$ is also in minutes.

$$T_{solar} = T_{std} + EoLD + EoT$$

If the resolution of the data is minute-wise, the minute counter in the day is represented as follows:

$$Day_{min} = Hour_{0to23} \times 60 + T_{solar}$$

Similarly, for hourly resolution data, the hour counter in the day is represented as follows:

$$Day_{hour} = Hour_{0to23} + \frac{T_{solar}}{60}$$

Here, $Hour_{0to23}$ is the hour counter for a day. $Day_{min}$ is the minute counter, and $Day_{hour}$ is the hour counter, both of which are to be referenced in solar time. If the data itself is in solar time, then

$$Day_{hour} = Hour_{0to23}$$

The solar angle calculations are performed such that they account for the tilt of the panel with respect to the ground (β) and the angular displacement of the panel normal from due south direction (γ). The definition of solar angles for this analysis is as specified in Duffie & Beckman, 2013.

The time corrections if calculated are applied to $Day_{hour}$ or $Day_{min}$ as per the choice of reference time resolution. The hour/minute angle (ω) could be appropriately calculated. Further, based on the time corrections applied, N was appropriately shifted. After applying this shift, the

declination angle (δ) was calculated. The declination angle and the latitude angle ($\Phi$) would aid in computing the sunrise/set time, number of daylight hours, incidence angle (θ), zenith angle ($\theta_z$), and altitude angles ($\alpha_s$). Relevant equations as specified in Duffie & Beckman, 2013 are summarised below:

$$\omega_{hour} = -15 \times (12 - Day_{hour})$$

$$\omega_{min} = -0.25 \times (720 - Day_{min})$$

$$\delta = \frac{180}{\pi} \times 0.006918 - 0.399912 \times cos(B) + 0.070257 \times sin(B) - 0.006758 \times cos(2B) + 0.000907 \times sin(2B) - 0.002697 \times cos(3B) + 0.00148 \times sin(3B))$$

$$\omega_{rise/set} = cos^{-1}(-tan\Phi \times tan\delta)$$

$$T_{rise/set} = 12 + \omega_{rise/set}/15$$

$$No.of\ daylight\ hours = \omega_{rise/set} \times (2/15)$$

$$\omega = \omega_{hour}\ or\ \omega_{min}$$ (Based on the choice of time resolution)

$$\theta = cos^{-1}(sin\delta \times sin\Phi \times cos\beta - sin\delta \times cos\Phi \times sin\beta \times cos\gamma + cos\delta \times cos\Phi \times cos\beta \times cos\omega + cos\delta \times sin\Phi \times sin\beta \times cos\gamma \times cos\omega + cos\delta \times sin\beta \times sin\gamma \times sin\omega)$$

$$\theta_z = cos^{-1}(cos\Phi \times cos\omega \times cos\delta + sin\Phi \times sin\delta)$$

$$\alpha_s = 90 - \theta_z$$

The solar azimuth angle (A or $\gamma_s$) is pivotal in illustrating the nature and direction of the sun's rays. There are two ways to illustrate this angle.

- It is the angular displacement from the south to the projection of the beam radiation on the horizontal plane. (It is the angle between the projections of the sun's ray with the N–S axis.) Displacements east of south are negative, and west of south are positive (ω negative for morning and positive for afternoon)(Duffie & Beckman, 2013):

  $$\gamma_s = sign(\omega) \times \left| cos^{-1}\left(\frac{cos\theta_z \times sin\Phi - sin\delta}{sin\theta_z \times cos\Phi}\right)\right|$$

- It is the angle, measured clockwise on the horizontal plane from the north-pointing coordinate axis to the projection of the sun's central ray. Summarising the equations provided in Stine & Geyer, 2001, we have:

Taking the sine expression for A'

$$A' = sin^{-1}\left(\frac{-cos\delta \times sin\omega}{cos\alpha}\right)$$

If $\left[cos\omega \geq \frac{tan\delta}{tan\Phi}\right]$ → A = 180 – A' Azimuth in 4th quadrant. Below EW line

If $\left[cos\omega < \frac{tan\delta}{tan\Phi}\right]$ → A = 360 + A' Azimuth in 1st quadrant. Above EW line

Taking the cosine expression for A

$$A'' = cos^{-1}\left(\frac{sin\delta \times cos\Phi - cos\delta \times cos \times sin\Phi}{cos\alpha}\right)$$

If $[Sin\omega > 0]$ → A = 360– A"

If $[Sin\omega \leq 0] \rightarrow A = A''$

The sine expression used for determining whether the time is before or after solar noon. The 'If' condition tests whether the solar azimuth is north or south of the east-west line.

It must be noted that due to the nature of their conventions, the angles A and $\gamma_S$ have the following relation

$A - \gamma_s = 180º$

Figure 7 provides the illustration of various solar angles.

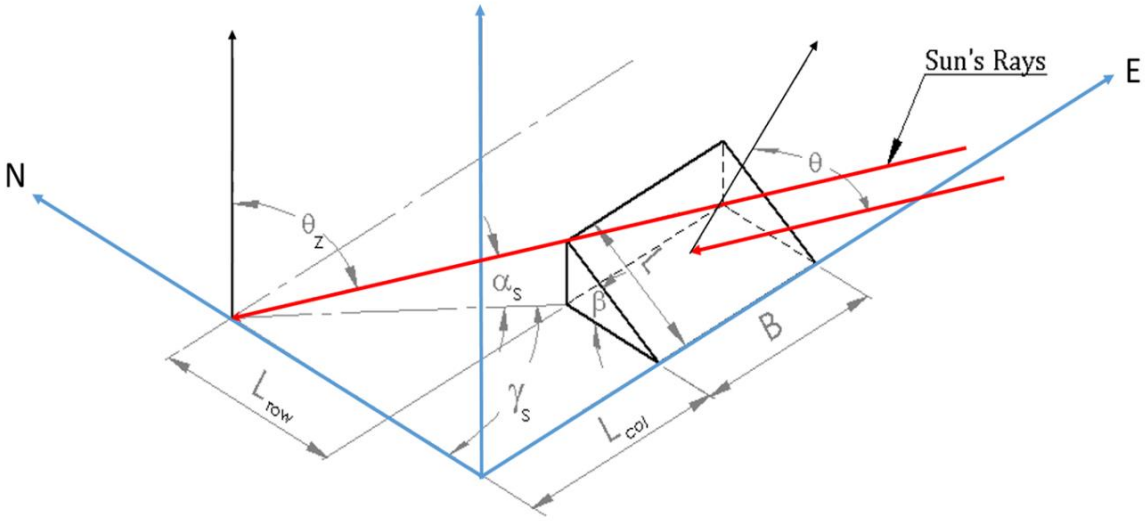


*Figure 7: Illustration of solar angles for a panel at fixed tilt facing due south*

The equations, so far, helped us precisely map conventions of time and the movement of the sun, as seen by the location of interest. Next, we move towards understanding the considerations for solar radiation.

## 2.3 Solar Radiation Model

The isotropic diffuse model proposed by Liu & Jordan, 1960 has been considered for this framework. This model considers the radiation on the titled surface to comprise of three components: the beam, isotropic diffuse, and solar radiation diffusely reflected from ground. Since the panels are tilted, the effective radiation components incident on the panel must be scaled appropriately. These scaling ratios are referred to as tilt factors. Here $R_b$, $R_d$ and $R_g$ are considered as the tilt factors for the Direct Normal Irradiance (DNI) or beam, Diffuse Horizontal Irradiance (DHI), or diffused and Global Horizontal Irradiance (GHI) of global components respectively.

The DNI is the component of radiation that is in the direction of the sun's rays. Hence, the radiation component incident on the horizontal surface parallel to its normal is:

$$G_b = DNI \times cos\theta_z$$

The beam radiation on a tilted surface is a function of the incident angle θ and can be illustrated as follows:

$G_{bT} = DNI \times cos\theta$

DHI and GHI were already accounted for as the isotropic diffused radiation component reaching the horizontal surface. The tilt factors to consider the effects of a titled panel are as follows:

$$R_b = \frac{Total\ DNI\ incident\ on\ tilted\ surface}{Total\ DNI\ incident\ on\ the\ horizontal\ surface} = \frac{DNI \times cos\theta}{DNI \times cos\theta_z} = \frac{cos\theta}{cos\theta_z}$$

$R_d = 0.5 \times (1 + cos\beta)$

$R_g = 0.5 \times (1 - cos\beta)$

$G_T$ is the net effective radiation incident on the tilted panel. This can be calculated as follows:

$G_T = G_b \times R_b + DHI \times R_d + GHI \times \rho \times R_g$

$G_T = DNI \times cos\theta + DHI \times R_d + GHI \times \rho \times R_g$

Here,

ρ = diffuse reflectance of the surroundings for total radiation (GHI)

This formulation does not consider the effect of incidence angle modifiers. The primary issue with taking incidence angle modifiers into consideration is that the precise refractive index/glass type and the thickness of the glass cover over a PV panel is not generally specified in module datasheets. Hence, $G_T$ has been considered in this model. Next, we move towards estimating the temperature built in the PV cells.

## 2.4 Cell Temperature Model

One of the most commonly used expressions to determine cell temperature (Ross, 1980) is:

$$T_{cell} = T_{amb} + G_T \times \left(\frac{NOCT - 20}{800}\right)$$

Here, in order to simplify the relation, it is assumed that the cell temperature increases linearly with irradiance. However, the coefficient, which captures the variation in cell temperature, depends on module installation, wind speed, ambient humidity, etc. This consideration leads to consider a single value to characterise a module type. This information is contained in Nominal Operating Cell Temperature (NOCT), which is defined as the cell temperature, when the ambient temperature is 20 °C, irradiance is 800 W/m2 and a wind speed of 1 m/s. NOCT values around 45 °C.

The main issue with this consideration is that it doesn't consider the effect of wind speeds, other than 1m/s or the module mounting condition. For CSTEM PV, we consider the approach developed by King et al., 2004, which factors varying wind speeds and the effects of module mount configuration (indicated in *Table 2*). The irradiance dependence is implicit in cell temperature, in this approach, and it can be illustrated by the following relation:

$T_{cell} = G_T \times exp(a_{CT} + b_{CT} \times WS) + T_{amb} + (\Delta T) \times G_T / G_{ref}.$

Here,

$T_{amb}$ = Ambient air temperature (ºC)

$G_{ref}$ = Reference solar radiation on the panel, 1000 W/m²

WS = Wind speed measured at standard 10-m height (m/s)

$a_{CT}$ = Empirically determined coefficient establishing the upper limit for module temperature at low wind speeds and high solar irradiance (ºC/ (W/m²))

$b_{CT}$ = Empirically determined coefficient establishing the rate at which module temperature drops, as wind speed increases ((ºC/ (W/m²)) × (1/ (m/s)) = (ºC/ (W/ms)))

ΔT = Temperature difference between the cell and the module back surface at an irradiance level of 1000 W/m². This temperature difference is typically 2 to 3 ºC for flat plate modules in an open rack mount. For flat plate modules with a thermally insulated back surface, this temperature difference can be assumed to be zero.

Table 2 provides a generic set of coefficients representative of flat plate PV modules for different module types and mounting configurations.

*Table 2: Empirically determined coefficients used to predict cell temperature (at a height of 10 m).*

| **Module type** | **Mount** | **$a_{CT}$** | **$b_{CT}$** | **ΔT (ºC)** |
|---|---|---|---|---|
| Glass/cell/ glass | Open rack | -3.47 | -0.0594 | 3 |
| | Closed roof mount | -2.98 | -0.0471 | 1 |
| Glass/cell/ polymer sheet | Open rack | -3.56 | -0.075 | 3 |
| | Insulated back | -2.81 | -0.0455 | 0 |
| Polymer/thin film/steel | Open rack | -3.58 | -0.113 | 3 |

With determination of $G_T$ and $T_{cell}$, we can determine the basis for estimating the module power output. This is done in 2 steps: first, we indicate the parameters of interest for PV module and PCUs (Section 2.5), and then, we elaborate about the operation of the PV module (Section 2.6)

## 2.5 PV Module and PCU Parameters of Interest

### 2.5.1 PV Module

A solar PV module is a combination of solar cells. The cells are connected in series to form a string, to achieve the required voltage level.These series strings are connected in parallel to form a module. Bypass diodes are connected across parallel strings to protect against hot spot damage when the PV panel is partially shaded by trees, fallen leaves or other obstructions. Figure 8 illustrates the structure of a generic solar PV module.

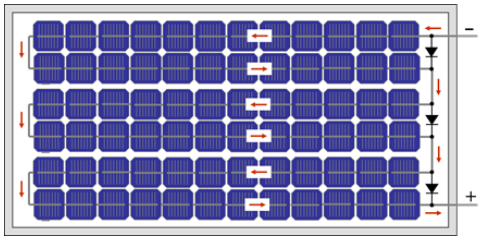

*Figure 8: A typical 72 cell PV module with bypass diodes*

*Source: Solmetric SunEye, 2011*

The parameters considered for design in this model are defined under the Standard Testing Condition (STC). It is a benchmark condition/criterion used to define reference power ratings of a solar PV module. The STC comprises of an incident solar irradiance of 1000 W/m$^2$, cell temperature of 25 °C, wind speed of 1 m/s, air mass[7] of 1.5. The STC is alternatively called Standard Rating Conditions (SRC). The parameters of interest openly available in datasheets are as follows:

- Short Circuit Current ($I_{sc}$) in A: It is defined as the current developed in the circuit when the output terminals are short circuited i.e. V = 0 or the load impedance at the output terminals = 0.
- Open Circuit Voltage ($V_{oc}$) in V: It is defined as the voltage developed in the circuit when the output terminals are open circuited i.e. I = 0 or the load impedance at the output terminals = 0.
- Maximum Power Point (MPP) parameters: The MPP is the operating point in the characteristic curve that generates maximum output power. The voltage at this point is termed as the maximum power point voltage ($V_{mpp}$ or $V_{mp}$) in V, the current, at this point, is termed the maximum power point current ($I_{mpp}$ or $I_{mp}$) in A, and hence, the maximum power ($P_{mpp}$ or $P_{mp}$ or $P_{max}$ or $P_{mod}$) in W.

$$P_{mpp} = V_{mpp} * I_{mpp}$$

- Temperature Coefficients in %/°C: The temperature coefficient of a parameter indicates the change in the parameter, when subjected to a unit change in cell temperature. Typically, temperature coefficient of $V_{oc}$, $I_{sc}$ and $P_{mp}$ are provided by module manufacturer datasheets. They are denoted as $K_{T\text{-}Voc}$, $K_{T\text{-}Isc}$ and $K_{T\text{-}Pmp}$ respectively.
- Dimensions of the module in mm or m: The length, breadth, and width of the solar panel are denoted as $L_{mod}$, $B_{mod}$ and $W_{mod}$ respectively.
- Module Degradation: Typically, the rating of the module at the end of year 1, year 10, and year 25 are provided. A linearized degradation rate has been derived and applied.

[7] Air Mass is the ratio of the mass of the atmosphere, through which, a beam radiation passes to the mass it would pass through if the sun were at the zenith (i.e. directly overhead). Thus, at sea level m = 1, when the sun is at the zenith and m =2 for a zenith angle $\theta_Z$ (further explained in the solar radiation and solar angles section) of 60°. For $\theta_Z$ from 0° to 70° at sea level, to a close approximation.
Air mass = 1 / (cos $\theta_Z$)
(Duffie & Beckman, 2013)

### 2.5.2 PCU or Inverter

PCU converts unregulated DC power, supplied by the solar PV array, to single phase AC or synchronous three-phase AC power. In case of a grid connected plant, this three-phase AC is made compatible with the power grid. Furthermore, PCU performs the following functions (Teodorescu et al., 2011):

- Operates maximum power point tracker, factoring the limits of converter (DC-DC), charge controller, and inverter (DC-AC). Maximum power trackers are devices that keep the impedance of the circuit of the cells at levels corresponding to the best operation, and convert the resulting power from the PV array so that its voltage is compatible with the load/grid (Duffie & Beckman, 2013)
- Filter the DC and the harmonic content on the AC side and make it compatible with the grid frequency and phase
- Control the grid disconnection relay (for grid-connected systems) and DC switch in case of a contingency/fault.

Since the operating voltage of the AC side is fixed, the amplitude of the current would be proportional to the generated DC power. The PCU, thereby, behaves like an electrical current source. The parameters of interest, openly available in datasheets, are as follows:

#### *2.5.2.1 AC Side*

- Maximum Continuous output power ($P_{PCU\ AC}$) in kVA or MVA: It is the maximum rated AC power that can be delivered by the PCU.
- Efficiency ($\eta_{PCU}$) in %: It is the ratio of the AC power output to the DC power input. Typically, peak and weighted average CEC[8] and/or European efficiency is listed. It is important to note the input voltage, over which, the stated peak efficiency is obtained. Since the utility interactive PCU always is loaded by the utility connection, if it is designed with the maximum power tracking, it will deliver maximum power to the grid over a wide range of PV input power, and will operate close to peak efficiency over most of the maximum power tracking range (Roger & Jerry, 2005). Since most datasheets do not provide this efficiency curve, hence, an approximate consideration would involve taking the *lowest quoted efficiency*.

#### *2.5.2.2 DC Side*

- Nominal DC power rating ($P_{nomDC}$) in kW: This is the nominal rated DC power of the inverter. If this parameter is not specified it can be derived by $P_{PCU\ AC}$ / $\eta_{PCU}$.

[8] The California Energy Commission (CEC), making use of other weighing coefficients, arrived at the CEC efficiency ($\eta_{CEC}$), which is typically suitable for locations with high annual irradiation levels. A criterion based on weighing factors, derived from annual irradiation distribution, has been established to determine the European efficiency ($\eta_{EURO}$). The European and the CEC efficiencies are defined by the following formulae (Antonio & Hegedus, 2003)

$$\eta_{EURO} = 0.03 * \eta_5 + 0.06 * \eta_{10} + 0.13 * \eta_{20} + 0.1 * \eta_{30} + 0.48 * \eta_{50} + 0.2 * \eta_{100}$$

$$\eta_{CEC} = 0.04 * \eta_{10} + 0.05 * \eta_{20} + 0.12 * \eta_{30} + 0.21 * \eta_{50} + 0.53 * \eta_{75} + 0.05 * \eta_{100}$$

The subscript in the above formulae correspond to the loading level on, in other words, the power output level of the PCU

- Maximum input voltage ($V_{DC\ max}$) in V: This is the maximum voltage from the PV array that can be tolerated by the PCU. Typically, this corresponds to the voltage built up in the PV array under open circuit condition, and it must be less than $V_{DC\ max}$.
- Operating DC voltage range in V: This corresponds the voltage range from the PV array that would sustain the operation of the PCU.
- Maximum Power Point Tracking (MPPT) range in V: This corresponds to the voltage range under which the MPPT unit would operate. ($V_{mppmin}$ to $V_{mppmax}$).
- Input start voltage ($V_{start}$) in V: This is the minimum voltage required to be built up by the PV system to trigger the PCU operation. Discussions with industry experts reveal that when explicitly not mentioned, $V_{start}$ can be considered as the mean of the MPPT range
- Nominal operating DC current ($I_{nomDC}$) in A: This generally corresponds to the current level at $V_{mppmin}$.
- Maximum input current ($I_{DC\ max}$) in A: This is the maximum current from the PV array that can be tolerated by the PCU. Typically, this corresponds to the current built up in the PV array under short circuit condition and must be less than $I_{DC\ max}$.

## 2.6 Electrical Operation of PV Module

Solar PV cell is typically represented by diode models. A brief description of these have been provided in Appendix – B. The detailed models (5 parameter, 4 parameter, and Bai et al., 2015 approximation) are appropriate methods for tracing the characteristic of the solar cell/module for any given operating condition. The more detailed the model, the better the accuracy of the parameters computed. But, these models require certain input, which generally, aren't specified in the module datasheets and/or these models are computationally intense and iterative.

From a pre-feasibility analysis standpoint, there is a need for a method which:

- Uses readily available information
- Is computationally less intense and preferably non-iterative.

Here, we consider the linear maximum power model, as described in Townsend, 1989. It is intended for calculating MPP output as a function of STC module data, cell temperature, and the effective radiation incident on the module. Albeit bit old and less versatile than the detailed models, it does not generate the entire I-V characteristic for an operating condition. But, it is still appreciably accurate and is used in programs which assess the performance of MPP systems (Klein & Beckman, 1983; Klein, Beckman, & Al., 1979; Menicucci & Fernandez, 1988; Whitaker et al., 1991). This is adopted by the system advisory model developed by the National Renewable Energy Laboratory for their simple efficiency solar PV model (Gilman, 2015). This is the basis for the power plant model in the work done by Klima et al., 2018. When comparing the output from the model with spatially and temporally coincident data of existing operational plants, it was found that the error margin was about $6 \pm 6$ %. In the model adopted in CSTEM PV, the module power output would be computed at an hourly resolution using the following relation:

$$P_{module\_output} = P_{mp} \times \left(G_T / G_{ref}\right) \times \left(1 + K_{T-Pmp} \times \left(T_{cell} - T_{cell-ref}\right)\right).$$

In order to consolidate the resource component and make the effective module power output as a function of the rated module power, the above expression can be re-written as:

$$P_{module\_output} = P_{mp} \times RP_{mod}$$

Here, $RP_{mod}$ is resource to module power factor.

The temperature dependence of module parameters such as short circuit current ($I_{sc\text{-}ref}$) and open circuit voltage ($V_{oc\text{-}ref}$) could be represented by their relationship with their temperature coefficients. Module short circuit current ($I_{sc}$) is assumed to be strictly proportional to irradiance. It increases slightly with cell temperature (this stems from a decrease in band gap and an improvement of minority carrier lifetimes).

$$I_{sc} = I_{sc-ref} \times \frac{G_T}{G_{ref}} \times \left(1 + K_{T-Isc} \times \left(T_{cell} - T_{cell-ref}\right)\right)$$

The open circuit voltage ($V_{oc}$) strongly depends on temperature (the main influence is that of the intrinsic concentration) decreasing linearly with it.

$$V_{oc} = V_{oc-ref} + K_{T-Voc} \times (T_{cell} - T_{cell-ref})$$

With the fundamentals of the electrical operation of a PV module explained, we move to the consideration for PV plant design (section 2.7) and sizing the PV system (section 2.8)

## 2.7 Consideration for PV Plant Design

The following are the important considerations in this model for designing the PV plant:

1. PV modules are of fixed-tilt configuration. It is also a general practice to consider the tilt of the module (and hence array) β, to be equal to the latitude of the location φ. Furthermore, the arrays are considered to face due south in case of the northern hemisphere, and due north in case of the southern hemisphere (Antonio and Hegedus, 2003; Markvart and Castaner, 2013). This makes the surface azimuth angle, γ = 0°
2. Based on discussions with industry experts, the maximum allowable height of the array structure is limited to 2m (~ 6.5 feet). This is to accommodate the ease of maintenance and the upkeep of the arrays. Additionally, a 0.5m (1.64 feet) ground clearance has been provided to protect the panels from the effects of soiling
3. The initial land area available was assumed to be an infinite plane with no undulations, and consists of a flat terrain profile
4. The auxiliary area requirement factors in the necessityfor additional land area for the placement of the inverter/PCU, office buildings, and extended pathways inside a plant. These have been considered based on consultations with sector experts. To account for this in the model, a curve fit equation was generated, to estimate the auxiliary land area requirement as a function the capacity of the plant (MWp)
5. A boundary spacing of 10m between the plant's inner periphery and the outer plant boundary was considered
6. An important consideration while performing the electrical sizing of the system entails:

a. The combined voltage of modules in series should not exceed the maximum tolerable Direct Current (DC) voltage of the inverter

b. The combined current of the module arrays in parallel should not exceed the maximum rated DC current of the inverter

These considerations are fundamental to deciding the system design point for the PCU (Antonio and Hegedus, 2003). In this model, we consider the midpoint voltage in the Maximum Power Point (MPP) range and the corresponding current to achieve the rated PCU power rating.

## 2.8 Sizing the Solar PV System

The core idea of design of the PV plant (grid/off-grid, utility/mini grid) is that the estimated capacity must *deliver power close to the rated capacity under the best solar conditions of the location*. Alternate design approaches that could be considered would deliver maximum power for the best economic value. This approach has not been considered for CSTEM PV.

The first step is to estimate the number of modules required for building a plant of target capacity in MWp DC ($P_{plant\text{-}target}$). A simple way to arrive at the number of modules required for $P_{plant\text{-}target}$ can be illustrated as follows:

$$No.\,of\ modules\ in\ Wp_{STC} = \frac{Target\ plant\ capacity}{Rated\ module\ power\ in\ STC} = \frac{P_{plant-target}}{P_{mod}}$$

The main drawback of this approach is that it cannot derive the combination of modules in series and parallel, per PCU.

An understanding of the electrical scale up, from PV cell to plant, is important in establishing a method that considers the above-mentioned approach.This can be illustrated as::

- A module is made up of PV cells that are connected in series to form cell strings, which determine its voltage rating (due to voltage addition). These cell strings are connected in parallel, which determine its current rating (due to current addition). The cell strings are also connected in parallel with bypass diodes to prevent reverse flow of current.
- Modules are also connected in series to form module strings, such that, the total $V_{oc}$ developed in the string is always below the $V_{DC\ max}$ of the PCU (Antonio & Hegedus, 2003; Markvart & Castaner, 2013; Roger & Jerry, 2005). The module strings are connected in parallel such that the total current developed in the modules will be below $I_{DC\ max}$ of the PCU. This combination of modules makes a PV array for one PCU.

Figure 9 illustrates the build-up of a solar PV system from a solar cell.

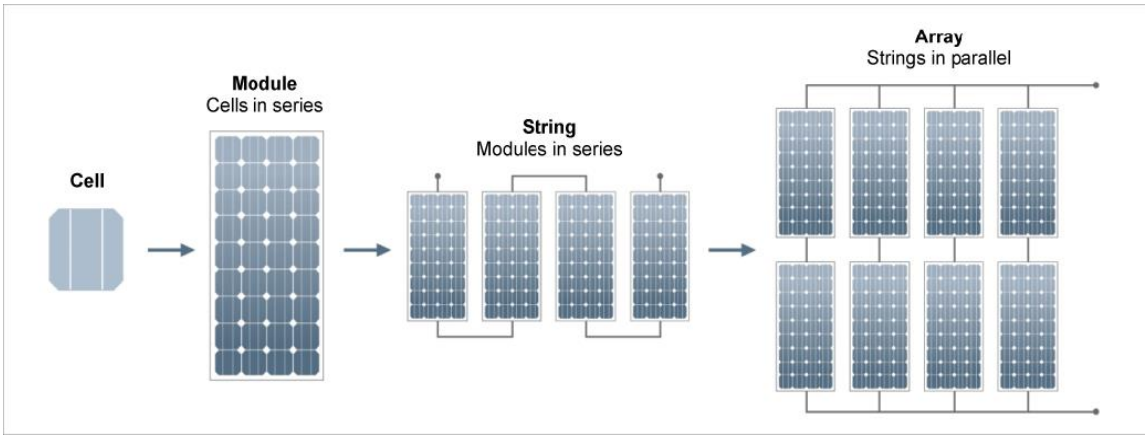


*Figure 9: Building up a solar PV configuration*

*Source: Your Home (Govt. Of Australia), n.d.*

With this as a premise, we designed the PV system. First, we estimated the number of PCUs ($N_{PCU}$) required for a given $P_{plant\text{-}target}$.

$$N_{PCU} = \left(\frac{P_{plant-target}}{P_{nomDC}}\right) = \left(\frac{P_{plant-target}}{(P_{PCU\ AC}\ /\eta_{PCU})}\right)$$

Since $N_{PCU}$ must be a whole number, the decimal portion of this result was neglected.

By virtue of specification of voltages in the PCU datasheets, they bear the following relation:

$V_{mppmin} < V_{start} < V_{mppmax} < V_{DC\ max}$.

The PCU design point is generically referred to as ($V_{PCU\text{-}Ref}$, $I_{PCU\text{-}Ref}$). We consider the midpoint of the Maximum Power Point Tracking (MPPT) range of the PCU as the design point (as indicated in point 6 of section 2.7). This reference point would provide an appreciable margin for variations across both limits of the MPPT range due to extreme temperature, etc. The corresponding voltage and rated current at this midpoint can be calculated as follows:

$$V_{PCU-Ref} = V_{mid} = \frac{V_{mppmin} + V_{mppmax}}{2}$$

$$I_{PCU-Ref} = I_{mid} = \frac{P_{nomDC}}{V_{mid}}$$

There is a provision for the user to specify an alternate PCU reference voltage, provided it lies within the MPP range of the PCU.

It is notable that during plant operation, the PCU operating voltage is free to fluctuate within the MPP range. The design point of the module involves the MPP condition at Standard Testing Condition (STC) ($V_{mp}$, $I_{mp}$). Hence, using this, the number of modules in series for voltage addition (forming 1 module string) can be calculated as:

$$m = \frac{V_{mid}}{V_{mp}}$$

The value of 'm' can be rounded up (as applied here) or rounded down to the nearest integer.

The DC power, seen by the PCU, is a product of voltage and current. The module strings account for matching the appropriate reference PCU voltage. The current matching is done by sizing the required number of module strings in parallel ('n') to meet the power rating of the PCU. Ideally, a single array of 'm x n' panels should meet the power requirements of the PCU. However, the

resultant array may not be feasible from a maintenance standpoint. Hence, the number of module strings in parallel is split into two components:

- 'n' module strings in parallel per array
- 'y' arrays in parallel per PCU.

The size of the array is limited by the height of the structure (as indicated in point 2 of Section 2.7). This consideration is agnostic to the dimensions of the module.

First, we estimated 'n', considering the array to be tilted at an angle of β with respect to the horizontal (ground surface) facing due south (γ = 0°, for sites in Northern hemisphere). The height of the array structure, not considering the ground clearance, can be generically represented as 'h'.

$$n = (h/(L_{mod} \times \sin\beta))$$

'n' is rounded down to the nearest integer to adhere to the array height restriction. Figure 10 illustrates the layout of a single PV array.

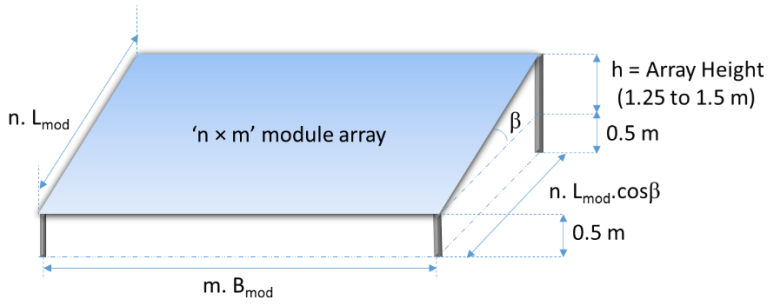


*Figure 10: PV array layout design*

In similar fashion, the number of arrays in parallel 'y' could be estimated as:

$$y = {I_{PCU-Ref}}/{(n \times I_{mp})}$$

'y' is rounded up to the nearest integer to limit the current addition at peak conditions (factoring losses), to be close to design point. In summary, the number of modules at various levels is indicated as follows:

No. of modules per string $= m$

No. of modules per array $= m \times n$

No. of modules per PCU $= N_{mod-PCU} = m \times n \times y$

No. of modules for the plant $= N_{plant} = m \times n \times y \times N_{PCU}$

Rated Capacity of the plant $(MW_p) = P_{plant} = N_{plant} \times P_{mod} / 1000000$

Pure module area of the plant $= N_{plant} \times L_{mod} \times B_{mod}$

To re-iterate the point made earlier in this section, *the core idea is to design a plant in such a manner that it generates approximately the target plant capacity, at the best local environmental conditions*. In this context, we must first identify the best operating conditions. This is can be determinedas follows:

$$P_{mod-max} = P_{mod} \times \max\ (RP_{mod})$$

The size of the PV modules supporting the PCU must be limited to the DC power rating of PCU ($P_{nomDC}$). When the DC power, generated by the PV array, exceeds $P_{nomDC}$, the PCU will 'clip' the power and limit its output to the rated value. The excess power is dumped as clipping losses. Generally, it is recommended that the system not be operated frequently in clipping mode. The exact criterion for clipping mode operation has not been specified in the datasheet. Additionally, it is unfavourable to design a system, which marginally underperforms. Hence, to optimize the utilisation of the system, the design must be refined appropriately. This should be in a way that ensures that *under the best solar resource conditions seen by the location of interest, the DC power seen by the PCU factoring the DC losses (soiling losses) is close to the PCU rating.* Depending on the solar resource availability, the PV array must be sized up or down, slightly, to meet this criterion. To do this we must estimate the maximum DC power seen by the PCU.

$$Max\ DC\ PCU\ power = P_{mod-max} \times (No.of\ modules\ per\ PCU) \times (Soiling\ Loss\ Factor) / 1000$$

$$P_{PCU-DC-Max} = P_{mod-max} \times N_{mod-PCU} \times (1 - soiling\ loss\ \%) / 1000$$

The addition/removal of PV modules in done is steps of 'm' modules, such that, the voltage level of the PCU is unaffected by the scaling of the modules. Next, an iterative process was followed to arrive at the most suitable combination modules for the PCU, considering the best solar conditions of the location of interest. The number of module strips of m, each added or removed, has been noted as Δm. Δm is positive if module strips are added and negative if module strips are removed.

If the original estimate of $P_{PCU\text{-}DC\text{-}Max}$ is greater than $P_{nomDC}$, then the number of modules per PCU ($N_{mod\text{-}PCU}$) is reduced by m modules at each iteration, and the $P_{PCU\text{-}DC\text{-}Max}$ is revised and compared until the comparison condition becomes false.

Alternatively, if the original estimate of $P_{PCU\text{-}DC\text{-}Max}$ is lesser than or equal to $P_{nomDC}$, then $N_{mod\text{-}PCU}$ is increased by m modules at each iteration, and the $P_{PCU\text{-}DC\text{-}Max}$ is revised compared until the comparison condition becomes false.

Post the iterative calculations, the revised number of modules in the plant ($N_{plant}$), the plant capacity ($P_{plant}$), and the pure module area of the plant was estimated. It must be noted that $P_{plant}$ represents the DC rating of the plant in MWp. The effective AC rating of the plant in MVA has been represented as follows:

$$Rated\ Capacity\ of\ Plant\ (MVA) = P_{plant-PCU} = N_{PCU} \times P_{PCU\ AC} / 1000000$$

Here, $P_{PCU\ AC}$ is the AC rating of PCU in kVA

Another metric of interest is the DC to AC ratio or the DC scaling factor. It typically represents the scale of DC side system for every unit AC system.

$$DC\ to\ AC\ ratio\ or\ DC\ scaling\ factor = N_{mod-PCU} \times P_{mod} / (P_{PCU\ AC} \times 1000)$$

The changes in plant area must be calibrated as per the adjustments in the plant's electrical configuration. To do this, we calculated the new 'y' from an electrical standpoint, post the estimation of the revised plant capacity:

$$y\ (new) = N_{mod-PCU} / (n \times m)$$

Here, 'y' represents the electrical sizing factor and can be a decimal number.

From an area estimation standpoint, a change of 'n' m strings results in a change in 'y' by one. If strings are to be added to a system, even a single-string addition would require an area of an entire array structure. Moreoever, if the strings are being reduced from the system, it would take 'n' m strings to reduce the array structure area requirement by one (reduce 'y' by 1). From this, we can infer that 'y' for area calculation ($y_{area}$) has be to be a whole number, and incorporate the nature of module string addition/reduction:

$$y_{area} = roundup\ (y)$$

After estimating the electrical sizing factors, we move towards estimating the physical area covered by the plant.

## 2.9 Plant Area Estimation

### 2.9.1 Inspiration

Nature has inspired some of the best engineering designs. One such case is inspired by the phyllo-taxis disc pattern, which is the configuration of florets on the head of a sunflower (Vogel, 1979). This concept was used to provide a theoretical design for the heliostat field arrangement in concentrated solar power plants (Noone, Torrilhon, & Mitsos, 2011). Our model draws inspiration from the prime spiral, also known as the Ulam spiral (Stein et al., 1964).

The Ulam spiral is a simple method of visualising prime numbers that reveal the apparent tendency of certain quadratic polynomials of generating an unusually large number of primes. Ulam began to number intersections, starting near the centre with 1, and moving out in a counter clockwise spiral. He began circling all the prime numbers. The prime numbers tend to crowd into diagonal lines as illustrated in Figure 11.

Near the centre of the spiral, the lining up of primes is to be expected because of great "density" of primes, and the fact that all primes, except 2, are odd (Gardener, 1971). The pattern presented by the Ulam's spiral has been used in applications ranging from identifying patterns in distribution of nucleotides in DNA (Cattani, 2011), to data record extractions for web technology applications (Anderson & Hong, 2013), and 'object and pattern' identification using raster models (Kitano, Katsuhiko, Kakimoto, Urakawa, & Araki, 2015). The model considered in CSTEM PV does not focus on the pattern of prime numbers. Instead, it focuses on the placement of numbers, which builds this rectangular/square spiral. This pattern is used to map the physical placement of PV arrays and PCU blocks towards building the plant.

A detailed record of this approach has been presented by Sridhar & N. C., 2019. This work compares the area estimates from the proposed methods to those of currently operational plants. It estimates the revised solar potential for India, considering the Land Use Land Cover details, as reported by ISRO, NRSC, RSAA, LRUMG, & LUCMD, 2014. Some brief details of the approach have been covered in this report.

| | | | | | | | | | |
|---|---|---|---|---|---|---|---|---|---|
| 100 | 99 | 98 | 97 | 96 | 95 | 94 | 93 | 92 | 91 |
| 65 | 64 | 63 | 62 | 61 | 60 | 59 | 58 | 57 | 90 |
| 66 | 37 | 36 | 35 | 34 | 33 | 32 | 31 | 56 | 89 |
| 67 | 38 | 17 | 16 | 15 | 14 | 13 | 30 | 55 | 88 |
| 68 | 39 | 18 | 5 | 4 | 3 | 12 | 29 | 54 | 87 |
| 69 | 40 | 19 | 6 | 1 | 2 | 11 | 28 | 53 | 86 |
| 70 | 41 | 20 | 7 | 8 | 9 | 10 | 27 | 52 | 85 |
| 71 | 42 | 21 | 22 | 23 | 24 | 25 | 26 | 51 | 84 |
| 72 | 43 | 44 | 45 | 46 | 47 | 48 | 49 | 50 | 83 |
| 73 | 74 | 75 | 76 | 77 | 78 | 79 | 80 | 81 | 82 |

*Figure 11: Ulam or the Prime Spiral*

*Source: Gardener, 1971*

### 2.9.2 Brief Summary on Area Estimation

We start by defining the time window operation. It is typically the hours during which the solar plant operates, such that, the shadows of the surrounding structures, like neighbouring PV arrays, do not affect the power output of any module. Here, we consider four-time windows of operation: sunrise to sunset[9], one hour post sunrise and one hour before sunset, two hours post sunrise and two hours before sunset, and three hours post sunrise and three hours before sunset. It is notable that these windows are of decreasing duration. This is because in the early hours of sunrise, the sun's rays are too oblique and cast longer shadows. This, in turn, would require a greater distance between array structures to ensure shadow-free panels, which lead to a higher land area requirement. The idea is to consider the decreasing length of shadows, subtended by the tilted panels for the hours beyond sunrise, for spacing between modules' structures thus, reducing the land requirements. This makes us choose the optimum time window, where the trade-off between the energy gains and additional land area needed, is suitable. The plant area is estimated in two steps. First, we estimate the inter-row and inter-column spacing for different time windows.

The length of shadow subtended by the tilted panel is computed for every hour along the E–W ($L_{col}$) and N–S ($L_{row}$) directions:

$$L_{row} = n \times L_{mod} \times \sin\beta \times \cos\gamma_s / \tan\alpha_s$$

$$L_{col} = n \times L_{mod} \times \sin\beta \times \sin\gamma_s / \tan\alpha_s$$

The maximum of $L_{row}$ and $L_{col}$ are identified as $D_{row}$ and $D_{col}$ respectively. A collection of these elements is represented as inter-row ($D_r$) and inter-column ($D_c$) spacing sets.

$$D_{row} = \text{Max}\,(L_{row}), \quad \text{here } D_{row} \in D_r$$

$$D_{col} = \text{Max}\,(L_{col}), \quad \text{here } D_{col} \in D_c$$

Next ,we determine the area of the PCU block. We consider '$y_{area}$' arrays of dimensions ($n \times L_{mod} \times \cos\beta$) $\times$ ($m \times B_{mod}$) each, arrange them in spiral patterns, and determine the appropriate spacing coefficients. Using these, the dimensions ($L_{PCU} \times B_{PCU}$) and the area of a PCU block is determined. We arrange '$N_{PCU}$' PCU blocks of the estimated dimensions and arrange

[9] To be specific we consider the earliest sunrise hour and latest sunset hour as seen the year.

them in them in the spiral pattern using the same algorithm, deriving the *'Effective plant area'*. Using this, the area contribution due to boundary spacing condition is applied to derive the *'Total plant area'*. Finally, the requirement for the auxiliary area is considered and the *'Gross plant area'* is derived. All these estimates are done for each time window.

Our next task involved identifying a suitable time window for operation. While it is tempting to make the decision criterion for this to be based on energy generation, our discussion with industry experts revealed that an area-based rationale could be of merit too (hence applied in CSTEM PV). The idea is to identify the time window which provides the closest gross plant area estimate to that of the reference/benchmark area required. We chose a benchmark of 5 acres/MWp as indicated by CERC, 2016b. Curious readers can check Sridhar & N. C., 2019 for the detailed explanation.

Two metrics of interest can be used to assess the effectiveness of the estimated plant area - Packing Density (PD), and Deviation Factor (DF).

### 2.9.3 Packing Density

PD is defined as the ratio of the active module area (pure module area of the plant) to the gross plant area for the chosen time window. This factor indicates the active land area utilised for power generation.

$$Packing\ Density\ (PD) = \frac{Pure\ module\ area\ of\ the\ plant}{Gross\ plant\ area}$$

### 2.9.4 Deviation Factor

To assess the extent of deviation in the estimated area with respect to the benchmark area, we estimate the DF. It is positive if the estimated area is greater than the benchmark area and negative if it is lesser.

$$Deviation\ Factor\ (DF) = \frac{Gross\ plant\ area\ (Acres) - P_{plant}\ \times Benchmark\ area}{P_{plant}\ \times Benchmark\ area}$$

We estimated the power output from the plant for the designed configuration and the chosen time window.

## 2.10 Estimation of PV Plant Output

The plant's output is estimated in three steps. First, the plant's hourly power output, is determined, keeping in mind all losses and disregarding module degradation (Section 2.10.1). Next, we determine the effect of module degradation on the power output over the plant's life term (Section 2.10.2). Finally, we determine the relevant plant performance metrics (Section 2.10.3).

### 2.10.1 Base Output Estimation

The losses are categorised into two components. The first one accounts for soiling losses caused due to deposition of dust and other particles. The second one accounts for the electrical losses,

on both the AC and DC sides. This includes loss in conductors and transformers. Additionally, the efficiency of the PCU ($\eta_{PCU}$) is factored too. The details of these losses have been considered as user inputs, in percentage. Using these, the loss factors were derived and used to estimate the hourly resource-to-plant power factor ($RP_{plant}$). Finally, the final plant output was derived for a given time window and hour. The relevant relations are indicated below:

$$Soiling\ Loss\ Factor = (\ 1 - Soiling\ loss\ \%)$$

$$Electrical\ Loss\ Factor = (1 - Electrical\ loss\ \%)$$

$$RP_{plant}(hour) = (Soiling\ Loss\ Factor) \times (Electrical\ Loss\ Factor) \times \eta_{PCU} \times RP_{mod}(hour) \times N_{plant}$$

$$P_{plant-AC}\ (hour) = P_{mod} \times RP_{plant}\ (hour)$$

$$Annual\ PV\ Generation = Q_{year} = \sum_{hour=0}^{8759} P_{plant-AC}\ (hour)$$

### 2.10.2 Plant Output Factoring Module Degradation

PV modules degrade over time. The module datasheets typically provide details about the ratings of the module at the end of year one, ten, and 25 (sometimes more). A linearized module degradation rate over the modules' lifetime can be derived using this criteria. The typical degradation details include: 97% of the module rating at the end of year one, 90% at the end of year ten, and 80% at the end of year 25. Accounting for the degradation, the net module rating per annum could be estimated. The hourly output of the module and the plant can be computed, using this. Figure 12 illustrates a typical linearized degradation curve.

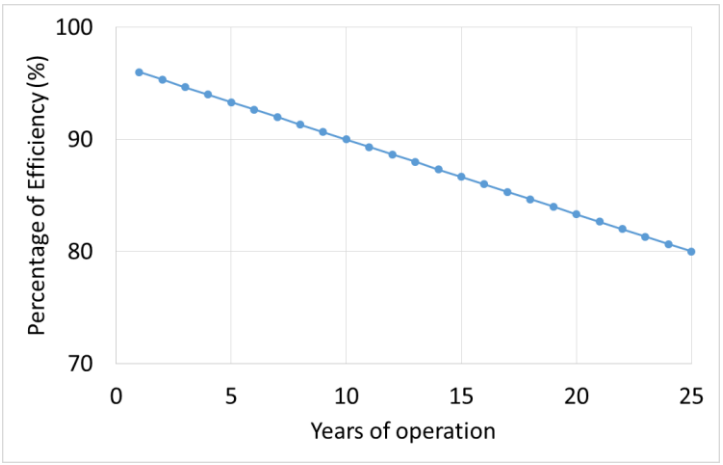


*Figure 12: Module degradation illustrated as dro-p in percentage of efficiency vs. years of operation*

The following equations can be used to illustrate the aspect of module degradation:

$$Net\ Module\ rating\ (year) = Net\ P_{mod}(year) = P_{mod} \times (Degraded\ rating\ (year))$$

$$P_{plant-AC}\ (hour, year) = Net\ P_{mod}(year)\ \times RP_{plant}\ (hour, year)$$

$$Q_{PV,year} = \sum_{hour=0}^{8759} P_{plant-AC}\ (hour, year)$$

### 2.10.3 Plant Performance Metrics

The three annual performance metrics of interest are Capacity Utilisation Factor (CUF), Performance Ratio (PR), and Solar to Electric Efficiency (SEE).

#### *2.10.3.1 Capacity Utilisation Factor*

CUF is the ratio of the actual output from a plant, over a year, to the maximum possible output from the plant for a year under ideal conditions. CUF does not directly consider environmental factors such as patterns of irradiance, which varies yearly.

$$CUF_{year}(\%) = \frac{Q_{PV,year}\ \times 100}{8760\ \times P_{plant}}$$

#### *2.10.3.2 Performance Ratio*

*PR*[10] is stated as a percentage and describes the relationship between the real and theoretical possible energy output of a solar PV plant. It shows the proportion of energy that is actually available for export to the grid after reducing the energy loss components (e.g., thermal losses, soiling, etc.) and energy consumption for operation. It can be computed by using a simplified version of the formula specified in (Chrosis Sustainable Solutions, 2012).

$$Annual\ solar\ radiation = Annual\ G_T\ (year) = \sum_{hour=\ 0}^{8759} G_T\ (hour)$$

$$PR_{year}\ (\%) = \left(\frac{Q_{PV,year}\ \times 100}{(Annual\ G_T\ (year)) \times \left(N_{plant}\right) \times (Net\ P_{mod}\ (year)/1000)}\right)$$

#### *2.10.3.3 Solar to Electric Efficiency*

*SEE or* $\eta_{SE}$ is the ratio of the actual output from a plant, over a year, to the actual incident solar radiation on the solar panels. It is a metric with a broader context and observes the efficiency of the entire process in terms of the ratio of sheer useful output energy to input energy:

$$SEE_{year}\ (\%) = \frac{Q_{PV,year}\ \times\ 100}{Annual\ G_t(year) \times\ Pure\ module\ area\ of\ the\ plant}.$$

[10] $PR = \frac{Energy\ fed\ to\ the\ grid}{Energy\ converted\ by\ solar\ plant}$

This concludes the description of the technical model. The next chapter summarises the details and considerations for the financial model.

# 3. Financial Model

The financial model has been built based onthe norms and considerations specified by CERC, 2016a. CERC stopped publishing the benchmark levelised tariff in 2017, and has since, moved towards project-specific tariff determinations for solar PV plants (CERC, 2017). However, the procedure considered in the 2016 regulations is still valid and widely accepted by stakeholders. Hence, this procedure was used as a base to build CSTEM's financial model. This model has been applied, and insights have been derived to understand the effect of the module's reliability to a PV plant's techno-economics (Sridhar & N. C., 2018). These insights have been accepted by various stakeholders and academic institutions. CSTEM's model has been generalised to accommodate the latest cost and financial metric-related inputs.

## 3.1 Methodology of Financial Model

Figure 13 illustrates the methodology of financial models, along with the core inputs and outputs. Section 3.2 and 3.3 briefly summarise the assumptions and considerations, providing context to important financial metrics computed.

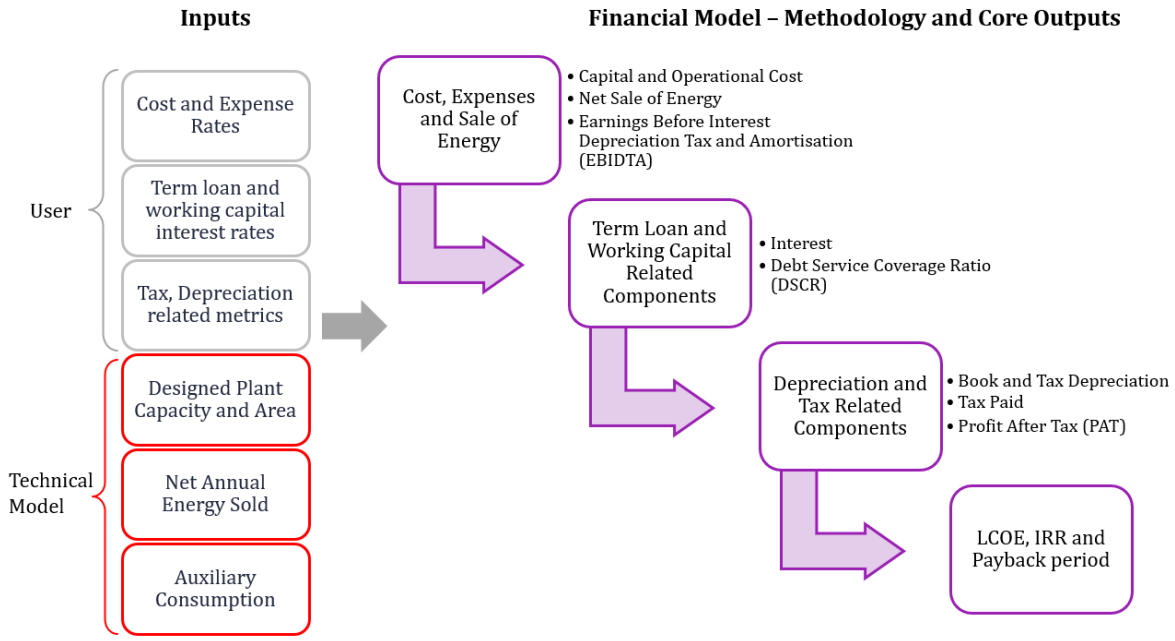


*Figure 13: Methodology of the financial model*

## 3.2 Assumptions and Consideration

### 3.2.1 Cost and Expenses

Capital cost and expense components can be divided into three categories: machinery, infrastructure, and other expenses. Table 3 illustrates the components covered in each category and provides appropriate remarks, as per CERC considerations.

*Table 3: Capital cost and expense components*

| Category | Component | Remark |
|---|---|---|
| Machinery | PV module | Price in ₹ / Wp. It is inclusive of custom clearing charges, transportation, and unloading |
| | PCU | Typically considered in ₹ Lakhs / MWp. This includes all taxes, duties, and major overhaul cost in 12th – 14th year of operation |
| | Batteries (if applicable) | Typically considered in ₹ / kWh. Overhaul costs not factored and are added additionally based on the discounted price, as per the year of replacement |
| Infrastructure | Land | Typically considered in ₹ Lakhs / Acre. The generic rate and area requirement considered by CERC is ₹ 5 Lakh/Acre and 5 Acres/MWp respectively. The land deployed for these projects is barren in nature. |
| | Mounting Structure | Considered in ₹ Lakhs / MWp |
| | Power Evacuation Infrastructure | Considered in ₹ Lakhs / MWp. Includes cost of DC cabling between Solar PV panels & PCUs including junction boxes, AC cabling, between PCU & substation, LT/HT panels, earthing arrangements, step-up outdoor type transformer, breaker, current transformers, potential transformers, auxiliary transformers, control cables, isolators, lightning arrestors, protection relays, time of day (ToD) meters/ tariff meters, peripheral lighting telemetry system for real time monitoring, etc. |
| | Tracking Systems (if applicable) | Considered in ₹ Lakhs / MWp |
| Other Expenses | Civil and General Works | Considered in ₹ Lakhs / MWp. This includes site preparation as such as levelling and mounting, and building control rooms to house PCU and systemic components. This also includes building approach roads, fencing or boundary walls, cable trenching, arranging water supply, lighting, etc. General works include security of solar farm, setting up of power backup generators; yard lighting, earthing kits, etc. |
| | Preliminary and Pre-operative Expenses | Considered in ₹ Lakhs / MWp. This includes transportation of equipment, storage of equipment at site, insurance, contingency, taxes, duties, Interest During Construction (IDC), financing costs, and other project management costs. |
| | Miscellaneous Expenses | Considered in ₹ Lakhs / MWp. This includes any other expenses not covered in the above categories. |

The operational and maintenance cost is considered in ₹ Lakhs / MWp for the base year. It accounts for all expenses, governing the day to expenses, such as salaries, bills, and spares. It is appropriately accounted for throughout the lifetime by considering an annual escalation rate.

### 3.2.2 Other Metrics Considered

The aspects considered include:

- Term loan-related components include debt-to-equity ratio, moratorium period, interest rate, and payment period. The working capital-related component is also factored in, with the appropriate interest rate.
- The return on equity component for both loan and post loan components
- Tax components, including minimum alternate tax and income tax-related components.
- The book depreciation of assets during the term loan period has been considered as an input. Post term loan, the book depreciation rate is internally computed, such that, at the end of plant life, the asset is depreciated to 90% of its value. Tax depreciation-related components are accounted implicitly.
- Tariff rate for purchase and sales of power (for grid-connected mini grids only)

Additionally, provisions for bulk capital subsidy, bid analysis (for utility scale plants), and feed in tariff (for mini grid plants) have also been provided.

## 3.3 Financial Metrics Computed

### 3.3.1 Net Sale of Energy

This is the revenue earned by the sale of 'net energy' (in Million Units, MU), which will be consumed by the intended customer. The intended customer depends on the type of system. For a utility scale PV plant, it is fed to the transmission grid and is then transacted to different utilities via contracts. In case of grid/off grid mini grids, the customers/establishments are physically connected to it. Also, for grid connected mini grid, the transmission or distribution grid is also a customer for selling the excess energy as well as the source for buying power during deficit energy.

For utility scale systems:

$$Net\ Saleable\ Energy_{year}\ (in\ MU) = Q_{Net\ Energy,year} = Q_{PV,year} - Q_{Aux,year}$$

For grid connected mini grid systems:

$$Net\ Saleable\ Energy_{year}\ (in\ MU) = Q_{Net\ Energy,year} = Q_{met\ load,year} + Q_{from\ grid,year} = Q_{load}$$

For off grid connected mini grid systems:

$$Net\ Saleable\ Energy_{year}\ (in\ MU) = Q_{Net\ Energy,year} = Q_{met\ load,year} = (Q_{load,year} - Q_{unmet\ load,year}) = (Q_{PV,year} - Q_{not\ utilised,year} - Q_{Aux,year})$$

For utility scale and off grid connected mini grid systems:

$$Net\ sale\ of\ Energy_{year}\ (₹\ Lakhs) = Q_{Net\ Energy,year} \times Tariff$$

For grid connected mini grid systems:

$$Net\ sale\ of\ Energy_{year}\ (₹\ Lakhs) = (Q_{met\ load,year} + Q_{to\ grid,year}) \times Tariff - Q_{from\ grid,year} \times Tariff_{buy}$$

### 3.3.2 Expenses, EBIDTA and Tax

The expenses primarily comprise of the annual operational and maintenance costs and 'Buy of energy' from the grid (for the grid connected mini grid cases). The Earnings Before Interest Depreciation Tax and Amortisation (EBIDTA) has been computed. It is an important metric as it indicates the net annual revenue available after expenses. The tax component consists of two parts: 1) Minimum Alternate Tax (MAT) and Income Tax (IT). The MAT component is accounted for with a five-year credit rollover. The IT component was computed by factoring in an implicit tax depreciation component, which aligns with financial experts' suggestions.

### 3.3.3 Net Present Value

Net Present Value (NPV) is the difference between the present value of cash inflows and outflows. It is used in capital budgeting to analyse the profitability of a projected investment or project (Investopedia, n.d.). Generally, an investment with a positive NPV will likely be profitable. Whereas, one with a negative NPV may possibly result in a net loss. The NPV of expenses and taxes were calculated in accordance with the following formula:

$$NPV\ of\ expenses\ and\ tax = \sum_{year=1}^{Plant\ life} \frac{Expenses_{year} + Tax_{year}}{(1+r)^{year}}$$

Here, 'r' refers to the discount rate used to determine the present value

Also, for the grid connected mini grid case, the expenses component also includes the 'Buy of energy' component from the grid.

### 3.3.4 Levelised Cost of Energy (LCOE)

*LCOE* refers to the cost, which when assigned to every unit of energy produced (or saved) by the system over the analysis period, will equal the Total Life Cycle Cost, when discounted back to the base year. This can be computed by the following formula (Short, Packey, & Holt, 1995)[11]:

$$LCOE = \frac{Expected\ Lifetime\ Costs\ of\ the\ System}{Expected\ Lifetime\ energy\ Output\ of\ the\ System}$$

[11] Cambell, 2008 and Ueckerdt, Hirth, Luderer, & Edenhofer, 2013 provide some very interesting insights with respect to understanding LCOE.

$$LCOE = \frac{Total\ discounted\ Life\ Cycle\ Cost}{\sum_{year=1}^{plant\ year} Q_{Net\ Energy,year}/(1+r)^{year}}$$

Here, Total discounted life cycle cost = capital cost + NPV (Expenses + tax)

### 3.3.5 Internal Rate of Return (IRR)

Ramaswamy et al., 2012 consider IRR as the rate at which the difference between the NPV of net income and capital cost is zero. According to their formulation, 'net income is the income obtained from the tariff minus the expenses for each year'. Since, the approach considered in CSTEM PV is post tax, we tweaked this net income to accommodate the tax component and defined it as 'net cash flows.' The net income defined here reflects EBIDTA. Hence, the revised formulation is as follows:

$$Net\ Cash\ Flows_{year} = EBIDTA_{year} - Tax_{year}$$

$$Capital\ Costs - \sum_{year=1}^{plant\ life} \frac{Net\ Cash\ Flows_{year}}{(1+r)^{year}} = 0$$

When solving the above relation for 'r', it would compute IRR.

### 3.3.6 Profit After Tax (PAT) and Debt Service Coverage Ratio

*PAT* reflects the profit at hand component, while *DSCR* is a measure of the cash flow available to pay current debt obligations. A DSCR greater than 1 means the entity – whether a person, company or government – has sufficient income to pay the current debt obligations., Whereas, a DSCR less than 1 means it does not have the capacity to do so (Investopedia, n.d.).

### 3.3.7 Payback Period

There are many interpretations for payback period. In this model, we consider the payback period to be the year when the sum of net cash flows equals or exceeds the project cost. Here the project cost is defined as the sum of capital cost and average margin money for the working capital.

This concludes the details related to the formulation of the financial model. The next chapter focuses on presenting a case example that illustrates the application of the technical and financial model.

# 4. Illustration via Simulated Case

In this chapter, we present an example case based on the technical and financial models presented, so far. We will illustrate the design of a *utility scale fixed panel solar PV plant*. This design can be optimised for the best solar conditions for a given location. The economic analysis would involve the following assessments:

- Basic viability: determination of LCOE and IRR
- Impact of bulk capital subsidy
- Viability of plant for a target bid

The core philosophy of the design approach can be summarised as follows:

- First, we assess the impacts caused by the choice of the location. This involves estimating the net effective solar hours available for generation and its spread across the year, factoring aspects related to solar geometry
- Next, we assess the availability of solar resource (solar radiation, ambient temperature, and wind speed) at the location of interest and its variations across the year.
- Based on the choice of technology and design criterion specified by the user, the solar PV plant is designed to ensure that it delivers the maximum rated DC power at the best solar conditions for the location.
- Based on this we estimate the plant area and chose a time window of operation, which provides a reasonable land area requirement.
- The last step in the technical model would be to determine the *hourly plant output* and study its variations across the year.
- We also estimated the performance capabilities, capital cost, operational costs, revenue from sales, and profit post tax for the designed plant
- The basic financial viability of the plant includes assessing its capacity to service debts and determine the minimum tariff required to recover all costs and expenses
- Finally, we assess the impact of the capital subsidy and the viability of target bid

Several considerations for the technical and financial models are in line with Sridhar & N. C., 2018. For the sake of completeness, they have been listed here appropriately.

## 4.1 Case Considerations and Inputs

### 4.1.1 Technical Model Inputs

We begin with the choice of location - for this analysis, we consider one with co-ordinates, 12.85 °N, 76.95°E (presented in map in Figure 14). The broader data related to the case has been indicated in Table 4.

*Table 4: Summary of case parameters*

| | |
|---|---|
| **Location** | 12.85 °N, 76.95°E |
| **Target Plant Capacity** | 10 MWp |
| **Duration of Useful Plant Life** | 25 years |
| **Tilt angle of the array and Orientation** | 12.85°, Due South (surface azimuth angle, γ = 0) |
| **PV Module (Technology / Model/ Rating) *** | Multi-crystalline / Tata Power Solar, TP300 Series / 288 Wp |

| | |
|---|---|
| **PCU (Model / Rating) *** | Eaton Power Xpert / 250 kW |
| **Array height / Ground clearance** | 1.3 m / 0.5 m |

** Detailed listing of parameters for PV module and PCU has been provided in Appendix – C.*


*Figure 14: Location of interest*

*Source: Google Maps*

Other considerations include:

- Module type and mount: *glass/cell/glass* type with an *open rack mount*.
- Albedo factor of the ground (ρ) ~ 0.14
- Auxiliary energy consumption of the plant is assumed to be 1% of the plant generation, with no module degradation
- Soiling and electrical losses are assumed to be 5% and 8% respectively
- Boundary spacing along the length and breadth is about 10 m
- Benchmark area considered for optimisation and determination of time window is 5 acres / MWp (as per CERC norms)
- The midpoint of the maximum power point voltage range of the PCU and the maximum power point voltage of the module has been chosen as the reference design point for power rating

### 4.1.2 Financial Model Input

The financial metrics include consideration of components related to:

- Capital expenditure
- Operation and maintenance
- Subsidy and target bid
- Loan-related metrics
- Return on equity and depreciation
- Taxes

A detailed listing of the financial metrics considered for this case has been presented in Appendix – C. Some specific assumptions of the financial model are listed below:

- The working capital considerations are in accordance with CERC norms, and is based on one month of operation and maintenance expenses (15% of which is allotted for spares) and two months of receivables, and 25% of the total working capital has been considered as Margin Money for Working Capital (MMWC)
- The Minimum Alternate Tax has been considered, with a five-year rollover
- We took into account book depreciation of assets to ensure that about 90% of the asset is depreciated by the end of plant life
- The tax depreciation of assets has been considered as follows:
    - Land at 0% (land value is not depreciated and hence not considered)
    - Buildings at 15% - this includes all aspects covered under civil and general costs
    - Plant and machinery at 50% - this includes all aspects covered under module, PCU, and mounting structure costs
    - Other assets at 25% - primarily consisting of power evacuation infrastructure costs.

## 4.2 Technical Outputs

### 4.2.1 Sunrise, Sunset and Day length

We determines the length of the day and solar hours for the location of interest. Figure 15 presents the sunrise and sunset time, as seen at the location, based on solar geometry analysis. The duration of solar hours for a day is the difference between the sunrise and sunset times for that day, as indicated in Figure 16. Furthermore, Figure 17 indicates the aggregate solar hours available in each month. Table 5 gives a quick summary of these parameters, along with the annual aggregate solar hours.

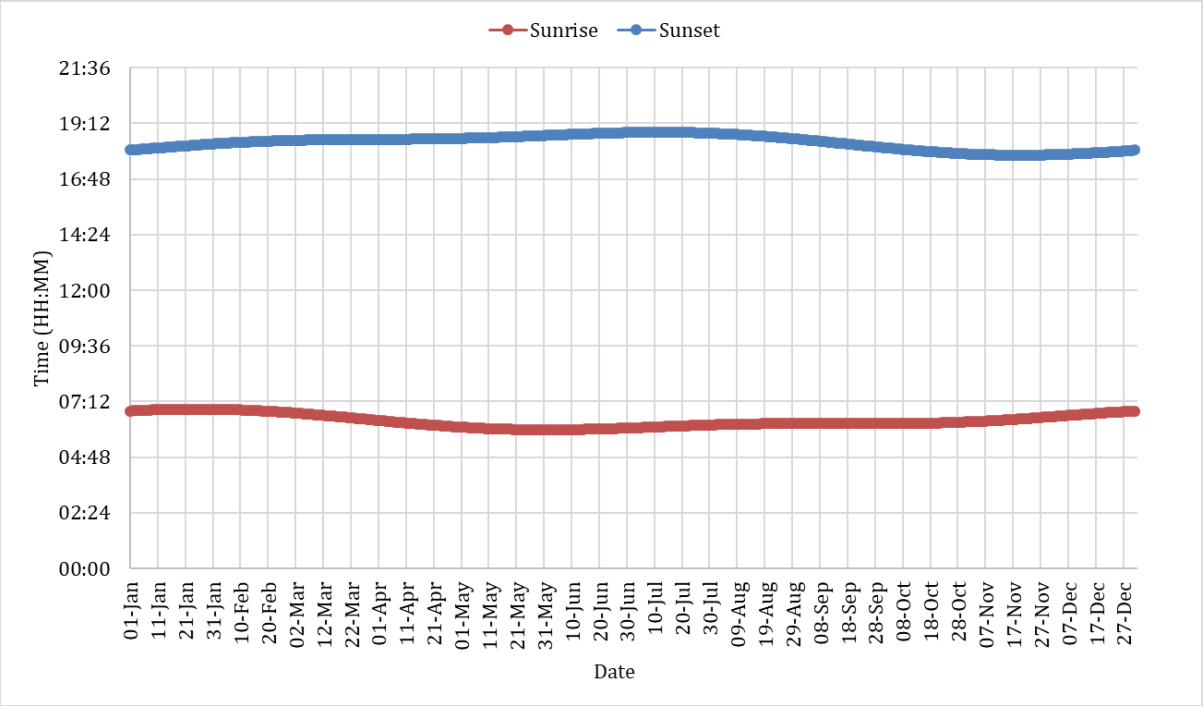


*Figure 15: Variation of sunrise and sunset time for 12.85 °N, 76.95°E*

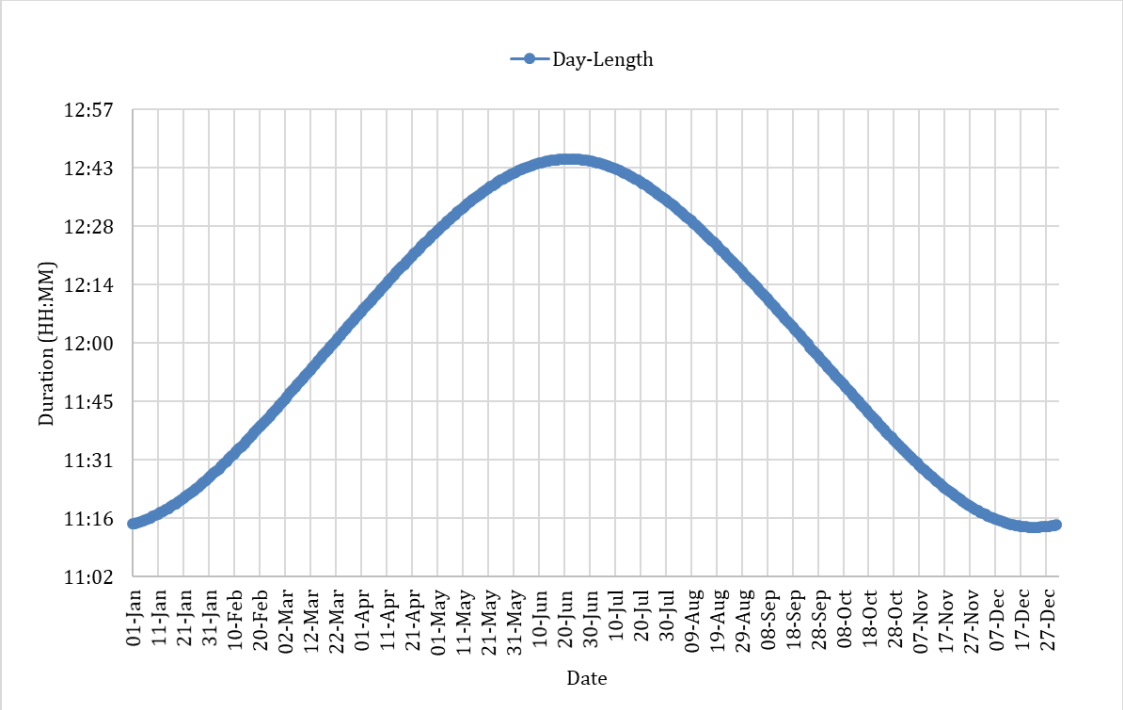


*Figure 16: Duration of the day for 12.85 °N, 76.95°E*

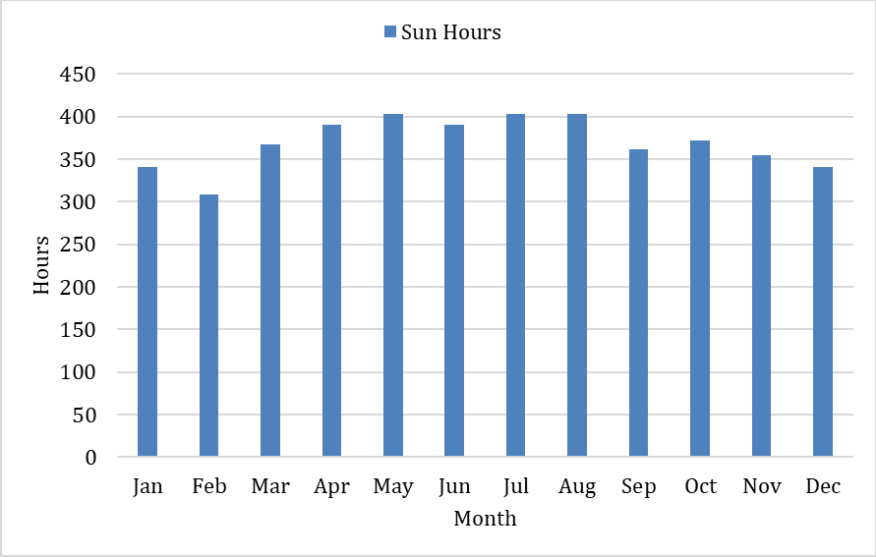


*Figure 17: Monthly variation of aggregate solar hours for 12.85 °N, 76.95°E*

*Table 5: Summary of sunrise, sunset and day-length for 12.85 °N, 76.95°E*

| | |
|---|---|
| **Earliest Sunrise (Date / Time)** | June 1, 05:58 |
| **Longest Day (Date / Duration)** | Jun 22, 12:45 |
| **Latest Sunset (Date / Time)** | July 12, 18:49 |
| **Earliest Sunset (Date / Time)** | Nov 20, 17:49 |
| **Shortest Day (Date / Duration)** | Dec 22, 11:14 |

| | |
|---|---|
| **Latest Sunrise (Date / Duration)** | Jan 25, 06: 52 |
| **Annual Solar Hours** | 4435 |

The details presented under this section clearly illustrate the seasonal variations in lengths of the day due to variations in sunrise and sunset times. It also verifies common knowledge that days are indeed shorter during winter and longer during summer.

### 4.2.2 Solar Resource Assessment

We assessed the hourly solar resource available at the location. Solar resource comprises of three components of radiation - DNI, DHI, and GHI; ambient temperature, and wind speeds. We derived monthly patterns for the variations of the available solar resource. Figure 18 presents the monthly aggregate spread of solar radiation. Figure 19 and Figure 20 illustrate the range of monthly ambient temperature and wind speed available at the site. These conditions reflect the weather conditions incident at the place throughout the year. Finally, to provide a broader view of the available solar resource, a summary of the available solar radiation and other resources have presented in Table 6 and Table 7 respectively.

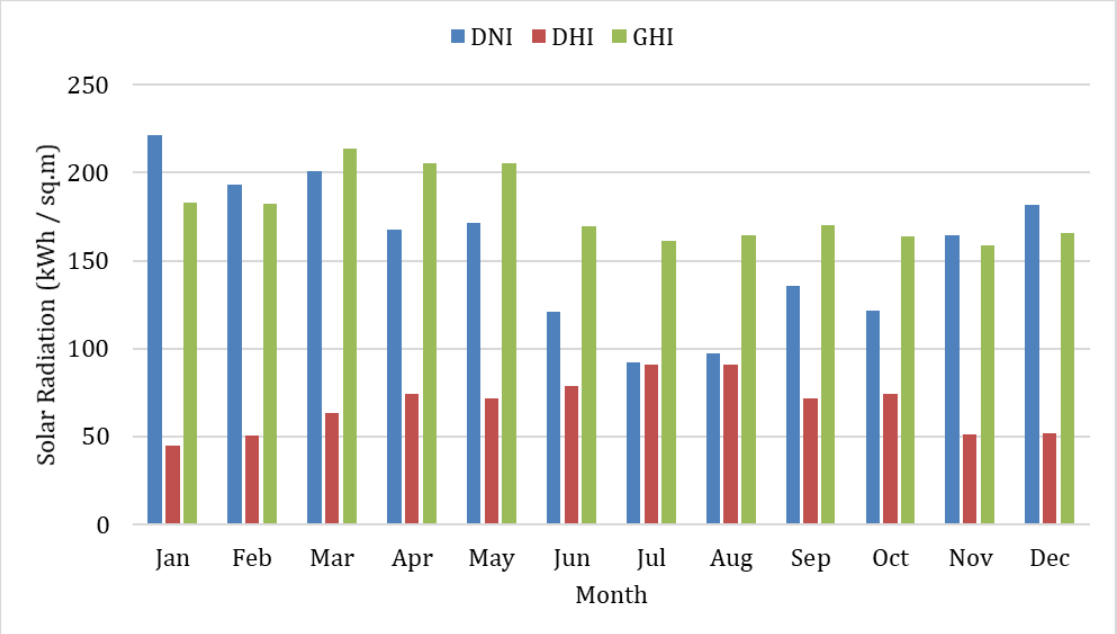


*Figure 18: Monthly aggregate solar radiation*

*Table 6: Summary of available solar radiation*

| **Component** | **Per Day Average (kWh / m²)** | **Annual Aggregate (MWh / m²)** |
|---|---|---|
| DNI | 5.12 | 1.87 |
| DHI | 2.23 | 0.81 |
| GHI | 5.87 | 2.14 |

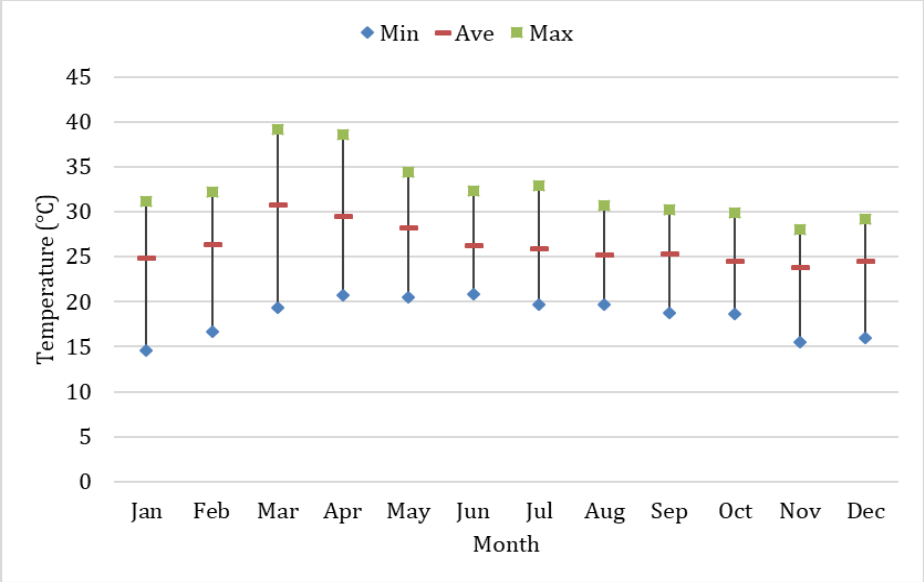


*Figure 19: Monthly range of ambient temperature during solar hours*

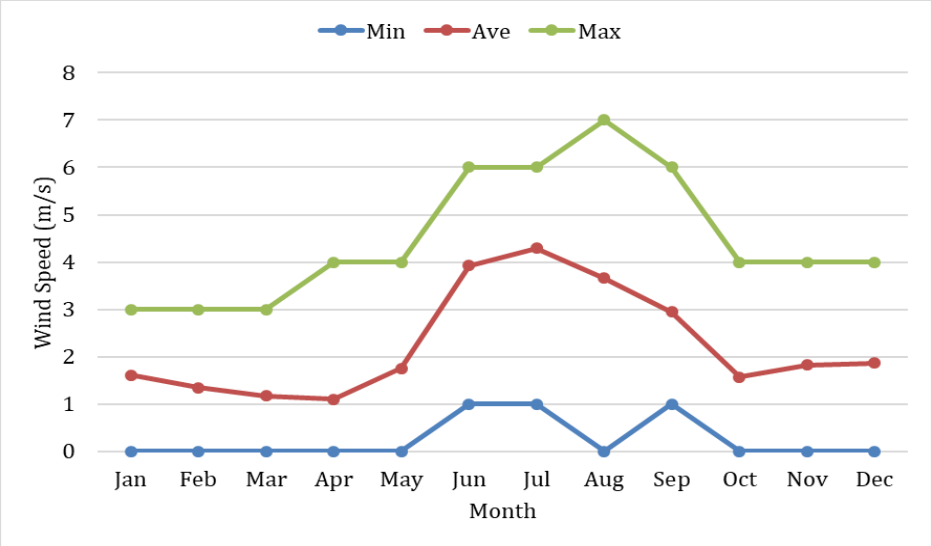


*Figure 20: Monthly range of wind speed during solar hours*

*Table 7: Summary of ambient temperature and wind speeds during solar hours*

| **Parameter** | **Minimum** | **Mean** | **Maximum** |
|---|---|---|---|
| Ambient Temperature (°C) | 14.63 | 26.36 | 39.19 |
| Wind Speed (m/s) | 0 | 2.30 | 7.00 |

Using these, we estimated the net incident radiation and cell temperature w.r.t to the module. Figure 21 and Figure 22 illustrate the monthly aggregate incident radiation and the monthly range of cell temperature, as seen in the module. These are the crucial parameters which determine the PV module's output. An interesting aspect to note, is that the cell temperature built up is significantly high compared to the ambient temperature. This is due to the effect of radiation and wind speeds.

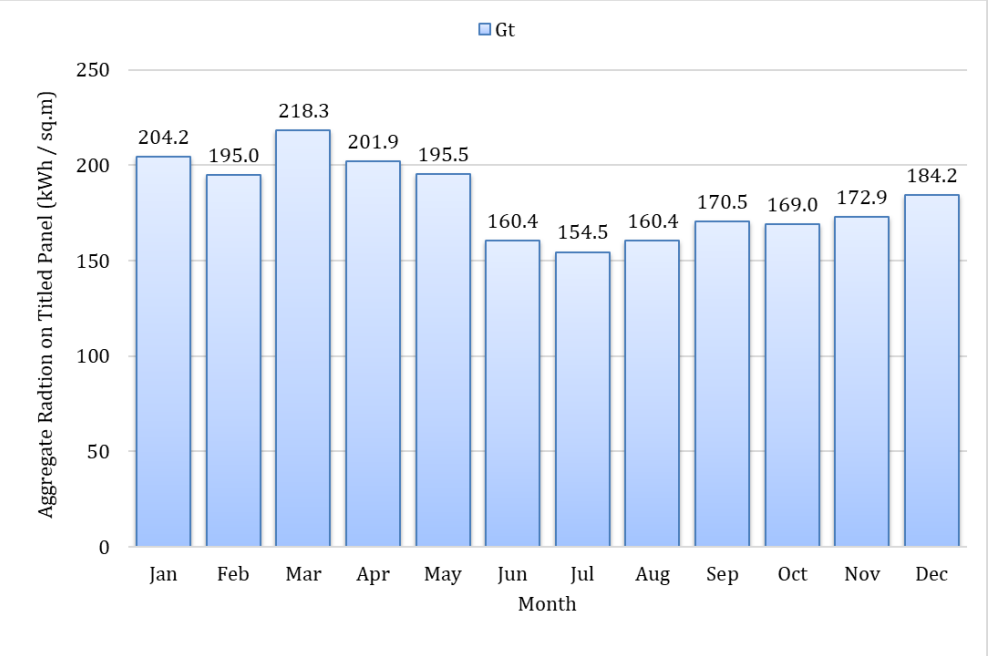


*Figure 21: Monthly aggregate radiation on tilted panel*

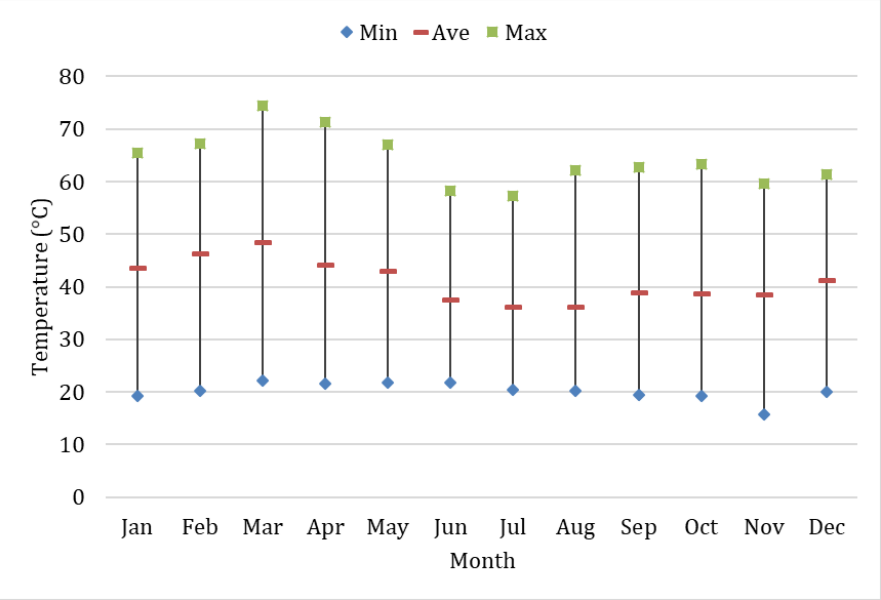


*Figure 22: Monthly range of cell temperature*

Using this, we estimate the hourly resource to power factor ($RP_{mod}$). We estimate the maximum $RP_{mod}$ ($RP_{mod\text{-}max}$) to be 0.895. This will used be in the next section to size the plant for the best solar conditions.

### 4.2.3 Determining Plant Size

Based on the user inputs, and considering the specifications of the module and PCU, we sized the PV plant. This has been summarised in Table 8. After deriving the initial plant size based on PCU limitations, we reworked it to derive an optimal plant size. This has been obtained by adding or removing module strings such that:

- The electrical limitations of the PCU are respected
- Under the best solar conditions ($RP_{mod\text{-}max}$), the pre-loss raw DC power generated by the PCU is close to its rated power

The decimal part in the revised 'y' represents a partially filled array. In this case, one array is partially filled with only 1 string instead of 5, as in others. Additionally, the Plant AC Capacity was based purely on the AC rating of the PCU and $N_{PCU}$.

*Table 8: Summary of the plant sizing parameters*

| **Parameter** | **Value** |
|---|---|
| Target plant capacity ($P_{plant\text{-}target}$) | 10 MWp |
| Number of PCUs for the Plant ($N_{PCU}$) | 40 |
| Number of modules in series per string for voltage addition (m) | 12 |
| Number of module strings in parallel per array for current addition (n) | 5 |
| Number of arrays in parallel for current addition per PCU (y) | 16 |
| Total number of modules per PCU | 960 |
| Total number of modules in the plant | 38,400 |
| Original Plant DC capacity | 11.0592 MWp |
| Number of module strings added (+) or removed (-) per PCU (m_change) | 6 |
| Revised 'y' | 17.2 |
| Revised total number of modules per PCU | 1032 |
| Revised total number of modules in the plant ($N_{Plant}$) | 41,280 |
| Revised Plant DC capacity ($P_{plant}$) | 11.88864 MWp |
| DC to AC ratio | 1.188864 |
| Plant AC Capacity ($P_{plant\text{-}PCU}$) | 10 MVA |

### 4.2.4 Estimating Plant Area and Optimal Generation Window

Based on the electrical sizing of the PV plant estimated in the above section, we determined the area of the plant and some related metrics. This can be done by incorporating the following steps:

- Define the time windows of interest/ generation windows
- Estimate the inter-row and inter-column spacing, and hence, plant area for each time window
- Determine plant area-related metrics and optimal time window

#### *4.2.4.1 Defining generation windows*

Based on Table 5's details, we defined the annual solar window for this location to range from the earliest sunrise to latest sunset (for this case: 5:58 to 18:49). Next, we defined the first-generation window. The basis for this was arrived by considering suggestions from academic experts. It was decided that:

- First-generation window would range from the earliest and latest day hours, for which, the solar altitude angle (αs) was greater than 1° (for this case: 6:30 to 18:30)
- Second-generation window would range from 1 hour, post the reference sunrise and 1 hour before reference sunset of the first-generation window (for this case: 7:30 to 17:30)
- Similarly, the third and fourth generation windows would be derived from the second and third generation windows, respectively. (for this case: 8:30 to 16:30 and 9:30 to 15:30).

It must be pointed that, as we moved to narrower generation windows, we would be reducing the effective generation hours appropriately. Figure 23 visually illustrates the various generation windows, in contrast to the variations in sunrise and sunset time.

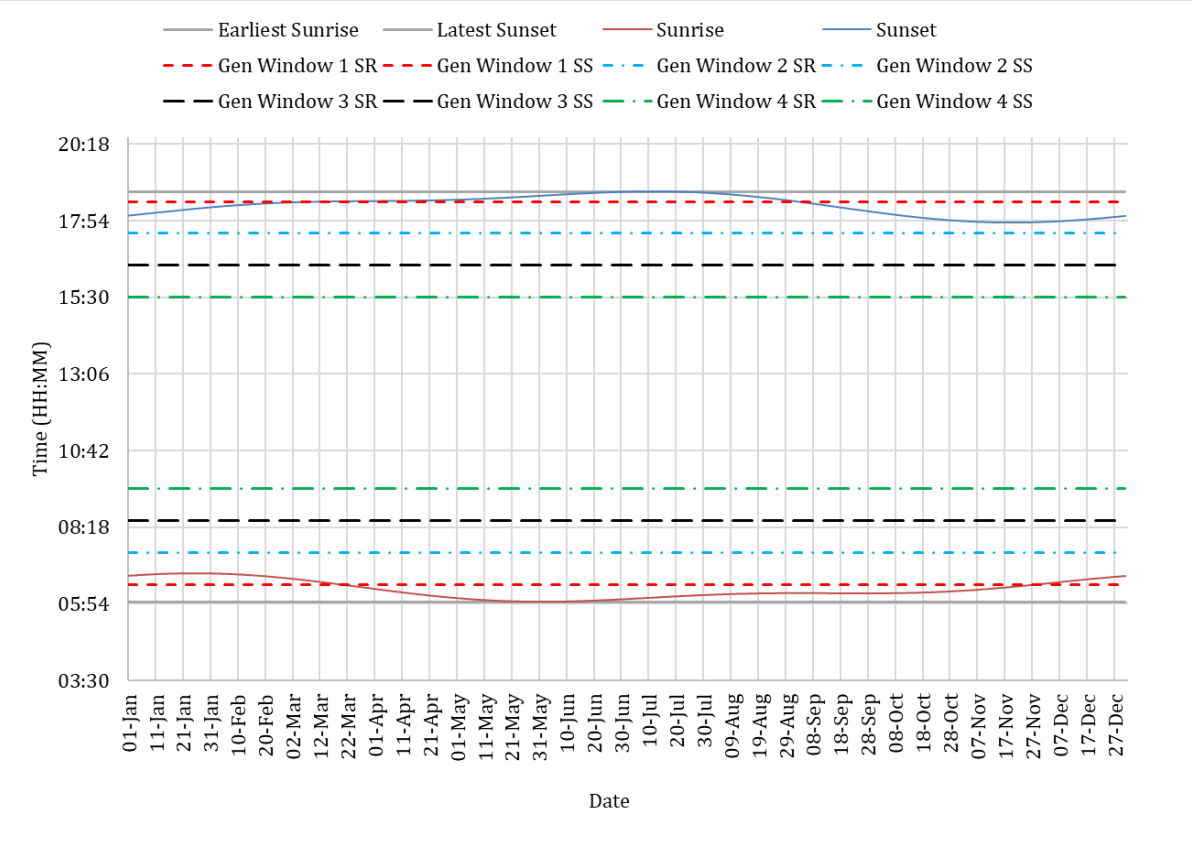


*Figure 23: Illustration of different generation windows*

### *4.2.4.2 Estimating the spacing and plant area*

Based on the steps presented in section 2.9.2, we determined the Drow and Dcol spacing, and the plant area estimates for each window. An illustration of Drow, Dcol ,and plant area, along with their respective reduction factor matrix[12] is shown in Figure 24, Figure 25, and Figure 26.

[12] It illustrates a set of factors, which compare the values for a reference window (a) to that of the following windows (b). Hence, the reduction factor would be a/b. The reduction factor for this analysis is expected to be greater than, or equal to, 1.

A)

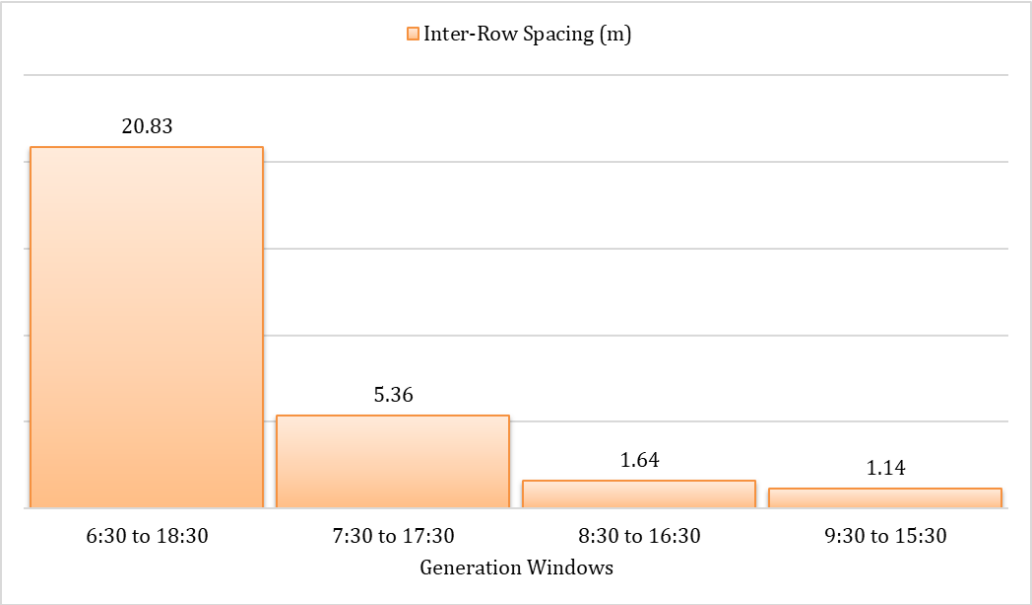


B)

| Reduction Factor Matrix (a/b) : Drow | | | | | |
|---|---|---|---|---|---|
| b | 6:30 to 18:30 | 1 | | | |
| | 7:30 to 17:30 | 3.89 | 1 | | |
| | 8:30 to 16:30 | 12.73 | 3.27 | 1 | |
| | 9:30 to 15:30 | 18.26 | 4.70 | 1.43 | 1 |
| Time windows | | 6:30 to 18:30 | 7:30 to 17:30 | 8:30 to 16:30 | 9:30 to 15:30 |
| | | a | | | |

*Figure 24: Variation of inter-row spacing (A) along with reduction factor matrix (B)*

A)

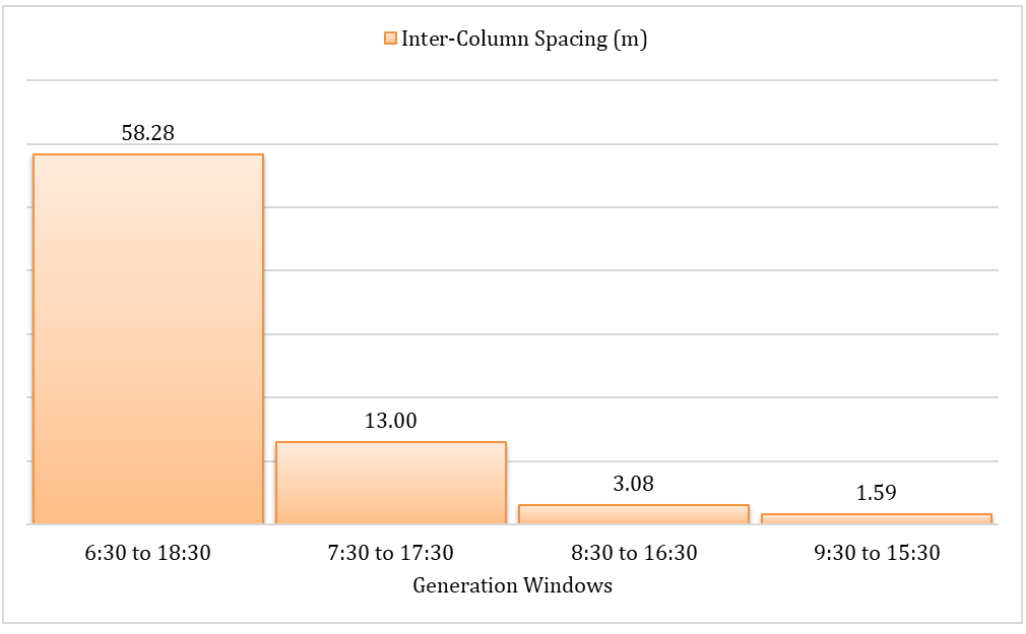


B)

| Reduction Factor Matrix (a/b) : Dcol | | | | | |
|---|---|---|---|---|---|
| b | 6:30 to 18:30 | 1 | | | |
| | 7:30 to 17:30 | 4.48 | 1 | | |
| | 8:30 to 16:30 | 18.95 | 4.23 | 1 | |
| | 9:30 to 15:30 | 36.72 | 8.19 | 1.94 | 1 |
| Time windows | | 6:30 to 18:30 | 7:30 to 17:30 | 8:30 to 16:30 | 9:30 to 15:30 |
| | | a | | | |

*Figure 25: Variation of inter-column spacing (A) along with reduction factor matrix (B)*

A)

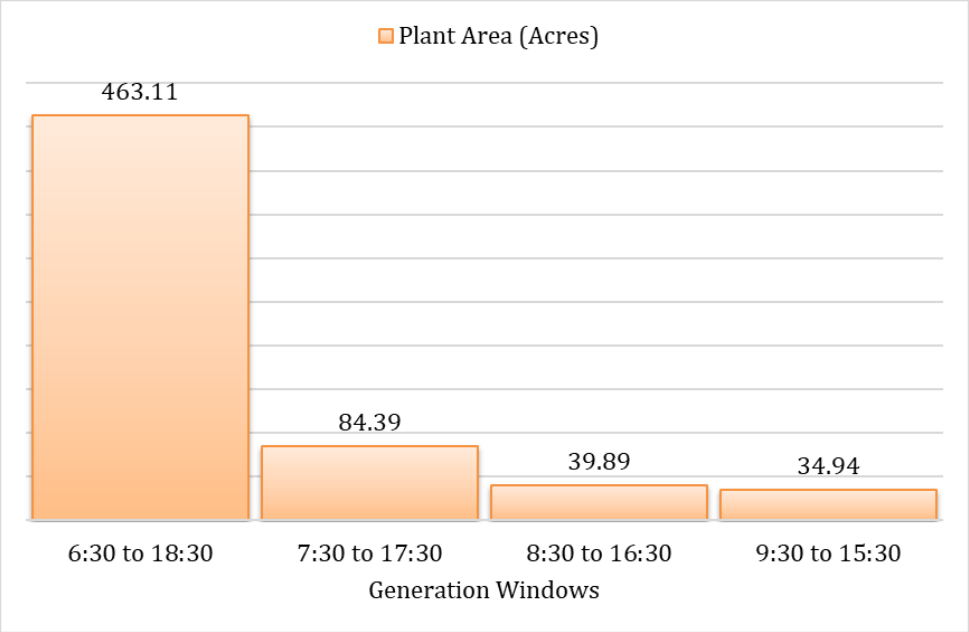


B)

| Reduction Factor Matrix (a/b) : Plant Area | | | | | |
|---|---|---|---|---|---|
| b | 6:30 to 18:30 | 1 | | | |
| | 7:30 to 17:30 | 5.49 | 1 | | |
| | 8:30 to 16:30 | 11.61 | 2.12 | 1 | |
| | 9:30 to 15:30 | 13.25 | 2.42 | 1.14 | 1 |
| Time Windows | | 6:30 to 18:30 | 7:30 to 17:30 | 8:30 to 16:30 | 9:30 to 15:30 |
| | | a | | | |

*Figure 26: Variation of plant area (A) along with reduction factor matrix (B)*

The figures above indicate that for narrower generation windows, the area requirements reduce significantly; while, for extreme windows the area requirement reduces by a factor of over 13.

#### *4.2.4.3 Determining optimal generation window and other metrics*

A narrower window also indicates reduction in effective generation hours, shadow free radiation on the panels, and hence, the effective generation from the PV plant[13]. The variation of these parameters, along their corresponding reduction factor matrix, has indicated in *Figure 27*, *Figure 28*, and *Figure 29*.

A)

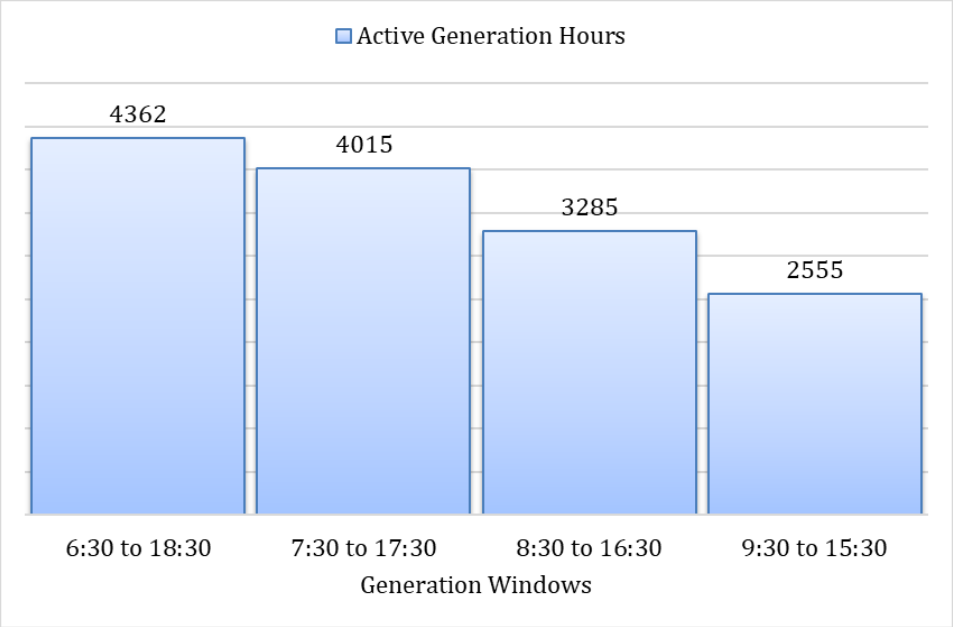


B)

| Reduction Factor Matrix (a/b) : Active Generation Hours | | | | | |
|---|---|---|---|---|---|
| b | 6:30 to 18:30 | 1 | | | |
| | 7:30 to 17:30 | 1.09 | 1 | | |
| | 8:30 to 16:30 | 1.33 | 1.22 | 1 | |
| | 9:30 to 15:30 | 1.71 | 1.57 | 1.29 | 1 |
| Time Windows | | 6:30 to 18:30 | 7:30 to 17:30 | 8:30 to 16:30 | 9:30 to 15:30 |
| | | a | | | |

*Figure 27: Variation of active generation hours (A), along with reduction factor matrix (B)*

A)

[13] Considering no module degradation

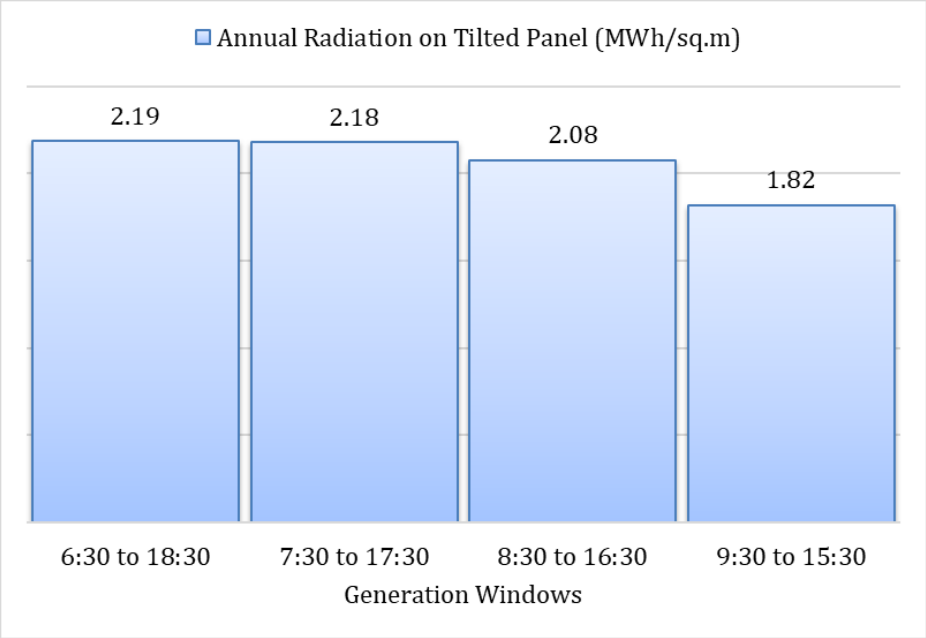


B)

| Reduction Factor Matrix (a/b) : Annual Radiation on Tilted Panel | | | | | |
|---|---|---|---|---|---|
| b | 6:30 to 18:30 | 1 | | | |
| | 7:30 to 17:30 | 1.00 | 1 | | |
| | 8:30 to 16:30 | 1.05 | 1.05 | 1 | |
| | 9:30 to 15:30 | 1.20 | 1.20 | 1.14 | 1 |
| Time Windows | | 6:30 to 18:30 | 7:30 to 17:30 | 8:30 to 16:30 | 9:30 to 15:30 |
| | | a | | | |

*Figure 28: Variation of annual radiation on titled panel (A), along with reduction factor matrix (B)*

A)

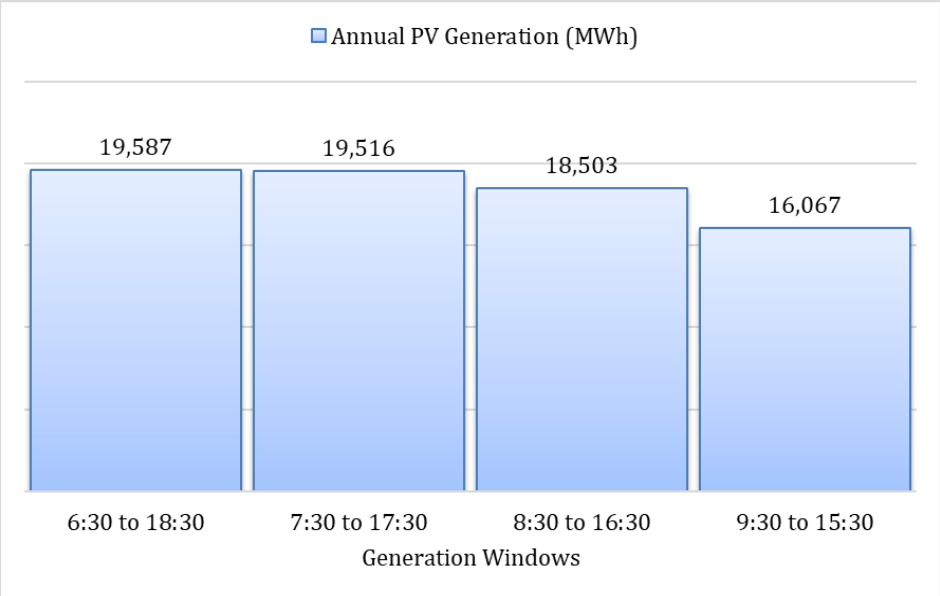


B)

| Reduction Factor Matrix (a/b) : Annual PV Generation | | | | | |
|---|---|---|---|---|---|
| b | 6:30 to 18:30 | 1 | | | |
| | 7:30 to 17:30 | 1.00 | 1 | | |
| | 8:30 to 16:30 | 1.06 | 1.05 | 1 | |
| | 9:30 to 15:30 | 1.22 | 1.21 | 1.15 | 1 |
| Time Windows | | 6:30 to 18:30 | 7:30 to 17:30 | 8:30 to 16:30 | 9:30 to 15:30 |
| | | a | | | |

*Figure 29: Variation of annual PV generation (A), along with reduction factor matrix (B)*

It can be seen that for the extreme windows, the reduction factor for generation hours and hence, the radiation and generation are significantly high. Putting this in context, w.r.t choice of optimal generation window, there are opposing ideas of interest:

- Minimise area requirement
- Maximise energy generation

A basis for this choice must ensure that there is minimum compromise on the above interests. In CSTEM PV we use the CERC norm of 5 acres/MWp as a benchmark to derive a 'Deviation factor' (DF) of the area (indicated in section 2.9.4) across different time windows. The optimal generation window is one whose DF is closest to zero. For this case, it works out to be *8:30 to 16:30* window. Along with deviation factor, other metrics such as Annual energy yield per unit area, PD, CUF, PR, and SEE have been computed, and have been summarised in *Table 9*. Optimal generation/time window is marked in red.

*Table 9: Summary of metrics related to generation windows*

| Generation Window | Annual Energy / Area (in MWh/Acre) | Deviation Factor (DF) | Packing Density (PD) | Capacity Utilisation Factor (CUF) | Performance Ratio (PR) | Solar to Electric Efficiency (SEE) |
|---|---|---|---|---|---|---|
| 6:30 to 18:30 | 42.29 | 6.79 | 0.04 | 18.81% | 75.34% | 11.19% |
| 7:30 to 17:30 | 231.26 | 0.42 | 0.23 | 18.74% | 75.31% | 11.18% |
| 8:30 to 16:30* | 463.84 | -0.33 | 0.50 | 17.77% | 74.94% | 11.13% |
| 9:30 to 15:30 | 459.81 | -0.41 | 0.57 | 15.43% | 74.27% | 11.03% |

**Optimal time window*

Next, we take a deeper look at the energy generated by the PV plant.

### 4.2.5 Estimating Components of Energy Generation

#### 4.2.5.1 Annual Energy Flow

First, we present a flow of energy from the sun that is effectively converted to AC generation[14] from the plant. *Figure 30* details the quantum of energy and *Figure 31* presents the energy generations as a percentage of the energy from the sun. Only 11.13% of the energy from the sun is converted to final useful AC energy. This is in line with SEE, estimated in *Table 9*. Post conversion to DC energy, the losses in the system are caused primarily due to soiling and electrical losses in the conductors and equipment. For our case, it works out to be 1,103 MWh and 2,447 MWh, which works out to be about 0.66% and 1.47% of the total solar energy incident on the panels, respectively.

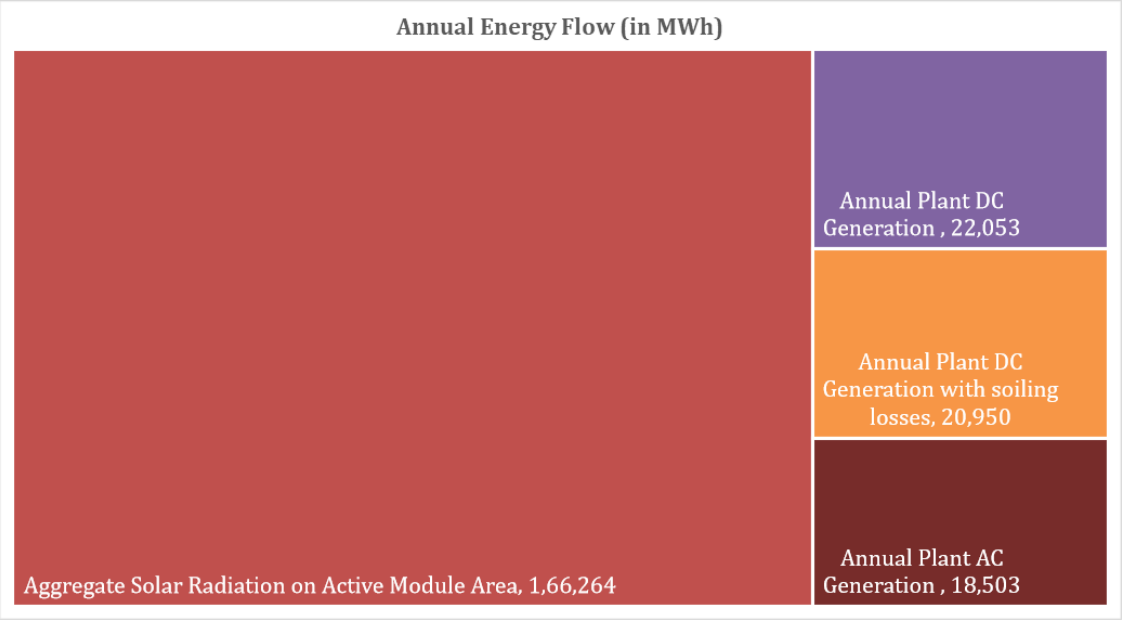


*Figure 30: Annual energy flow*

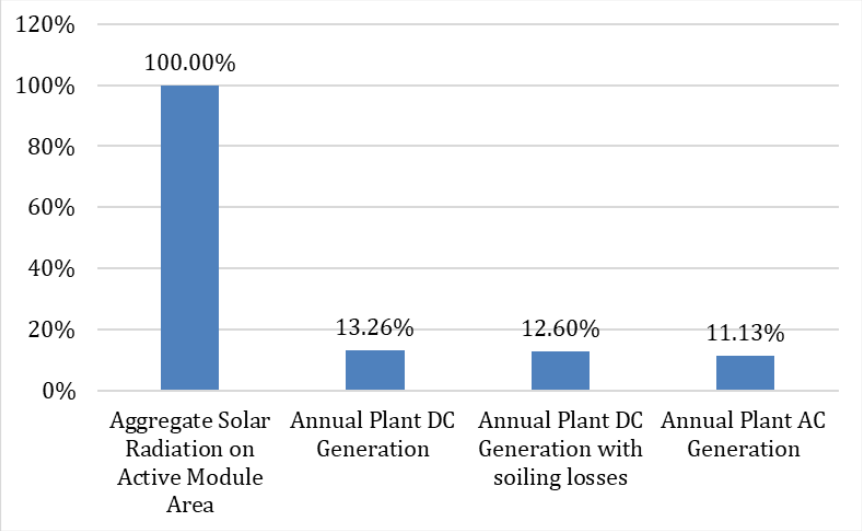


*Figure 31: Energy generation as a percentage of incident solar energy*

[14] Considering no module degradation

#### *4.2.5.2 Monthly and daily aggregate generation*

We explored the monthly variation in aggregate energy generation, and their percentage share in the annual generation (indicated in *Figure 32*). This helps provide an idea of the variation of solar energy across seasons. We also presented day-to-day variations of aggregate power generation in *Figure 33*. This illustrates the intra-seasonal variations in generation for this location. Furthermore, even the hourly generation profile has been estimated. Although it is not presented here, it will be presented in the web tool.

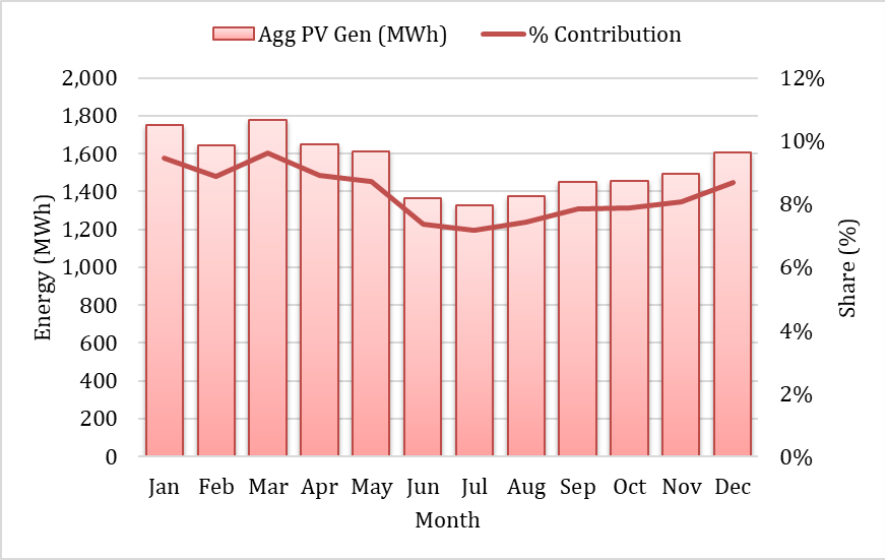


*Figure 32: Variation in monthly energy generation*

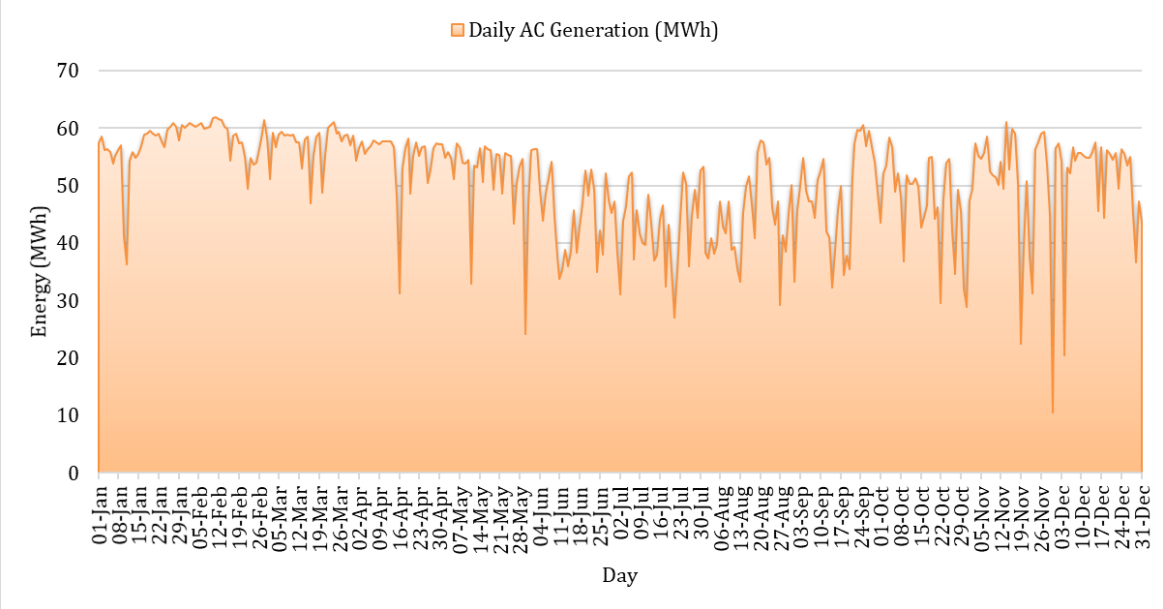


*Figure 33: Variation of daily aggregate energy generation*

The above detailed output help us obtain a generic understanding of the nature and spread of energy generation. Next, we move towards deriving some unique perspectives, which would be of interest to select sector experts.

#### 4.2.5.3 Select insights on plant generation

First, we present a histogram, which illustrates the hours of generation across different generation deciles (*Figure 34*). This would help system planners formulate contingencies in design, and help in assessing regulatory risks.

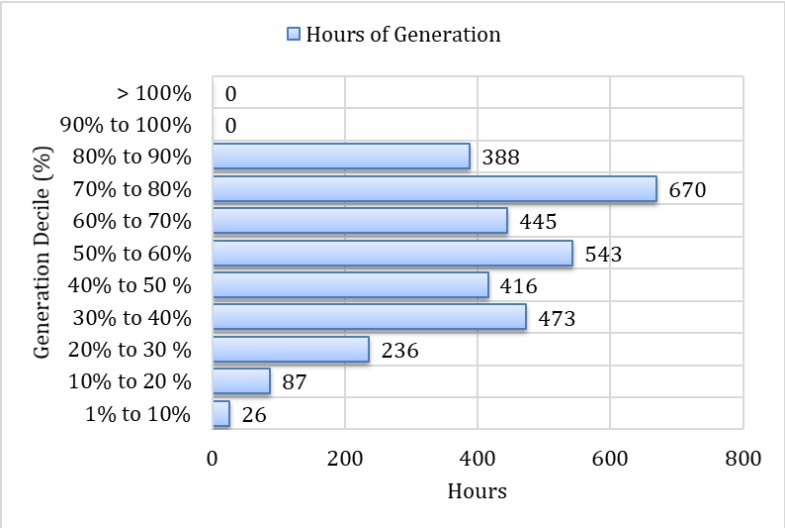


*Figure 34: Histogram of generation hours for different deciles*

Next, we present, the minimum, mean, and maximum power generated by the plant for a given day hour of interest (*Figure 35*).

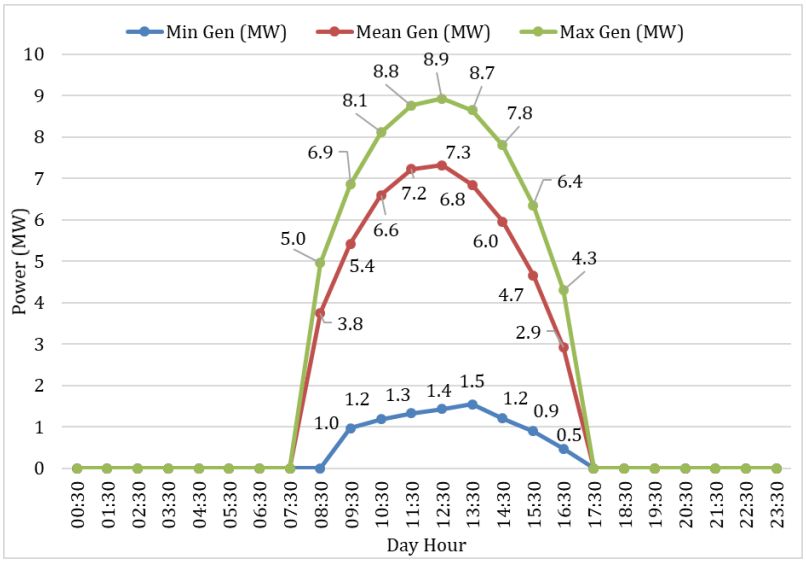


*Figure 35: Range of power generation for every day hour*

This would be of interest for power system planners, as it would provide them with a tangible perspective of the best, worst, and most anticipated state of the plant. It can play a crucial role in deciding system contingencies and scheduling of support generation.

Finally, we looked at the spread of cumulative energy generation, spread across day hours (*Figure 36*). This indicates the most crucial hours of generation, and the percentage share of generation, spread across each day hour.

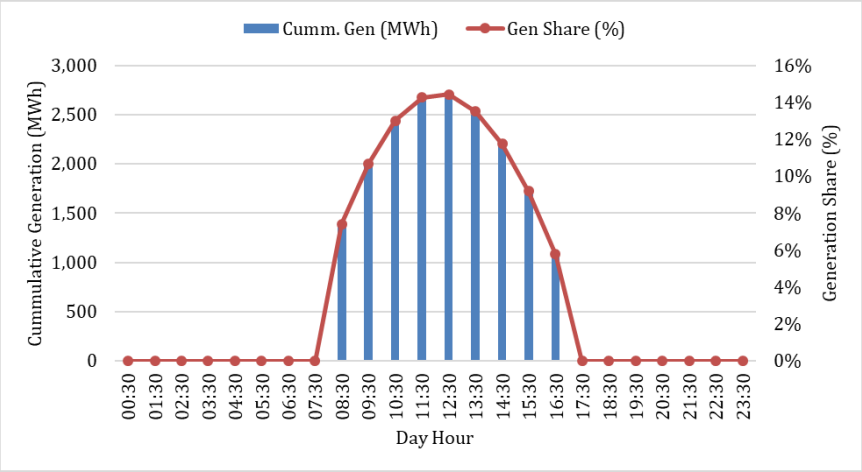


*Figure 36: Day hour wise cumulative generation and its percentage share*

### 4.2.6 Estimating effect of module degradation

We estimated the effect of module degradation on the annual solar energy generation (indicated in *Figure 37*). The annual generation mimics the pattern of module degradation. It also degrades to about ~80% w.r.t generation, with no module degradation (year 0).

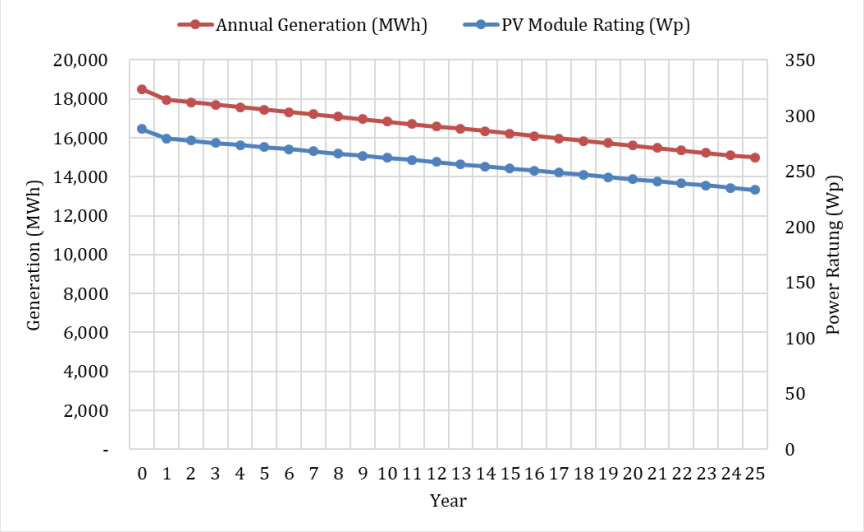


*Figure 37: Year-on-year module degradation and annual generation*

We estimated the CUF and the SEE, as indicated in *Figure 38*, to provide insights about the year-on-year plant performance. It must be pointed out that the pattern of CUF and SEE mimics that of module degradation (as indicated in *Figure 37*).

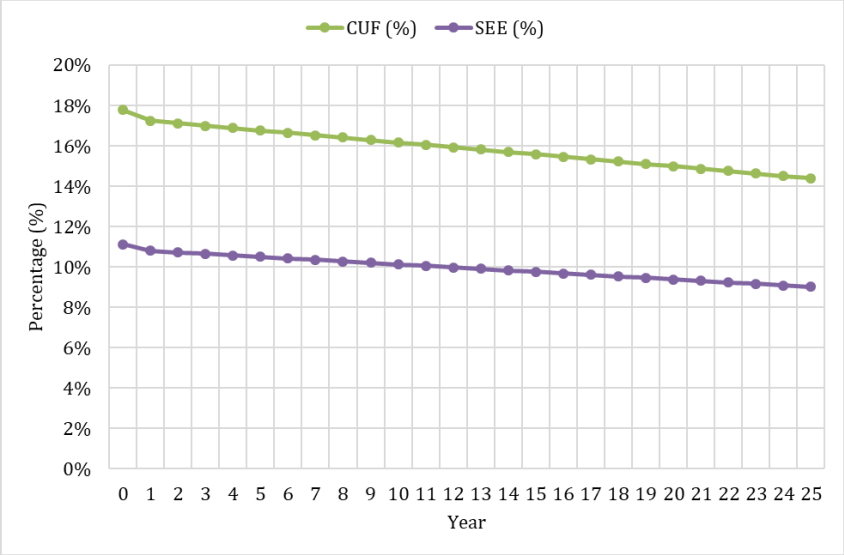


*Figure 38: Year-on-year CUF and SEE*

### 4.2.7 Summary of Technical Outputs

The plant was simulated using the technical model, which has been summarised in *Table 10*. The core outputs from the technical model, which passed to the financial model, involve the plant capacity, annual generation, and land area requirement.

*Table 10: Summary of technical outputs*

| **Parameter** | **Details** |
|---|---|
| Location | 12.85 °N, 76.95°E |
| Target Plant Capacity | 10 MWp |
| Simulated Plant Capacity | 11.88864 MWp |
| PV Module (Technology / Model/ Rating) | Multi-crystalline / Tata Power Solar, TP300 Series / 288 Wp |
| Total Number of Modules in the Plant | 41280 |
| PCU (Model / Rating) | Eaton Power Xpert / 250 kW |
| Total Number of PCUs in the Plant | 40 |
| Active Module Area | 19.78 Acres |
| Optimal Generation Window | 8:30 to 16:30 |
| Plant Area | 39.89 Acres |
| Annual Radiation on the Tilted Panel | 2.08 MWh / $m^2$ |
| Annual PV Generation range* | 18,503 to 14,987 MWh |
| CUF range* | 17.77% to 14.39% |
| SEE range* | 11.13% to 9.01% |

**No module degradation (year 0) to the end of plant life*

## 4.3 Financial Outputs

Three aspects of financial analysis have been performed for this case:

- Basic viability: includes estimation of LCOE, IRR, and payback period[15]
- Impact of subsidy: include determining LCOE and payback period
- Assessment of target bid include determining IRR and payback period at the bid

Apart from these, several other metrics such as sale of energy, EBIDTA, PAT and DSCR have also been estimated and compared, for all three cases.

### 4.3.1 Estimating capital costs

*Figure 39* presents details of capital cost components. We can combine these components into three categories - machinery, infrastructure, and other expenses. The components have been appropriately colour coded in the figures.

A)

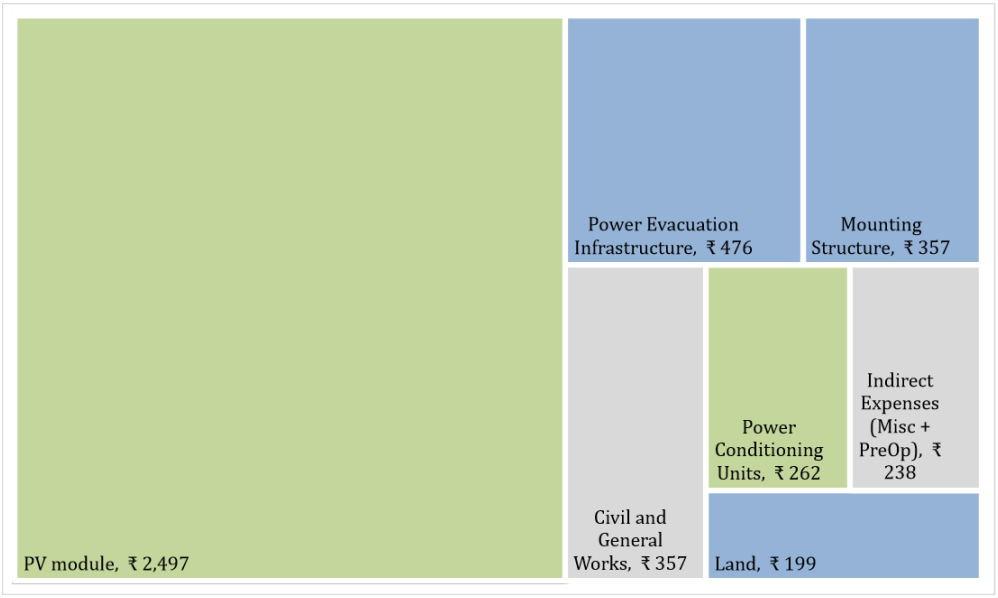


B)

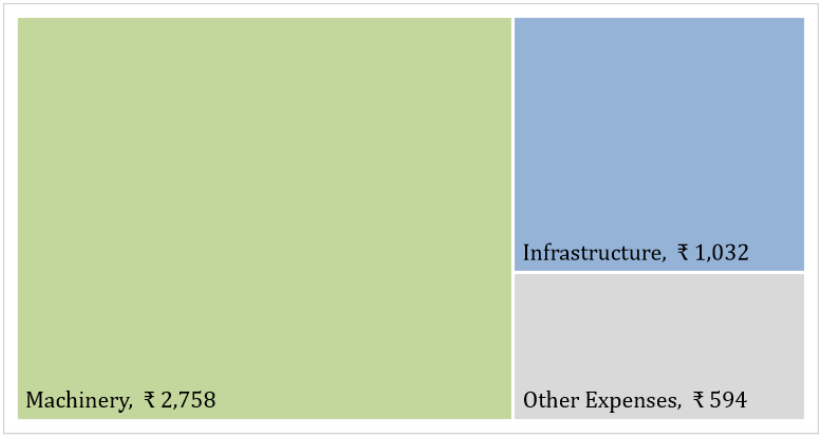


*Figure 39: Capital cost components*

[15] IRR and Payback period are estimated at LCOE

Machinery, infrastructure, and other expenses amount to about 63%, 24%, and 14% of the capital cost, respectively. *Figure 40* compares these components with the subsidy case.

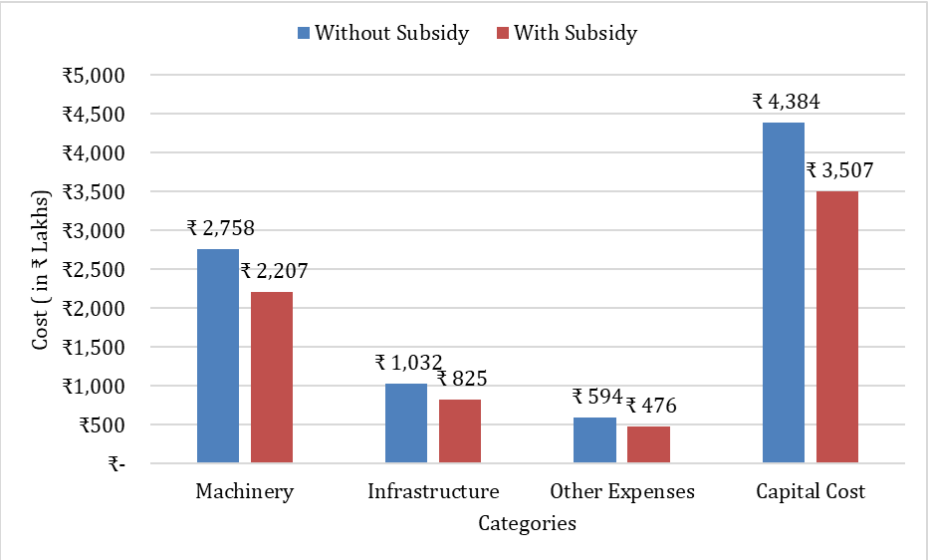


*Figure 40: Comparison of capital cost for subsidy and non-subsidy case*

### 4.3.2 Estimating other financial metrics

For all three cases, the energy generation considered, is the same. The net generation, post consideration of auxiliary consumption, has been presented in *Figure 41*, along with generation as percentage w.r.t no module degradation.

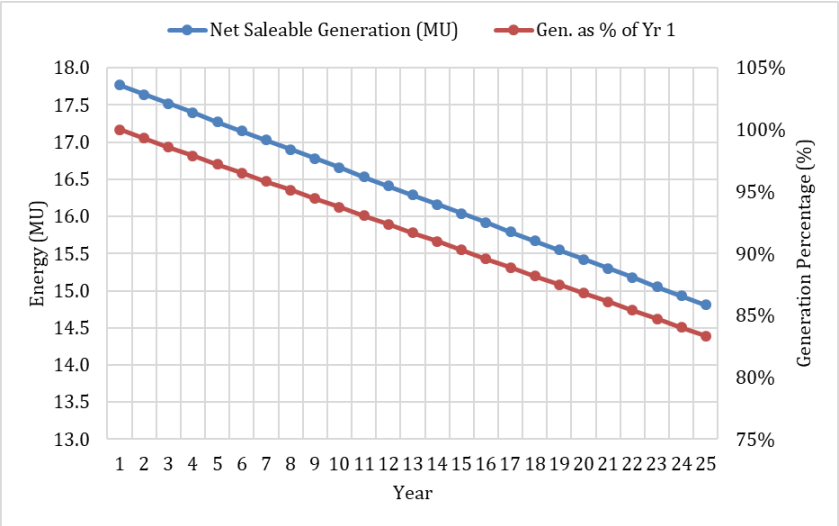


*Figure 41: Net saleable generation and generation percentage*

Based on the net saleable generation, the actual of sale of energy for all cases has been estimated, and presented in *Figure 42*.

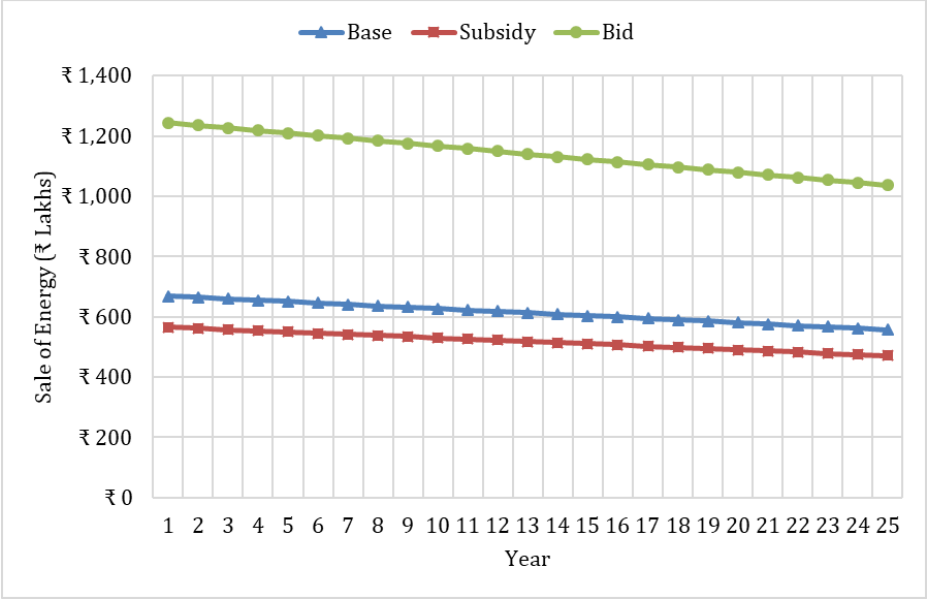


*Figure 42: Sale of energy*

Based on the sale of energy, we determined EBIDTA (indicated in *Figure 43*) and EBIDTA as a percentage of sale of energy(indicated in *Figure 44*). EBIDTA is an indication of revenue, post accounting for day-to-day operational expenses of the plant.

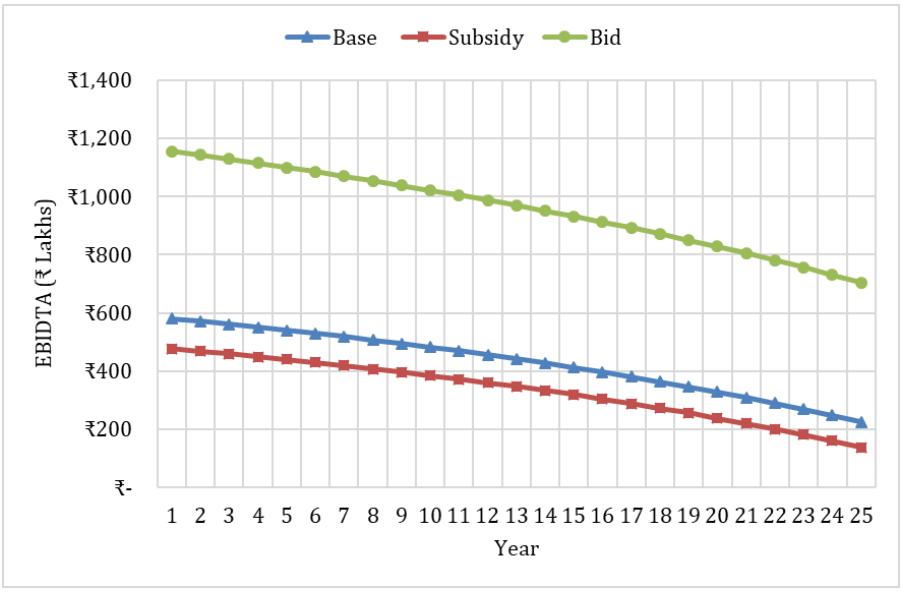


*Figure 43: Earnings Before Interest Depreciation Taxation and Amortisation (EBDITA)*

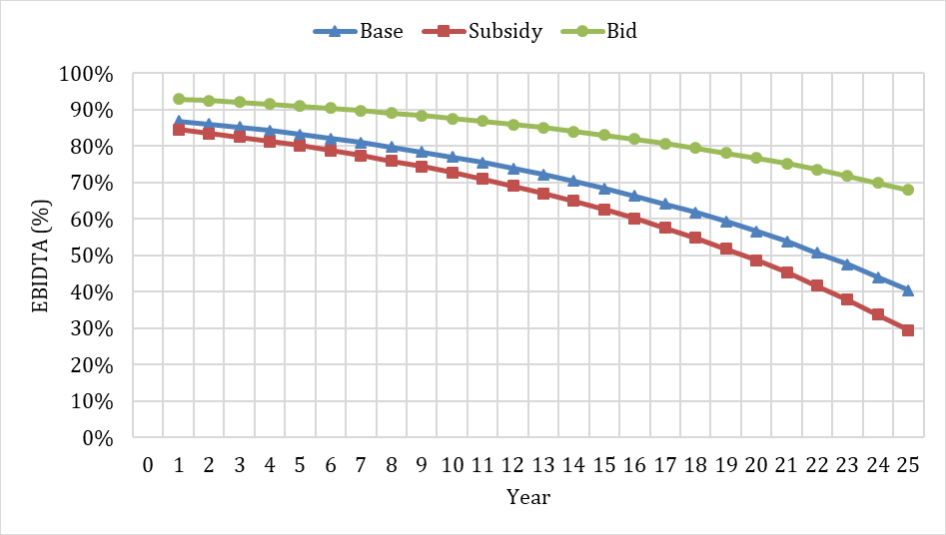


*Figure 44: EBIDTA as a percentage of sale of energy*

We determined the ability of the plant to service its debt obligations. Hence, we determine DSCR (indicated in *Figure 45*). It must be pointed that the curves for base and subsidy case, overlap. For both cases, the year-on-year values are greater than 1, implying that the project is capable of repaying its debt obligations.

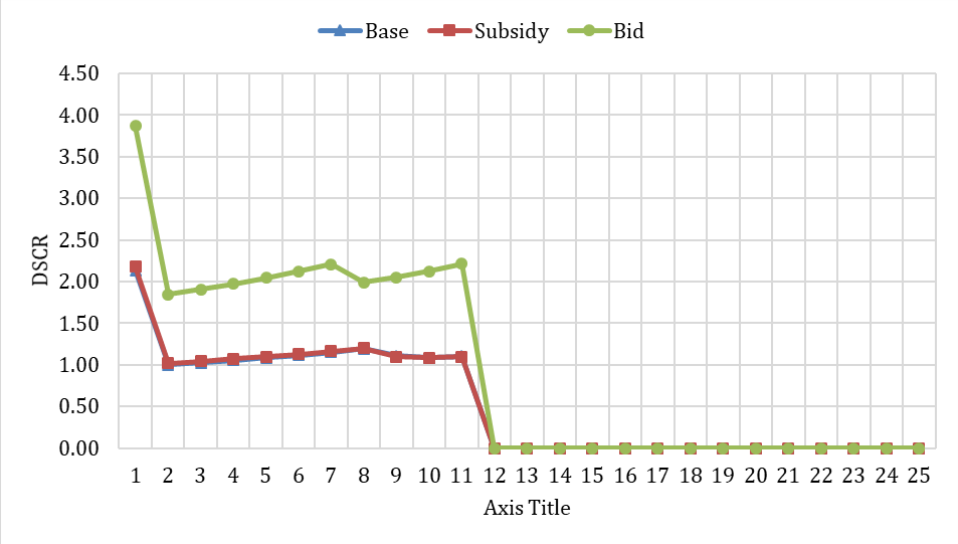


*Figure 45: Debt Service Coverage Ratio (DSCR)*

Finally, we determined Profit After Tax (PAT) based on the inputs provided by the user. PAT, for all three cases, was determined and has been indicated in *Figure 46*. Furthermore, PAT as a percentage of sale of energy has been determined and presented in *Figure 47*. The spike in the curves was caused by the completion of loan term. The bid case indicates that PAT % is significantly higher than the base case, and this indicates that the bid is a profitable one.

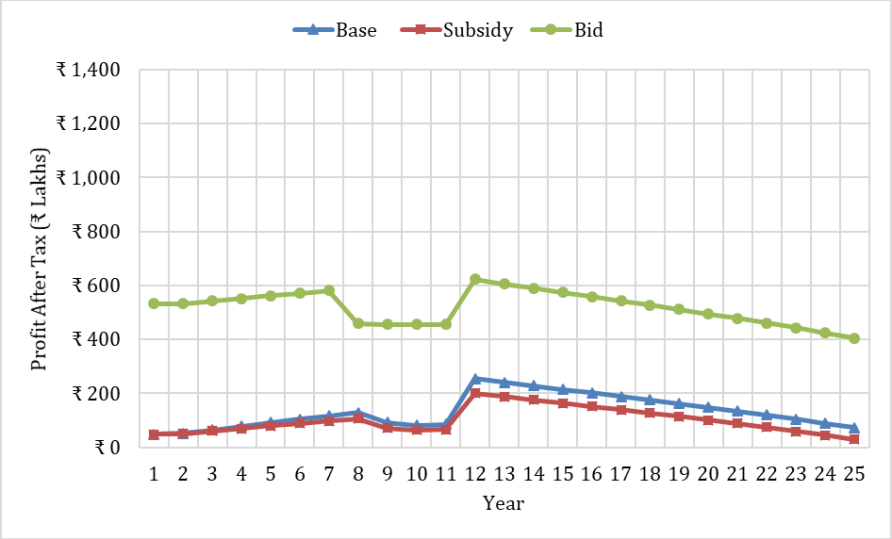


*Figure 46: Profit After Tax (PAT)*

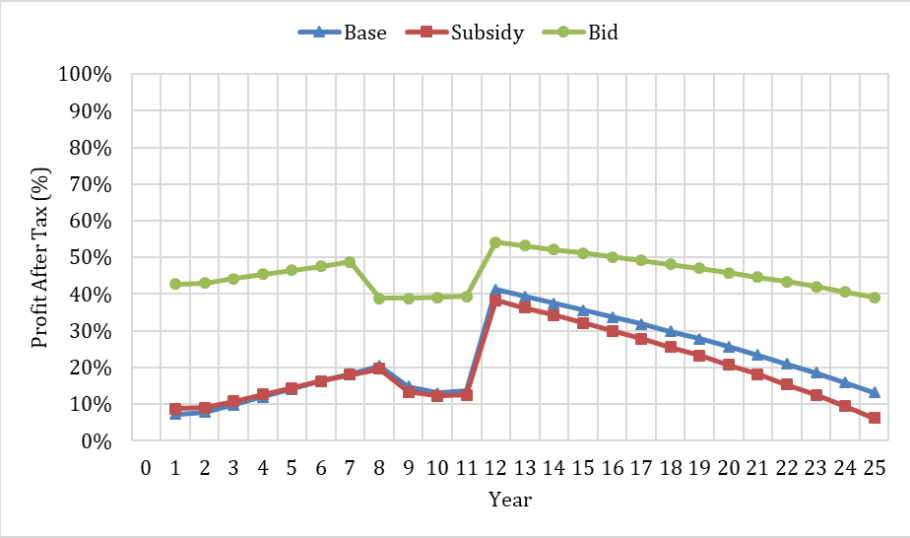


*Figure 47: PAT as a percentage of sale of energy*

The LCOE for the base and subsidy case has been estimated. These have been presented in *Figure 48* and *Figure 49*, respectively. The percentage share of each component has been indicated in *Table 11*.

*Table 11: Percentage share of LCOE components*

| **Component** | **% share for base case** | **% share for subsidy case** |
|---|---|---|
| Expenses | 31.4% | 35.0% |
| PV module | 39.1% | 37.2% |
| PCU | 4.0% | 3.8% |
| Land | 3.2% | 2.8% |
| Mounting Structure | 5.6% | 5.4% |
| Power Evacuation Infrastructure | 7.4% | 6.9% |
| Civil and General Works | 5.6% | 5.4% |

| | | |
|---|---|---|
| Indirect Expenses | 3.7% | 3.5% |

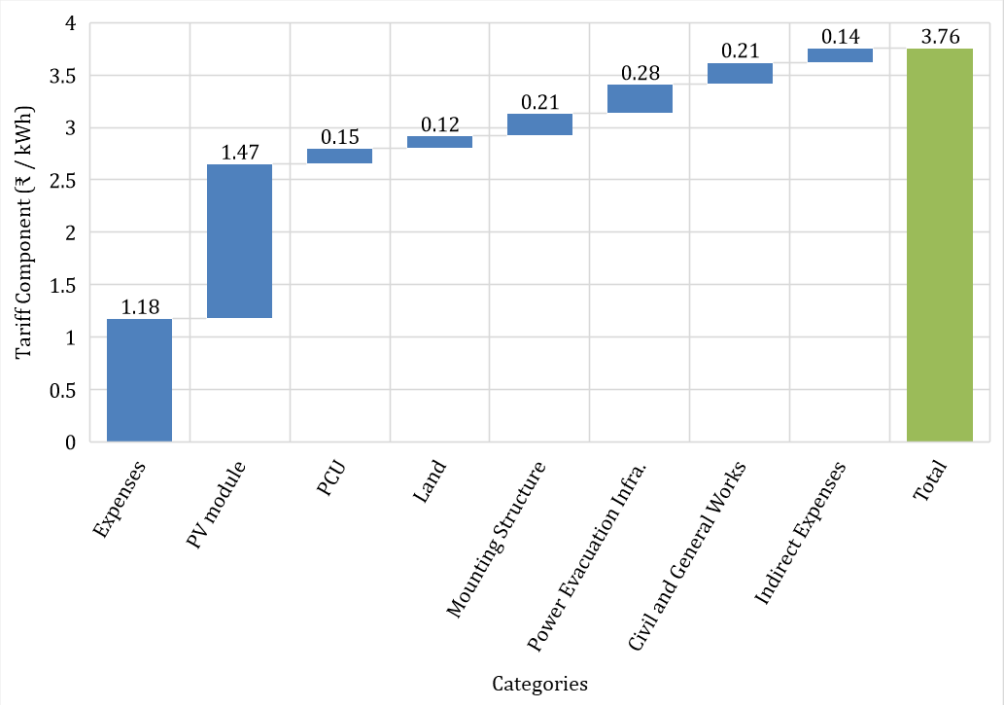


*Figure 48: LCOE for base case*

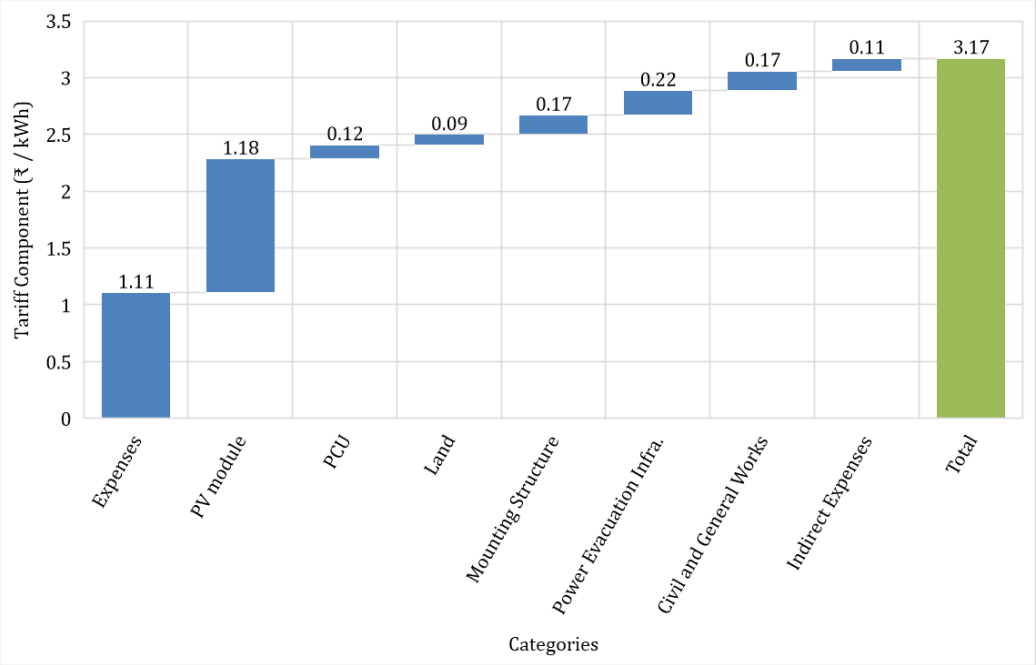


*Figure 49: LCOE for subsidy case*

### 4.3.3 Summary of the Financial Outputs

The summary of the financial outputs has been presented in *Table 12*. It also presents IRR and payback period for the respective cases. Overall, the plant is viable for both subsidy and bid cases.

*Table 12: Summary of the financial outputs*

| Base Case Viability | |
|---|---|
| Capital Cost | ₹ 4384.26 Lakhs |
| LCOE | ₹ 3.76 / kWh |
| IRR @ LCOE | 8.67 % |
| Payback Period @ LCOE | 9 years |
| Average DSCR | 1.86 |
| With Subsidy | |
| Bulk Subsidy Percentage | 20% |
| Capital Cost | ₹ 3507.42 Lakhs |
| LCOE | ₹ 3.17 / kWh |
| Average DSCR | 1.82 |
| Bid Analysis | |
| Target Bid | ₹ 7.00 / kWh |
| IRR | 21.59 % |
| Payback Period | 5 years |
| Average DSCR | 3.78 |

This concludes our illustration of the CSTEM PV model for utility plants via a simulated case study.

# 5. Conclusions and Way Forward

The current version of CSTEM PV tool can cater to techno-economic analysis for utility scale and mini-grid PV plants. This report covers the details of the solar and financial models. These are common for both utility and mini grid applications. A detailed report on the storage and load models will be released separately. This report further illustrates the models described with a case study for a utility scale solar plant.

The current version of the tool could be used to derive site-related outputs such as:

- Resource availability and utilisation (solar and land)
- Energy generation potential and its variations
- Capital cost and operational cost for setting up the plant
- The financial viability of the plant, along with the impact of subsidies
- The viability of a target bid

We aim to cover the following aspects in future versions of the tool:

- Module tracking (single and dual axis)
- Storage technologies for grid-connected systems (flow and Li-ion batteries)
- Variety of load dispatch strategies and battery sizing
- Different business and tariff models
- GIS integration to project national level insights for:-
    - Seasonal resource availability
    - Seasonal generation availability
    - Spread of annual CUF, SEE, etc. across the country
    - Integrated site selection and first order techno-economic viability

# Appendices

# 6. Appendix – A

## Solar Angles

Definition of solar angles (Duffie & Beckman, 2013):

**φ** Latitude ($-90º \leq \varphi \leq 90º$).

It is the angular location north or south of the equator

Convention: + for ºNorth, - for ºSouth

**δ** Declination angle ($-23.45º \leq \delta \leq 23.45º$)

The angular position of the sun at solar noon (i.e. when the sun is on the local meridian), with respect to the plane of the equator, north is considered positive. The value is assumed to be constant for an entire day. δ is close to zero at the equinoxes 21/22 March and 22/23 September) , it is close to +23. 45º at the summer solstice (June 21/22) and - 23.45º at the winter solstice (December 21/22).

Convention: From 21-22 March to 22-23 September δ is generally positive and from 24-25 September to 19-20 March it is generally negative.

**β** Tilt angle of the panel or the slope ($0º \leq \beta \leq 180º$)

It is the angle between the plane of surface of interest and the horizontal. Generally panels are fixed at an angle of $\beta = \Phi$ (latitude))

Convention: It is always positive, 0º when panel is parallel to ground surface.

**γ** Surface Azimuth angle ($-180º \leq \gamma \leq 180º$)

The deviation of the projection on a horizontal plane of the normal to the surface from the local meridian. If the panel is aligned along North – South direction, facing south, then $\gamma = 0$.

Convention: Zero at due south, negative towards east, positive towards west.

**ω** Hour angle ($-180º \leq \omega \leq 180º$)

The angular displacement of the sun east or west of the local meridian due to rotation of the earth on its axis at 15º per hour;

Convention: Negative in the morning, -90º at sunrise (6 am solar time) 0 at solar noon, positive after noon up to midnight, 90º at sunset (6 pm solar time)

**θ** Incidence angle ($0º \leq \theta \leq 90º$)

The angle between the beam radiation on a surface and the normal to that surface.

Convention: 90º at sunrise, $|\delta|$ at solar noon (minimum for that day) and finally 90º at sunset

**$\theta_Z$** Zenith angle ($0º \leq \theta_Z \leq 180º$)

The angle between the vertical and the line to the sun, that is, the angle of incidence of beam radiation on a horizontal surface.

Convention: approximately 90º at sunrise and sunset, decreases from 90º after sunrise, $\theta_z = |\delta - \Phi|º$ at solar noon, increases beyond 90º after sunset)

**$\alpha_s$** Solar altitude angle ($-90º \leq \alpha_s \leq 90º$)

The angle between the horizontal and the line to the sun that is the complement of zenith angle.

Convention: Negative before sunrise, 0º at sunrise and increases to 90º at solar noon and decreases to 0º at sunset and becomes up to sunset.

**$\gamma_s$** Solar azimuth angle ($-180º \leq \gamma_s \leq 180º$) – South Reference

The angle range is valid only for N/S latitudes between 23.45º and 66.45º. The angular displacement from south of the projection of beam radiation on the horizontal plane. It is generally negative from midnight to solar noon, approximately 0º at solar noon and positive from after noon to midnight. It is basically the angle between the projections on the sun's ray with the N-S axis.

Convention: Angle is measured from due south, displacements east of south are negative and west of south are positive. (ω – for mornings and + for afternoon)

# 7. Appendix – B

## Models for Electrical Operation of a PV Cell / Module

A solar cell typically being a semiconductor junction, could be represented by an ideal diode whose I-V characteristics could be represented by the following equation:

$$I_D = I_0 \,.\, (e^{qV/\varepsilon kT} - 1)$$

Here,

$I_D$ = Diode Current (A)

$I_0$ = Reverse saturation current of the diode (A)

q = Charge of an electron ($1.602 \times 10^{-19}$ C)

k = Boltzmann constant ($1.381 \times 10^{-23}$ J/K)

T = Junction temperature (K)

ε = Diode ideality factor (typically lies between 1 and 2), for an ideal cell ε = 1.

V = Voltage developed at the output terminals (V)

When this junction is illuminated, as is the case in a PV cell, a photocurrent $I_{ph}$ is generated. An ideal PV cell could be represented as a current source with intensity $I_{ph}$, connected in parallel with a diode, and the corresponding I-V characteristic (illustrated in Figure 50) of the setup could be described by Shockley's PV cell equation (Shockley, 1950).

$$I = I_{ph} - I_0 . (e^{qV/\varepsilon kT} - 1)$$

Here,

I = Current output of a solar photovoltaic cell (A)

$I_{ph}$ = Photocurrent generated in the cell due to incident light. (A)

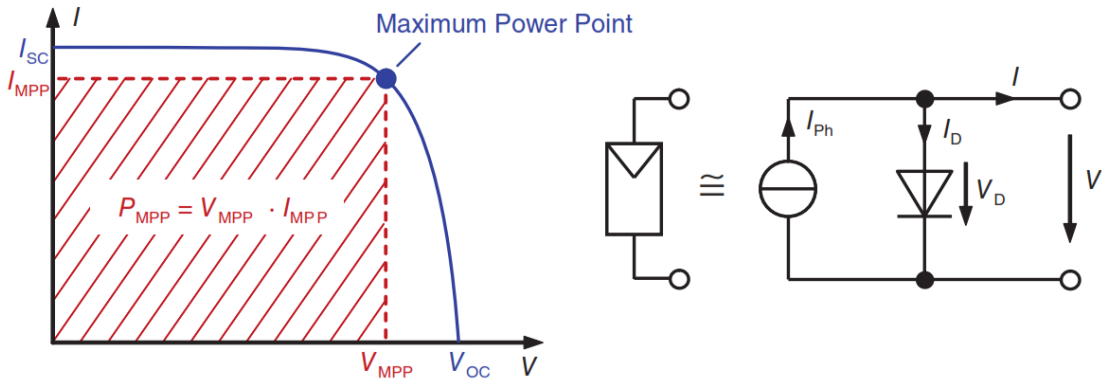


*Figure 50: Characteristic Curve of a loss-less solar cell and its simplified equivalent circuit*

*Source: Mertens, 2014*

The parameters illustrated in the characteristic curve have already been defined in Section 2.5 in the PV module section. The electrical circuit representation of the standard PV model in Figure 51 also considers the electrical losses in the cell. This is also known as the single diode representation of the system.

Simplified Model:

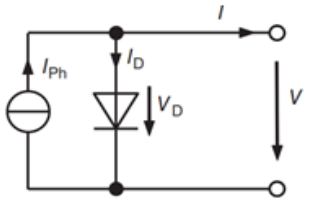


Standard Model:

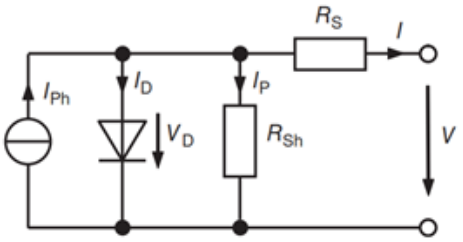


*Figure 51: Equivalent circuit for electrical description for solar cells and solar module*

*Source: Mertens, 2014*

The ohmic losses caused by the front contacts of the solar cell and at the metal semiconductor interface has been accounted for with the series resistance ($R_s$). The leaking current at the edge of the solar cell as well as any point short circuits of the p-n junction are accounted for as shunt resistance ($R_{sh}$).

Applying the Kirchhoff's current law (KCL) on the circuit of the standard model, we get:

$$I = I_{ph} - I_D - I_p$$

$$I = I_{ph} - I_0.\left(e^{(V+I.R_s)/a} - 1\right) - \frac{V + I.R_s}{R_{sh}}$$

Here $a = \frac{\varepsilon kT}{q}$ (Modified diode ideality factor)

Also, for a DC system power P = V×I

$$\frac{dV}{dI} = -R_s - \frac{a.R_{sh}}{a + I_0.R_{sh}.e^{\left(\frac{V+I.R_s}{a}\right)}}$$

The 5 parameters: a, $R_s$, $R_{sh}$, $I_{ph}$, and $I_0$ define the operation of the PV cell and these vary with incident radiation $G_T$, cell temperature $T_{cell}$ and incidence angle θ. We first would develop the equations required to determine them.

The general module parameters are specified at STC or SRC conditions. Hence, we use these conditions to determine the 5 parameters at STC (subscripted as ref) and translate these parameters for any operating condition. Here, $T_{cell\text{-}ref} = 25ºC$, $G_{T\text{-}ref} = 1000\ W/m^2$, $M_{am\text{-}ref} = 1.5$. The information available from the datasheets include at STC, $I_{sc\text{-}ref}$, $V_{oc\text{-}ref}$, $I_{mp\text{-}ref}$, $V_{mp\text{-}ref}$, $P_{mp\text{-}ref}$. Hence, the conditions (applied to KCL eqn.) that could be used for determining the 5 parameters at STC ($a_{ref}$, $R_{s\text{-}ref}$, $R_{sh\text{-}ref}$, $I_{ph\text{-}ref}$, $I_{0\text{-}ref}$) are as follows:

At short circuit, $I = I_{sc\text{-}ref}$ and $V = 0$

At open circuit, $I = 0$ and $V = V_{oc\text{-}ref}$

At MPP, $I = I_{mp\text{-}ref}$ and $V = V_{mp\text{-}ref}$

At MPP, $\frac{dP}{dV}\ at\ V_{mp} = 0$

At $I = I_{sc\text{-}ref}$, $\frac{dI}{dV} \cong \frac{-1}{R_{sh-ref}}$

$$I_{sc-ref} = I_{ph-ref} - I_{0-ref} * \left( e^{\frac{I_{sc-ref} * R_{s-ref}}{a_{ref}}} - 1 \right) - \frac{I_{sc-ref} * R_{s-ref}}{R_{sh-ref}}$$

$$0 = I_{ph-ref} - I_{0-ref} * \left( e^{\frac{V_{oc-ref}}{a_{ref}}} - 1 \right) - \frac{V_{oc-ref}}{R_{sh-ref}}$$

$$I_{mp-ref} = I_{ph-ref} - I_{0-ref} \cdot \left( e^{\frac{(V_{mp-ref} + I_{mp-ref} * R_{s-ref})}{a_{ref}}} - 1 \right) - \frac{V_{mp-ref} + I_{mp-ref} * R_{s-ref}}{R_{sh-ref}}$$

At MPP, $\frac{dP}{dV}\ at\ V_{mp} = 0$

$$P = VI, \qquad \frac{dP}{dV} = I + V\frac{dI}{dV},$$

$$at\ MPP\ \ \frac{dV}{dI} \Rightarrow \frac{-V_{m-ref}}{I_{m-ref}} = -R_{s-ref} - \frac{a_{ref} . R_{sh-ref}}{a_{ref} + I_{0-ref} . R_{sh-ref} . e^{\left(\frac{V_{m-ref} + I_{m-ref} . R_{s-ref}}{a_{ref}}\right)}}$$

At $I = I_{sc\text{-}ref}$, $V = 0$

$$\frac{dV}{dI_{sc}} = -R_S - \frac{a . R_{sh}}{a + I_0 . R_{sh} . e^{\frac{I_{sc} . R_s}{a}}}$$

$$I_0 . R_{sh} . e^{\frac{I_{sc} . R_s}{a}} \Longrightarrow 0, \qquad \frac{dV}{dI_{sc}} = -R_s - R_{sh}$$

$$R_s \ll R_{sh}\ and\ R_s \approx 0 \Rightarrow \frac{dI_{sc}}{dV} = \frac{-1}{R_{sh}}$$

The formulation above indicates that these equations of interest are non-linear and would have to be iteratively solved. Therefore, for obtaining the value of $a_{ref}$, $R_{s\text{-}ref}$, $R_{sh\text{-}ref}$, $I_{ph\text{-}ref}$, $I_{0\text{-}ref}$, the required parameters are $I_{sc\text{-}ref}$, $V_{oc\text{-}ref}$, $I_{mp\text{-}ref}$, $V_{mp\text{-}ref}$ and slope of the IV curve at the short circuit point $\frac{dI_{sc}}{dV}$. The slope: $\frac{dI_{sc}}{dV}$ is not generally provided in the module datasheets, and due to the nature of this point, a very high precision estimate is required for a sound analysis.

An approach called the 4 parameter model suggested by De Soto, 200 4, where it is assumed that Rsh → ∞, could be considered to estimate the other parameters ($a_{ref}$, $R_{s\text{-}ref}$, $I_{ph\text{-}ref}$, $I_{0\text{-}ref}$). The authors claim that this approach is not recommended for amorphous cell types.

The KCL equation reduces to:

$$I = I_{ph} - I_0.\left(e^{(V+I.R_s)/a} - 1\right)$$

Hence the equations under

At short circuit, $I = I_{sc\text{-}ref}$ and $V = 0$

At open circuit, $I = 0$ and $V = V_{oc\text{-}ref}$

At MPP, $I = I_{mp\text{-}ref}$ and $V = V_{mp\text{-}ref}$

Reduce to,

$$I_{sc-ref} = I_{ph-ref} - I_{0-ref} * \left(e^{\frac{I_{sc-ref} * R_{s-ref}}{a_{ref}}} - 1\right)$$

$$0 = I_{ph-ref} - I_{0-ref} * \left(e^{\frac{V_{oc-ref}}{a_{ref}}} - 1\right)$$

$$I_{mp-ref} = I_{ph-ref} - I_{0-ref}.\left(e^{\frac{(V_{mp-ref} + I_{mp-ref} * R_{s-ref})}{a_{ref}}} - 1\right)$$

Considering at MPP, $\frac{dP}{dV}\ at\ V_{mp} = 0$

$$\frac{dV}{dI} \Rightarrow \frac{-V_{m-ref}}{I_{m-ref}} = -R_{s-ref} - \frac{a_{ref}}{I_{0-ref}.e^{\left(\frac{V_{m-ref} + I_{m-ref}.R_{s-ref}}{a_{ref}}\right)}}$$

Another expression for calculating $a_{ref}$ which could be used under Rsh → ∞ condition

$$a_{ref} = \frac{K_{T-Voc} * T_{cell-ref} - V_{oc-ref} + \varepsilon.N_s}{\frac{K_{T-Isc} * T_{cell-ref}}{I_{ph-ref}} - 3}$$

Here $N_S$ = Number of cells in series in a module.

For translating the parameters to other operating conditions, we have the following relations (Townsend, 1989):

($T_{cell}$ and $T_{cell\text{-}ref}$ in Kelvin for 1st 2 eqns.)

$$\frac{a}{a_{ref}} = \frac{T_{cell}}{T_{cell-ref}}$$

$$\frac{I_0}{I_{0-ref}} = \left[\frac{T_{cell}}{T_{cell-ref}}\right]^3 * e^{\frac{\varepsilon.N_s}{a_{ref}}*\left(1-\frac{T_{cell-ref}}{T_{cell}}\right)}$$

$$I_{ph} = \frac{G_T}{G_{T-ref}} * \left(I_{ph-ref} + K_{T-Isc} * (T_{cell} - T_{cell-ref})\right)$$

Factoring the effect of air mass ($M_{am}$)

$$I_{ph} = \frac{G_{eff}*M_{am}}{G_{T-ref}*M_{am-ref}} * \left(I_{ph-ref} + K_{T-Isc} * (T_{cell} - T_{cell-ref})\right)$$

Here

$$M_{am} = \frac{1}{cos\theta_z}$$

The equations showcased above can help us obtain values of a, $I_0$ and $I_{ph}$ for an operating condition, based on the level of approximation ($R_{sh}$ = finite or $R_{sh} = \infty$). $R_s$ and $R_{sh}$ can be calculated using the 5 parameter or the 4 parameter model equations.

The 4-parameter model, although a simpler model than the 5-parameter model, is still computationally extensive. The author recommended that it not be used for amorphous/thin film-based technologies.

An approach suggested by Bai et al., 2015 provides a non-iterative approximation of the 5 parameter model. But it requires $I_{sc\text{-}ref}$, $V_{oc\text{-}ref}$, $I_{mp\text{-}ref}$, $V_{mp\text{-}ref}$, $\frac{dV}{dI}$ at V= $V_{oc\text{-}ref}$, and $\frac{dV}{dI}$ at I = $I_{sc\text{-}ref}$. The approximations and equations for the parameters are listed below:

$$e^{V_{oc}/a} - 1 \approx e^{V_{oc}/a};\ I_0 * \left(e^{I_{sc}*R_S/a} - 1\right), \left(e^{(V_m+I_m*R_s)/a} - 1\right) \rightarrow neglected$$

$$R_s = \frac{\left(V_{mp} * \left(\frac{dV}{dI}|_{V_{oc}} - \frac{dV}{dI}|_{I_{sc}}\right) * \left(\frac{dV}{dI}|_{I_{sc}} * (I_{sc} - I_{mp}) + V_{mp}\right) - \frac{dV}{dI}|_{V_{oc}} * \left(\frac{dV}{dI}|_{I_{sc}} * I_{mp} + V_{mp}\right) * \left(\frac{dV}{dI}|_{I_{sc}} * I_{sc} + V_{oc}\right)\right)}{\left(I_{mp} * \left(\frac{dV}{dI}|_{V_{oc}} - \frac{dV}{dI}|_{I_{sc}}\right) * \left(\frac{dV}{dI}|_{I_{sc}} * (I_{sc} - I_{mp}) + V_{mp}\right) + \left(\frac{dV}{dI}|_{I_{sc}} * I_{mp} + V_{mp}\right) * \left(\frac{dV}{dI}|_{I_{sc}} * I_{sc} + V_{oc}\right)\right)}$$

$$R_{sh} = -R_s - \frac{dV}{dI}|_{I_{sc}}$$

$$I_{ph} = I_{sc} * \left(1 + \frac{R_s}{R_{sh}}\right)$$

$$a = \frac{\left(\left(\frac{dV}{dI}|_{V_{oc}} + R_S\right) * \left(\frac{dV}{dI}|_{I_{sc}} * I_{sc} + V_{oc}\right)\right)}{\left(\frac{dV}{dI}|_{V_{oc}} - \frac{dV}{dI}|_{I_{sc}}\right)}$$

$$I_0 = \frac{\left(I_{ph} - \frac{V_{oc}}{R_{sh}}\right)}{\left(e^{V_{oc}/a} - 1\right)}$$

We could obtain an approximate slope would by using the MPP point and $V_{oc}$, MPP and $I_{sc}$ points to get the slope. But, it must be pointed that due to the placement of the $I_{sc}$ point, even a small change in the value's precision could lead to a wider variation in the computed parameters. Hence, due to the sensitive nature of the assumption, this method has not been considered in CSTEM PV.

# 8. Appendix – C

## 8.1 Module Specifications

*Table 13: Relevant details for Tata Power Solar TP288 PV Module*

| **Parameter** | **Data** |
|---|---|
| Manufacturer | Tata Power Solar |
| Technology | Multi Crystalline |
| Model | TP300 Series – TP288 |
| Module Power Rating ($P_{mod}$ or $P_{max}$) at STC | 288 Wp |
| Open Circuit Voltage ($V_{oc}$) at STC | 44.6 V |
| Short Circuit Current ($I_{sc}$) at STC | 8.45 A |
| Voltage at Maximum Power Point ($V_{mp}$) at STC | 36.3 V |
| Current at Maximum Power Point ($I_{mp}$) at STC | 7.95 A |
| Length of Module ($L_{mod}$) | 0.992 m |
| Breadth of Module ($B_{mod}$) | 1.955 m |
| Temperature Coefficient of $P_{max}$ | -0.42 % / °C |
| Temperature Coefficient of $V_{oc}$ | -0.293 % / °C |
| Temperature Coefficient of $I_{sc}$ | 0.058 % / °C |
| Module Rating at the end of year 1 | 97% |
| Linearised Year on Year Degradation rate | -0.667 % / year |

*Source: Tata Power Solar, 2018*

## 8.2 PCU Specifications

*Table 14: Relevant Parameters of Eaton Power Xpert 250 kW PCU*

| **Parameter** | **Data** |
|---|---|
| Manufacturer | Eaton Corporation |
| Model | Eaton Power Xpert Solar |
| Weighted CEC efficiency | 96% |
| AC Power Rating | 250 kVA |
| Nominal DC Power Rating | 250 kW |
| Minimum Voltage at Maximum Power Point Range | 300 V |
| Maximum Voltage at Maximum Power Point Range | 500 V |
| PCU Start Voltage | 400 V |
| Maximum Permissible DC Voltage | 600 V |
| Nominal DC Current | 860 A |
| Maximum Permissible DC Current | 1340 A |

*Source: Eaton, 2015*

## 8.3 Financial Parameters

*Table 15: Relevant Financial Parameters for the case*

| **Category** | **Parameters** | **Data** |
|---|---|---|
| Capital Expenditure | PV module rate | ₹ 21 / Wp |
| | Land rate | ₹ 5 Lakhs / Acre |
| | Mounting structure rate | ₹ 30 Lakhs / MWp |
| | Civil and general works rate | ₹ 30 Lakhs / MWp |
| | PCU or Inverter rate | ₹ 22 Lakhs / MWp |
| | Power evacuation infrastructure rate | ₹ 40 Lakhs / MWp |
| | Preliminary and pre-operation costs | ₹ 20 Lakhs / MWp |
| | Miscellaneous expenses | ₹ 0 Lakhs / MWp |
| Operation and Maintenance (O&M) | O&M cost for 1st year | ₹ 7 Lakhs / MWp |
| | O&M escalation rate per annum | 5.72 % |
| Subsidy | Bulk Capital Subsidy | 20% |
| Target Bid | Bid | ₹ 7 / kWh |
| Loan related metrics | Debt share | 70% |
| | Term Loan term | 11 years |
| | Moratorium period | 1 year |
| | Term Loan interest rate | 8.5% |
| Return on Equity | During Term Loan | 15% |
| | Post Term Loan | 15% |
| Depreciation | During Term Loan | 5.83% |
| Taxes | Income Tax Rate | 30% |
| | Minimum Alternate Tax Rate | 15% |

## 9. References

Anderson, N., & Hong, J. (2013). Visually Extracting Data Records from Query Result Pages. In Z. shikawa, Y., Li, J., Wang, W., Zhang, R. (Ed.), *Web Technologies and Applications 15th Asia-Pacific Web Conference*. Retrieved from https://link.springer.com/chapter/10.1007/978-3-642-37401-2_40#citeas

Antonio, H., & Hegedus, S. (2003). *Handbook of photovoltaic science and engineering*. https://doi.org/10.1002/9780470974704

Azure Power. (2015). 100 MW plant in Jodhpur, Rajasthan.

Bai, J., Cao, Y., Hao, Y., Zhang, Z., Liu, S., & Cao, F. (2015). Characteristic output of PV systems under partial shading or mismatch conditions. *Solar Energy*, *112*, 41–54. https://doi.org/10.1016/j.solener.2014.09.048

Bridge To India. (2019). *India RE Outlook 2019*. Retrieved from https://bridgetoindia.com/report/india-re-outlook-2019-i-january-2019/

Brigham, E. F., & Houston, J. F. (2007). Fundamentals of financial management. In *Engineering and Process Economics* (Vol. 3). https://doi.org/10.1016/0377-841X(78)90069-4

Cambell, M. (2008). The drivers of levelized cost of electricity for utility-scale photovoltaics. Retrieved May 15, 2016, from SunPower Website website: https://us.sunpower.com/sites/sunpower/files/media-library/white-papers/wp-levelized-cost-drivers-electricity-utility-scale-photovoltaics.pdf

Cattani, C. (2011). On the existence of wavelet symmetries in Archaea DNA. *Computational and Mathematical Methods in Medicine*, *2012*. https://doi.org/http://dx.doi.org/10.1155/2012/673934

CEA. (2016). *Perspective Transmission Requirements for 2022 - 36*. Retrieved from http://www.cea.nic.in/reports/others/ps/pspa2/ptp.pdf

CEA. (2018a). *All India Installed Capacity Report - Dec 2018*. Retrieved from http://cea.nic.in/reports/monthly/installedcapacity/2018/installed_capacity-12.pdf

CEA. (2018b). *Growth of Electricity Sector in India From 1947- 2018*. Retrieved from http://www.cea.nic.in/reports/others/planning/pdm/growth_2018.pdf

CEA. (2018c). *Load Generation Balance Report 2018-19*. Retrieved from http://www.cea.nic.in/reports/annual/lgbr/lgbr-2018.pdf

CERC. (2016a). *Determination of Benchmark Capital Cost norm for solar PV and solar thermal power projects applicable during FY 2016-17* (No. Petition no. 17/SM/2015). India: Central Electricity Regulatory Comission (CERC).

CERC. (2016b). *Determination of levellised generic tariff for FY 2016-17* (No. (Petition No. SM/03/2016 (Suo-Motu))). India: CERC.

CERC. (2017). *CERC (Terms and Conditions for Tariff determination from Renewable Energy Sources) Regulations, 2017*. Retrieved from http://www.cercind.gov.in/2017/regulation/Noti131.pdf

Chrosis Sustainable Solutions. (2012). Chrosis Whitepapers - PR vs CUF. Retrieved May 15, 2016, from Chrosis Website website: http://chrosis.de/wp-content/uploads/2012/12/PR-vs-CUF-WP.pdf

CSTEP. (2017). *CSTEP's Solar Techno Economic Model - CSTEM*. Retrieved from

http://cstem.cstep.in/cstem/

De Soto, W. (2004). *Improvement and validation of a model for photovoltaic array performance* (University of Wisconsin - Madison). Retrieved from http://digital.library.wisc.edu/1793/7602

Duffie, J. A., & Beckman, W. A. (2013). Solar Engineering of Thermal Processes: Fourth Edition. In *Solar Engineering of Thermal Processes: Fourth Edition*. https://doi.org/10.1002/9781118671603

Eaton. (2015). *Datasheet Power Xpert Solar 250 kW Inverter*. Eaton.

Gardener, M. (1971). *Martin Gardener's Sixth book of Mathematical Diversions from Scientific American*. University of Chicago Press.

Gilman, P. (2015). *SAM Photovoltaic Model Technical Reference*. https://doi.org/NREL/TP-6A20-64102

Hegedus, S., & Luque, A. (2011). Achievements and Challenges of Solar Electricity from Photovoltaics. In *Handbook of Photovoltaic Science and Engineering* (pp. 1–38). https://doi.org/10.1002/9780470974704.ch1

Hittinger, E., Wiley, T., Kluza, J., & Whitacre, J. (2015). Evaluating the value of batteries in microgrid electricity systems using an improved Energy Systems Model. *Energy Conversion and Management*. https://doi.org/10.1016/j.enconman.2014.10.011

Honsberg, C., & Bowden, S. (n.d.). Photovoltaic Education Network. Retrieved January 1, 2017, from pveducation.org website: http://www.pveducation.org/

IEA. (2019). *Global Energy & CO2 Status Report 2018*. Retrieved from https://webstore.iea.org/global-energy-co2-status-report-2018

Investopedia. (n.d.). Investopedia. Retrieved June 20, 2016, from http://www.investopedia.com/

Iqbal, M. (1983). An Introduction to Solar Radiation. In *An Introduction to Solar Radiation*. https://doi.org/10.1016/B978-0-12-373750-2.50017-3

ISRO, NRSC, RSAA, LRUMG, & LUCMD. (2014). *Land Use / Land Cover database on 1:50,000 scale, Natural Resources Census Project*. Retrieved from https://bhuvan-app1.nrsc.gov.in/2dresources/thematic/2LULC/lulc1112.pdf

Kalogirou, S. A. (2009). Solar Energy Engineering: Processes and Systems. In *Solar Energy Engineering*. https://doi.org/10.1016/B978-0-12-374501-9.00014-5

King, D. L., Boyson, W. E., & Kratochvil, J. A. (2004). Photovoltaic array performance model. In *Sandia Report No. 2004-3535*. https://doi.org/10.2172/919131

Kitano, H., Katsuhiko, H., Kakimoto, Y., Urakawa, T., & Araki, O. (2015). Computation simulation: Local Inhibitory Synapses Activate Cortical Regions Around the Lesion. *International Symposium on Nonlinear Theory and Its Applications*. Retrieved from http://www.ieice.org/nolta/symposium/archive/2015/articles/B2L-C5-6151.pdf

Klein, S. ., & Beckman, W. A. (1983). *PV f-char User's Manual: Microprocessor version*. Middleton, WI.

Klein, S. ., Beckman, W. A., & Al., E. (1979). *TRNSYS -- A Transient Simulation Program*. Madison.

Klima, K., Sridhar, H., Dash, V., Bharadwaj, M. D., Kumar, P., & Apt, J. (2018). *Performance Comparison of Solar Photovoltaic Models for Plant Siting in India*. https://doi.org/CSTEP WS

2019 04

Langella, R., Testa, A., & Ventre, C. (2014). A new model of lead-acid batteries lifetime in smart grid scenario. *ENERGYCON 2014 - IEEE International Energy Conference*. https://doi.org/10.1109/ENERGYCON.2014.6850597

Liu, B. Y. H., & Jordan, R. C. (1960). The interrelationship and characteristic distribution of direct, diffuse and total solar radiation. *Solar Energy*, *4*(3), 1–19. https://doi.org/10.1016/0038-092X(60)90062-1

Markvart, T., & Castaner, L. (2013). *Practical Handbook of Photovoltaics Fundamentals and Applications* (T. Markvart & L. Castaner, Eds.). USA: Elsevier Science Inc.

Menicucci, D., & Fernandez, J. . (1988). *User's Manual for PVFORM: A Photovoltaic system simulation program for standalone and grid interactive applications*. https://doi.org/SAND85-0376 UC-276

Mertens, K. (2014). *Photovoltaics: Fundamentals, Technology and Practice* (First; G. Roth, Ed.). John Wiley & Sons.

MNRE. (2019a). Physical Progress (Achievements). Retrieved June 27, 2019, from MNRE website website: https://mnre.gov.in/sites/default/files/uploads/State wise installed Capacity as on 31.05.2019.xlsx

MNRE. (2019b). Solar Energy Received by India. Retrieved June 26, 2019, from MNRE website website: https://mnre.gov.in/solar

NITI Aayog. (2016). *Report of the expert group on 175 GW RE by 2022*. Retrieved from http://niti.gov.in/writereaddata/files/writereaddata/files/document_publication/report-175-GW-RE.pdf

Noone, C. J., Torrilhon, M., & Mitsos, A. (2011). Heliostat field optimization: A new computationally efficient model and biomimetic layout. *Solar Energy*, *86*, 792–823.

NREL. (2015). TMY. Retrieved from https://nsrdb.nrel.gov/tmy

Paiva, G., Pimentel, S., Marra, E., & de Alvarenga, B. (2015). *Photovoltaic Energy Prediction Analysis Considering Tilt and Azimuthal Orientation in Brazil* (pp. 1–6). pp. 1–6.

PIB. (2015). Revision of Cumulative targets under National Solar Mission from 20,000 MW by 2021-22 to 1,00,000 MW by 2022. *PIB Website*. Retrieved from http://pib.nic.in/newsite/PrintRelease.aspx?relid=122566

Ramachandra, T. V., Jain, R., & Krishnadas, G. (2011). Hotspots of Solar Potential in India. *Renewable and Sustainable Energy Reviews*, *15*(6), 3178–3186. https://doi.org/10.1016/j.rser.2011.04.007

Ramaswamy, M. ., Krishnan, R., Chandrasekaran, V. ., Thirumalai, N. ., Rao, B. S., Suresh, N. ., … Kumar, A. V. (2012). *Engineering Economic Policy Assessment of Concentrated Solar Thermal Power Technologies for India*. Retrieved from http://www.cstep.in/uploads/default/files/publications/stuff/CSTEP_Concentrated_Solar_Thermal_Power_Technologies_Report_2012.pdf

Roger, M., & Jerry, V. (2005). Photovoltaic Systems Engineering. In *CRC Press LLC* (Second).

Ross, R. G. (1980). FLAT-PLATE PHOTOVOLTAIC ARRAY DESIGN OPTIMIZATION. *Conference Record of the IEEE Photovoltaic Specialists Conference*, pp. 1126–1132. Retrieved from http://www.scopus.com/inward/record.url?eid=2-s2.0-0018916158&partnerID=tZOtx3y1

SERIIUS. (2012). Solar Energy Research Institute for India and United States. Retrieved June 29, 2019, from SERIIUS website website: https://www.seriius.org/

Shi, Y., Xu, B., Tan, Y., Kirschen, D., & Zhang, B. (2018). Optimal Battery Control Under Cycle Aging Mechanisms in Pay for Performance Settings. *IEEE Transactions on Automatic Control*. https://doi.org/10.1109/TAC.2018.2867507

Shockley, W. (1950). *Electrons and Holes in semiconductor: With applications to transistor electronics*. New York: D Van Nostrand Company Inc.

Short, W., Packey, D. J., & Holt, T. (1995). A Manual for the Economic Evaluation of Energy Efficiency and Renewable Energy Technologies. In *NREL/TP-462-5173*. https://doi.org/10.2172/35391

Solanki, C. S. (2015). *Solar Photovoltaics: Fundamentals, Technologies and Application* (Third). New Delhi: PHI Learning Private Limited.

Solmetric SunEye. (2011). Shade Measurement Overview. Retrieved July 4, 2019, from Slideshare.net website: https://www.slideshare.net/phoberg/shade-measurement-overview

Sridhar, H., & N. C., T. (2018). *Effect of Module Reliability on Techno-Economics of a Utility Scale Solar Photovoltaic Plant in India*. https://doi.org/(CSTEP-Report-2018-02)

Sridhar, H., & N. C., T. (2019). *Rectangular Spiral Inspired Approach for Quantifying Land Use and Potential Capacity for Solar Photovoltaic Power Plants in India*. https://doi.org/10.31219/osf.io/bn5e6

Stein, M. ., Ulam, S. ., & Wells, M. . (1964, May). A Visual Display of Some Properties of the Distribution of Primes. *Mathematical Association of America Stable*, *71*(5), 516–520. https://doi.org/10.2307/2312588

Stine, W. B., & Geyer, M. (2001). Power From The Sun. Retrieved August 14, 2015, from powerfromthesun.net website: http://www.powerfromthesun.net/book.html

Tata Power Solar. (2018). *Datasheet TP 300 series, 72 cell Multi-Crystalline solar photovoltaic modules*. Retrieved from https://www.tatapowersolar.com/wp-content/uploads/2018/03/14055248/Datasheet-TP300-4BB-5BB-DCR.pdf%0A

Teodorescu, R., Liserre, M., & Rodriguez, P. (2011). *Grid converters for photovoltaic and wind power systems* (First). West Sussex: John Wiley & Sons.

Townsend, T. U. (1989). *A Method for Estimating the Long -term Performance of Direct Coupled Photovoltaic Systems* (University of Wisconsin - Madison). Retrieved from https://minds.wisconsin.edu/handle/1793/46720?show=full

Tsanakas, I. (John, & Botsaris, P. (2009). *Non-destructive In Situ Evaluation of a PV Module Performance using Infrared Thermography*.

Ueckerdt, F., Hirth, L., Luderer, G., & Edenhofer, O. (2013). System LCOE: What are the costs of variable renewables? *Energy*, *63*, 61–75. https://doi.org/10.1016/j.energy.2013.10.072

Vogel, H. (1979). A better way to construct the sunflower head. *Mathermatical Biosciences*, *44*(3–4), 179–189. https://doi.org/https://doi.org/10.1016/0025-5564(79)90080-4

Whitaker, C. M., Townsend, T. U., Wenger, H. J., Iliceto, A., Chimento, G., & Paletta, F. (1991). Effects of irradiance and other factors on PV temperature coefficients. *Photovoltaic Specialists Conference, 1991., Conference Record of the Twenty Second IEEE*, 608–613 vol.1. https://doi.org/10.1109/PVSC.1991.169283

Your Home (Govt. Of Australia). (n.d.). PV system cell to array. Retrieved January 1, 2017, from Yourhome website website: http://www.yourhome.gov.au/energy/photovoltaic-systems


CENTER FOR STUDY OF SCIENCE, TECHNOLOGY AND POLICY,
#18 & 19, 10th Cross, Mayura Street,
Papanna Layout, Nagashettyhalli, RMV II Stage,
Bengaluru-560094, Karnataka (India)
Email: cpe@cstep.in

CENTER FOR STUDY OF SCIENCE, TECHNOLOGY AND POLICY,
Studio #206, International Home Deco Park (IHDP),
Plot No. 7, Sector 127, Taj Expressway,
Noida-201301, Uttar Pradesh (India)
Email: cpe@cstep.in


Center for Study of Science, Technology and Policy

**Bengaluru**
#18 & 19, 10th Cross,
Mayura Street,
Papanna Layout,
Nagashettyhalli, RMV II
Stage,
Bengaluru-560094,
Karnataka (India)

**Noida**
Studio #206,
International Home Deco
Park (IHDP),
Plot No. 7, Sector 127,
Taj Expressway,
Noida-201301,
Uttar Pradesh (India)

Email: cpe@cstep.in
www.cstep.in